

Aus der Klinik für Allgemein-, Viszeral- und Transplantationschirurgie
Klinikum der Ludwig-Maximilians-Universität München



Characterization of Peripheral Immune Events in Primary Colorectal Cancer Patients

Dissertation

zum Erwerb des Doktorgrades der Medizin
an der Medizinischen Fakultät der
Ludwig-Maximilians-Universität München

vorgelegt von

Can Lu

aus

Heze city, Shandong province, China

Jahr

2022

Mit Genehmigung der Medizinischen Fakultät der
Ludwig-Maximilians-Universität zu München

Erster Gutachter:	PD Dr. med. Florian Kühn
Zweiter Gutachter:	Prof. Dr. Jens Neumann
Dritter Gutachter:	Priv. Doz. Dr. Clemens Gießen-Jung
ggf. weitere Gutachter:	_____ _____
Dekan:	Prof. Dr. med. Thomas Gudermann
Tag der mündlichen Prüfung:	20.09.2022

Table of Contents

Table of Contents	3
Zusammenfassung.....	6
Abstract.....	7
List of Figures.....	8
List of Tables.....	9
List of Abbreviations.....	10
1. Introduction.....	14
1.1 Colorectal Cancer.....	14
1.1.1 The Nature of Colorectal Cancer	14
1.1.2 Treatment Strategies	15
1.1.2.1 EGFR Inhibitors.....	16
1.1.2.2 VEGF/VEGFR Inhibitors	16
1.1.2.3 Immune Checkpoint Inhibitors	17
1.2 Immunology of Colorectal Cancer.....	18
1.2.1 Neutrophils.....	19
1.2.2 Monocytes.....	19
1.2.3 Dendritic Cells	20
1.2.4 Myeloid-Derived Suppressor Cells.....	20
1.2.5 Natural Killer and Natural Killer T Cells.....	21
1.2.6 Adaptive Immune System	22
1.3 FACS Analysis of Human Immune Cells	23
1.3.1 Innate Immune Cells	24
1.3.1.1 Neutrophils, Monocytes and Dendritic Cells.....	24
1.3.1.2 Myeloid-derived Suppressor Cells.....	25
1.3.1.3 Natural Killer and Natural Killer T Cells.....	25
1.3.2 T lymphocytes.....	26
1.3.3 B Lymphocytes	28

1.4 Hypothesis and Specific Aims	29
2. Material and Methods	31
2.1 Materials	31
2.1.1 Devices.....	31
2.1.2 Consumables	31
2.1.3 Chemicals and Antibodies.....	31
2.1.5 Software	33
2.2 Methods.....	34
2.2.1 Study Population.....	34
2.2.2 Flow Cytometry Antibody Staining.....	34
2.2.3 Flow Cytometry Data Analysis	37
2.2.4 Construction of Diagnostic Model.....	44
2.2.5 Gene Expression Profile Collection and Processing.....	45
2.2.6 xCell Algorithm	48
2.2.7 Differential Expression Analysis	48
2.2.8 Gene Ontology Enrichment Analysis.....	48
2.2.9 Correlation Analysis.....	48
2.2.10 Statistical Analysis	49
3. Results	50
3.1 Patients with CRC Exhibiting Systemic Immune Suppression	50
3.2 Diagnostic Model allowed Differentiation of CRC Patients from Healthy Controls	59
3.3 NR3C2, CAMK4, and TRAT1 Associated with the Composition of Th cells.....	62
3.4 Right-sided CRC Patients demonstrating Similar Systemic Immune Landscape with Left-sided Ones.....	65
3.5 Correlation of Clinical Test Parameters with Immune Subsets in CRC Patients...	68
4. Discussion.....	71
4.1 Distributional Characteristics of Circulating Immune Subsets in CRC patients ...	71

4.2 Construction of a Diagnostic Model based on the Circulating Immune Subsets ..	74
4.3 Prediction of Molecular Mechanism Regulating the Level of Circulating Th cells using Bioinformatics Analysis	75
4.4 Distributional Comparison of Circulating Immune Subsets between Right-sided CRC patients and Left-sided ones.....	77
4.5 Correlation Analysis between Clinical Test Parameters and Circulating Immune Subsets in CRC Patients.....	78
4.6 Research Significance	79
4.7 Limitations and Future Directions	79
5. Conclusion	81
6. References.....	82
7. Appendix.....	98
Acknowledgement.....	103
Affidavit	104
Confirmation of Congruency	105
List of publications.....	106

Zusammenfassung

Das Zusammenspiel von Tumor- und Immunzellen kann das Fortschreiten von Darmkrebs (CRC) beeinflussen. Bislang ist die Auswirkung von kolorektalen Karzinomzellen auf die systemischen Immunprofile unzureichend untersucht. Das Ziel dieser Arbeit war die detaillierte Charakterisierung von Immunzellen im peripheren Blut von Patienten mit kolorektalem Karzinom.

Die Zusammensetzung der Untergruppen und der Immunphänotyp von B- und T-Lymphozyten, Neutrophilen, Monozyten, dendritischen Zellen (DCs), myeloiden Suppressorzellen (MDSCs), NK- und NKT-Zellen wurden in peripheren Blutproben von 12 CRC-Patienten und 11 gesunden Kontrollpersonen mittels Multicolor-Durchflusszytometrie untersucht. Logistische Regressionsanalysen und maschinelle Lernalgorithmen (Support Vector Machine Learning) wurden durchgeführt, um ein diagnostisches Modell zur Unterscheidung von CRC-Patienten und gesunden Kontrollpersonen anhand der Immunzelluntergruppen zu erstellen. Darüber hinaus wurden die Expressionmuster der peripheren Blut- und Gewebeproben verwendet, um die Gene mit unterschiedlicher Expression (DEGs) bei CRC-Patienten im Vergleich zu normalen Kontrollen zu analysieren. Es wurde eine Korrelationsanalyse durchgeführt, um DEGs zu finden, die mit der Verteilung von Untergruppen von Immunzellen assoziiert sind und um die zugrunde liegende Beziehung zwischen Immunzellzusammensetzungen und klinischen Testparametern bei CRC-Patienten weiter zu untersuchen.

Ergebnisse: Im Gegensatz zu gesunden Kontrollpersonen wiesen CRC-Patienten einen geringeren Anteil an B- und T-Lymphozyten, T-Helferzellen (Th-Zellen), nicht-klassischen Monozyten, DCs und einen erhöhten Anteil an polymorphkernigen MDSCs sowie eine geringere Expression von CD69 sowohl auf CD56dim- als auch auf CD56bright-NK-Zellen auf. Ein diagnostisches Modell, das sieben Immununtergruppen integriert, wurde erstellt, um CRC-Patienten und gesunde Kontrollen mit einer AUC von 1.000 (95% CI 1.000-1.000) zu unterscheiden. Darüber hinaus wurden NR3C2, CAMK4 und TRAT1 als Kandidatengene identifiziert, die die Anzahl der zirkulierenden Th-Zellen bei Patienten mit CRC regulieren. Rechtsseitige Karzinome wiesen eine ähnliche systemische Immunlandschaft auf wie linksseitige Karzinome.

Zusammenfassend zeigte sich bei Patienten mit kolorektalem Karzinom eine eindeutige Suppression der systemischen Immunantwort. Die veränderte Zusammensetzung der zirkulierenden Untergruppen von Immunzellen bei CRC könnte den regionalen Immunstatus der Tumormikroumgebung ergänzen und zur Entdeckung immunbezogener Biomarker für die Diagnose von CRC beitragen.

Abstract

Background The interaction between tumor and immune cells is known to affect the progression of colorectal cancer (CRC), but the effect of CRC cells on the systemic immunity remained unclear. We aimed to perform a comprehensive evaluation of circulating immune subsets and gene expression analysis of CRC patients.

Methods The subset composition and phenotype of B and T lymphocytes, neutrophils, monocytes, dendritic cells (DCs), myeloid-derived suppressor cells (MDSCs), NK, and NKT cells were investigated in peripheral blood samples from 12 CRC patients and 11 healthy controls by multicolor flow cytometry. Circulating immune subsets were utilized to construct a diagnostic model. Furthermore, we performed the bioinformatics analyses to obtain the differential expression genes (DEGs) and immune cells between CRC patients and normal controls. Correlation analysis was conducted to discover regulatory genes and clinical test parameters associated with distribution of circulating immune subsets.

Results In contrast to healthy controls, CRC patients had a reduced proportion of B and T lymphocytes, T helper (Th) cells, non-classical monocytes, DCs, and an increased proportion of polymorphonuclear MDSCs, as well as reduced expression of CD69 on both CD56^{dim} and CD56^{bright} NK cells. A diagnostic model integrating seven immune subsets was constructed to discriminate CRC patients and healthy controls with an AUC of 1.000 (95% CI 1.000-1.000). Moreover, NR3C2, CAMK4 and TRAT1 were identified as candidate genes regulating the number of circulating Th cells in CRC patients. Right-sided CRC patients had a similar systemic immune landscape with left-sided ones. In addition, we found a robust positive correlation between immune subsets and three clinical test parameters, including gamma-glutamyltransferase, aspartate aminotransferase, and alanine aminotransferase.

Conclusions The immune suppression of systemic immune responses is evident in CRC patients. The altered composition of circulating immune subsets in CRC could complement the regional immune status of the tumor microenvironment and contribute to the discovery of immune-related biomarkers for the diagnosis of CRC.

List of Figures

Figure 1: Flow cytometry gating strategy applied for the identification of circulating B lymphocyte subsets	41
Figure 2: Flow cytometry gating strategy applied for the identification of circulating T lymphocytes subsets	42
Figure 3: Flow cytometry gating strategy applied for the identification of circulating innate immune cell subsets	43
Figure 4: Flow diagram of identifying and selecting eligible GEO datasets	46
Figure 5: The pre-processing of merged GEO datasets	47
Figure 6: Analysis flow diagram of the study	52
Figure 7: The circulating immune subsets distribution in CRC patients compared to healthy controls	54
Figure 8: The peripheral blood immunophenotype of NK and NKT cells in CRC patients compared to healthy controls	55
Figure 9: Diagnostic model for differentiating CRC patients from healthy controls	60
Figure 10: Differential expression genes between normal and CRC in blood and tissue samples	63
Figure 11: Identification of candidate genes associated with the composition of circulating Th cells	64
Figure 12: The circulating immune subsets distribution in right-sided CRC patients compared to left-sided ones	67
Figure 13: Correlation analysis between circulating immune subsets and clinical test parameters	69

List of Tables

Table 1 Flow cytometry panels applied to identify peripheral blood B-, T-, and Innate immune subsets	36
Table 2 Immunophenotyping of B lymphocytes, T lymphocytes, and Innate immune subsets	38
Table 3 Clinical characteristics of healthy controls and CRC patients.....	53
Table 4 Comparison of circulating immune subsets between CRC patients and healthy controls	56
Table 5 The accuracy of individual immune subset or the combination of different immune subsets as the classifier to distinguish CRC patients from healthy controls by Support Vector Machine learning algorithm.....	61
Table 6 Clinical characteristics of left-sided CRC patients and right-sided ones	66
Table 7 Clinical test parameters correlated with immune subsets	70
Table 8 Identification of circulating immune subsets to differentiate CRC patients from healthy controls through univariable logistic regression.....	98
Table 9 Correlation analysis between circulating Th cells and common DEGs in healthy controls	100
Table 10 Correlation analysis between circulating Th cells and common DEGs in CRC patients	101

List of Abbreviations

%	Percentage
Min	Minute
EGFR	Epidermal growth factor receptor
VEGF	Vascular endothelial growth factor
VEGFR	Vascular endothelial growth factor receptor
Th	T helper
CRC	Colorectal cancer
IBD	Inflammatory bowel diseases
SCRC	Sporadic colorectal cancer
HCRC	Hereditary colorectal cancer
CAC	Colitis-associated colorectal cancer
APC	Adenomatous polyposis coli
MMR	Miss match repair
CIN	Chromosomal instability
MSI	Microsatellite instability
OS	Overall survival
RSC	Right-sided CRC
LSC	Lest-sided CRC
TNM	Tumor-Nodes-Metastasis
KRAS	KRAS proto-oncogene
BRAF	B-Raf proto-oncogene
PI3KCA	Phosphatidylinositol-4,5-bisphosphate 3-kinase
TP53	Tumor protein p53
SMAD4	SMAD family member 4
EREG	Epiregulin
AREG	Amphiregulin
mCRC	Metastatic CRC
NCCN	National comprehensive cancer network
ErbB	Erythroblastosis oncogene B
HER	Human epidermal growth factor receptor

MEK	MAP kinase-ERK kinase
ERK	Extracellular signal-regulated kinase
AKT/PKB	Protein kinase B
JAK	Janus kinase
STAT3	Signal transducer and activator of transcription 3
FDA	Food and Drug Administration
PIGF	Placental growth factor
PFS	Progression-free survival
PD-1	Programmed cell death 1
CTLA-4	Cytotoxic T-lymphocyte associated protein 4
TIGIT	T cell immunoreceptor with Ig and ITIM domains
LAG3	Lymphocyte activating 3
HAVCR2	Hepatitis A virus cellular receptor 2
BTLA	B and T lymphocyte associated
dMMR	Deficient miss match repair
MSI-H	High microsatellite instability
pMMR	Proficient miss match repair
MSS	Microsatellite stable
MiRNA	MicroRNA
DFS	Disease-free survival
TAM	Tumor-associated macrophage
DC	Dendritic cell
LMR	Lymphocyte-to-monocyte ratio
CTLs	Cytotoxic T cells
MDSC	Myeloid-derived suppressor cell
M-MDSC	Monocytic myeloid-derived suppressor cell
PMN-MDSC	Polymorphonuclear myeloid-derived suppressor cell
E-MDSC	Early-stage myeloid-derived suppressor cell

Tregs	Regulatory T cells
NK	Natural Killer
NKT	Natural killer T
APC	Antigen-presenting cell
Th1	Helper T type 1
Th17	Interleukin 17-producing T helper
Bregs	Regulatory B cells
SSC	Side-scatter
FSC	Forward-scatter
SSC-H	SSC-height
SSC-W	SSC-width
FSC-H	FSC-width
FSC-W	FSC-width
CEACAM8	Carcinoembryonic antigen-related cell adhesion molecule 8
cDC1	Classical DC1
cDC2	classical DC2
pDCs	Plasmacytoid DCs
KIR	Killer immunoglobulin-like receptors
ADCC	Antibody-dependent cellular cytotoxicity
TCR	T-cell receptor
CD8T	CD8 ⁺ cytotoxic T
TCM	Central memory T
TEM	Effector memory T
cADPR	Cyclization of NAD ⁺ to cyclic ADP-ribose
Th2	Helper T type 2
BCR	B cell antigen receptor
GCs	Germinal centers
CSM	Class-switched memory
NCSM	Non-class switched memory
T2-MZP	Transitional 2 marginal-zone precursor
PB	Peripheral blood

FMO	Fluorescence minus one
MFI	Median fluorescence intensity
GEO	Gene Expression Omnibus
TCGA	The Cancer Genome Atlas
DEGs	Differential expression genes
GO	Gene Ontology
FDR	False discovery rate
SVM	Support vector machine
ICs	Immune cells
AUC	Area under curve
AJCC	American Joint Committee on Cancer
COPD	Chronic obstructive pulmonary disease
THEMIS	Thymocyte-expressed molecule involved in selection
AST	Aspartate aminotransferase
ALT	Alanine aminotransferase

1. Introduction

1.1 Colorectal Cancer

1.1.1 The Nature of Colorectal Cancer

Colorectal cancer (CRC) is the third most frequent carcinoma and the second leading cause of cancer-associated death globally, accounting for 1.8 million new cases and 900,000 deaths annually [1]. Although the incidence of CRC tends to be stabilized in highly developed economies, the worldwide incidence of this disease may increase to 2.5 million new cases in 2035 as the continuing progress trends in developing countries [2]. To date, inflammatory bowel diseases (IBD)[3], obesity and overweight[4-6], sedentary behavior[7], red meat consumption[8], family history of CRC[9] are well-established risk factors for the development of CRC. Clinically, presenting symptoms of CRC are varied among patients and lack uniqueness. However, most patients may present with rectal bleeding, changes in bowel habits, unintended weight loss, and abdominal pain [10]. Etiologically, CRC has been subdivided into sporadic colorectal cancer (SCRC), hereditary colorectal cancer (HCRC), and colitis-associated colorectal cancer (CAC).

SCRC, accounting for two-thirds of CRC, refers to cancer originating from the colorectum without known attribution to germline causes or significant family history of cancer or inflammatory bowel diseases [11]. According to the classification of alteration frequencies, SCRC could be subcategorized into hypermutated groups (15%) and non-hypermutated ones (85%) [11]. Even though around one-third of CRCs are diagnosed in subjects with a family history of the disease, only 15% of these patients are identified as HCRC with identified causes from germline mutations in genes pertaining to essential biological processes, such as adenomatous polyposis coli (APC) gene, DNA mismatch repair (MMR) genes, etc. [12]. Currently, it is widely accepted that three molecular pathways have a fundamental role in the adenoma-carcinoma progression sequence of SCRC and HCRC: Chromosomal Instability (CIN) pathway, Microsatellite Instability (MSI) pathway, Serrated Neoplasia pathway [13]. CAC is a

recognized and feared complication of IBD with the feature of non-infectious chronic inflammation of the gastrointestinal tract [14]. Moreover, although CAC is only responsible for 1-2% of all cases of CRC[15], 10-15% of annual deaths in IBD patients were caused by CAC [16]. Due to the controversial reports about the prognosis of CAC, a newly published meta-analysis indicated that CAC patients have much worse overall survival (OS) than patients with non-IBD CRC, which may largely attribute to aggressive histological characteristics and lower rates of R0 resections at the primary tumor sites [17]. Meanwhile, owing to the effect of relapsing intestinal chronic inflammation, CAC follows a different progression pattern compared to the other two types of CRC, called dysplasia-carcinoma sequence [18]. In addition, although both CAC and SCRC have a similar distribution of CIN and MSI, p53 mutations were considered the early events in CAC, whereas the inactivation of APC mainly characterizes SCRC as the initial event for the carcinogenesis [19, 20].

1.1.2 Treatment Strategies

Treatment strategies for CRCs largely depend on the tumor stage at presentation, the location of primary carcinoma, mutational characteristics, metastatic sites as well as the therapeutic aims [2]. Removal of cancer is always the core purpose of the clinical treatments on patients with CRC, so surgical resection remains the cornerstone for curative-intent treatment. For those cases with unresectable tumors or who are intolerant to surgery, chemotherapy and radiotherapy are the prioritized options for restraining disease in such patients [21]. Accumulating studies show that chemotherapy could significantly extend the OS time in CRC patients with or without metastases, resulting in chemotherapy acting as the backbone of CRC treatment [22-24]. However, chemotherapy has some limitations such as inevitable systematic toxicity, unsatisfying response rate, and unpredictable intrinsic or acquired drug resistance. Therefore, new approaches have received enormous investments to improve or even substitute available CRC chemotherapy [21].

Despite significant advances in diagnostic and therapeutic options in the past decades, nearly 25% of the patients have synchronous metastases at the initial diagnosis, and virtually 50% of primary CRC patients could develop distant metastases during this disease [25]. Furthermore, after receiving completed resection of CRC, the 5-year survival rate is approximately 60%, while the rate drops to 12% for mCRC [26]. Therefore, there is a pressing need to develop more effective approaches for medical intervention. With a better understanding of the molecular and genetic biology of CRC, targeted therapies and immunotherapy have become promising strategies for advanced late-stage cases.

1.1.2.1 EGFR Inhibitors

EGFR, belonging to the ErbB (erythroblastosis oncogene B)/HER (human epidermal growth factor receptor) family, plays a vital role in promoting colorectal carcinoma development via activating various downstream intracellular signaling pathways, including RAS/RAF/MEK/ERK, PI3K/AKT, and JAK/STAT3 pathways [27, 28]. Two inhibitors of EGFR, cetuximab, and panitumumab, have obtained approval from the United States of America Food and Drug Administration (FDA) to treat mCRC harboring wild-type RAS (RAS-WT). These two inhibitors, ones of immunoglobulins, could directly bind to the external domain of EGFR to induce its internalization and degradation. According to the phase III ASPECCT study findings, cetuximab and panitumumab have similar clinical outcomes in improving the OS time of mCRC patients [29]. However, due to the complicated communications among molecular in different pathways of EGFR and genetic mutations, innate or acquired resistance for the above two inhibitors frequently occurs even in mCRC with RAS-WT [21]. Consequently, dozens of new drugs targeting the EGFR pathway are still under clinical investigation worldwide.

1.1.2.2 VEGF/VEGFR Inhibitors

Vascular endothelial growth factor (VEGF), belonging to VEGF family containing five members (VEGF-A, -B, -C, and D and placental growth factor (PlGF)), could bound to tyrosine kinase VEGF receptors of endothelial cells to promote angiogenesis

acted as an essential role in tumor progression. Although FDA has approved four anti-VEGF/VEGFR agents in the past two decades, bevacizumab is the only drug permitted as a first- and second-line targeting-VEGF agent for mCRC so far. Bevacizumab, a humanized monoclonal antibody, could directly neutralize VEGF-A in the tumor microenvironment. Although bevacizumab only presents significant partial improvement in either OS or progression-free survival (PFS)[30, 31], this agent stably shows effectiveness in different subgroups of mCRC patients, such as elderly subjects (over 70 years old)[32], patients with or without KRAS mutations[33, 34], and cased with left- or right-sided colorectal carcinoma [33]. Unsurprisingly, mCRC could also show resistance to anti-VEGF agents, which may attribute to the compensatory activation of alternative signaling pathways and secretion of angiogenesis-associated substances. Hence, amounts of new anti-VEGF/VEGFR drugs are under investigation in clinical trials to further optimize the treatment effects of target therapy.

Although anti-EGFR and anti-VEGF therapies have shown sound effects against mCRC, multiple studies suggested that anti-EGFR agents combined with chemotherapy are recommended as the first-line treatment for metastatic LSC patients with RAS-WT while anti-VEGF drugs should always be considered as an alternative [35-37].

1.1.2.3 Immune Checkpoint Inhibitors

Immune checkpoints, also called inhibitory immunoreceptors, refer to molecules expressed on the immune cells to prevent the over-activation of immune responses, including but not limited to PD-1, CTLA-4, TIGIT, LAG3, HAVCR2, and BTLA. In contrast to approaches directly blocking pathways that promote tumor development, evidence suggested that enhancing intratumoral immunorecognition and subsequent immune responses might be promising alternative ways to counter against cancer. Pembrolizumab and nivolumab, humanized IgG4-based PD-1 antibodies, have gained FDA approval for the treatment of mCRC with MMR deficient (dMMR) or high MSI (MSI-H) [21]. The Keynote-177 study investigated pembrolizumab versus standard of

care chemotherapy in mCRC patients with MSI-H in the first-line setting, which showed estimated median PFS values of 16.5 months and 8.2 months, respectively [38]. Thus, FDA has approved pembrolizumab as the first-line treatment with MSI-H advanced CRC in 2020, which likely led to the paradigm shift in treatment. In addition, owing to the decent effects and safety of combined therapy with nivolumab and ipilimumab (CTLA-4 antibody) on mCRC patients with MSI-H [39], this doublet regimen has acquired FDA approval as an alternative therapy for patients with chemotherapy-refractory mCRC with MSI-H. On the other hand, CRC patients with MMR proficient (pMMR) or microsatellite stable (MSS), constituting a large proportion of patients, virtually have no response to immune checkpoint blockade. Even though the underlying mechanism of this resistance remains unclear, strategies to improve immune checkpoint inhibitor response on these patients are still under research [40].

1.2 Immunology of Colorectal Cancer

Many types of biomarkers, including miRNAs, circulating tumor cells, circulating tumor DNA, and genetic mutations, have been proposed to predict the responses to therapeutics and stratify CRC patients according to the risk classification [41]. However, these approaches are virtually characterized by tumor-cell-centric nature, overlooking the intrinsic heterogeneity of the tumor microenvironment and immune elements. Moreover, accumulating studies confirmed that the interplay between tumor processes and the host immune responses have a fundamental role in shaping the progression of CRC [42-44]. The immunoscore based on the quantification of CD3⁺ and CD8⁺ lymphocytes at the invasive margin and the core of the carcinoma have been proven to be more reliable than tumor-node-metastasis (TNM) staging as a prognostic marker in patients with CRC [45, 46]. However, it must be realized that the immunoscore only represents the local immune infiltration profiles in the tumor tissues and has a limited capacity for evaluating a wide range of potential tumor-infiltrating immune cell subsets.

Furthermore, cancer immunity is considered a combination of the intratumoral immune events and the systemic immune response of the peripheral blood [47]. A previous study also showed that circulating CD16⁺ NKT-like cells was negatively associated with disease-free survival (DFS) in CRC patients [48]. Since anti-tumor adaptive immune cell subsets of neoplasia are mainly sourced from the blood via the chemotaxis process, immunophenotyping of circulating immune cells could comprehensively provide systemic features which complement local characteristics of the intratumoral immune status. In contrast to the tumor-infiltrating immune cells, the circulating immune profiles have the advantage of being continuously measured to potentially reflect the responses of therapy and possibly inform the suitable treatment options in the future. The defense system in the tumor tissue and blood consists of immune cell subsets belonging to innate and adaptive immune systems.

1.2.1 Neutrophils

Neutrophils are indispensable immune cells in defending against invading microorganisms and facilitating wound healing [49]. Recent studies have shown that tumors could prime neutrophils to polarize into diversified functional states by which they exhibit pro- or anti-tumorigenic roles in cancer development [49]. Interestingly, Governa et al.[50] revealed that tumor-infiltrating CD66⁺ neutrophils were positively associated with the OS in patients with CRC, whereas Rao et al.[51] conclude an opposite finding that intratumoral CD66⁺ neutrophil is a poor prognostic marker for CRC patients. There are still controversies to debate on the clinical significance of neutrophils. Moreover, two studies failed to characterize the circulating neutrophils. Therefore, it is necessary to explore the features of circulating neutrophils in CRC patients.

1.2.2 Monocytes

Monocytes, a heterogeneous population of mononuclear phagocyte systems, are recently considered critical regulators of cancer development and metastasis, with different subsets performing opposing roles in enabling tumor growth and preventing

metastatic spread of tumor cells [52]. They also act as the main source of tumor-associated macrophages (TAMs) and dendritic cells (DCs) that orchestrate the tumor microenvironment [53]. It is proven that tumor-infiltrating CD68⁺ macrophages were negatively associated with the OS of patients with stage III CRC [54]. Since systemic inflammation has been demonstrated to be related to the tumor progression and metastasis of CRC[55], a meta-analysis indicated that low lymphocyte-to-monocyte ratio (LMR) in the peripheral blood was associated with poor prognosis in CRC patients [56]. Besides, Shibutani et al.[57] also pointed out that the peripheral monocyte count was strongly associated with the density of tumor-associated M2-like macrophages with anti-inflammation function. However, there are few reports on the distributional characteristics of circulating monocytes subsets in CRC patients.

1.2.3 Dendritic Cells

DCs, one of the essential antigen-presenting cells, could initiate adaptive immune responses and secret costimulatory molecules to drive cytotoxic T cells (CTLs) clonal expansion [58]. In terms of DC's ability to induce a wide range of immune responses, DC-based vaccine research aiming to boost adaptive immunity to cancer has grown rapidly in recent years [59, 60]. Due to the diversified subsets and functional plasticity, DCs could elicit anti-tumor and pro-tumor functions in the tumor microenvironment [61]. While there are contradicting reports about the clinical significance of DCs, one systematic review integrating twelve studies concluded that tumor-associated activated and mature DCs in CRC might be linked to good clinical outcomes, including OS and DFS [62]. Until now, no relevant studies investigated the distribution of circulating DCs in individuals with CRC.

1.2.4 Myeloid-Derived Suppressor Cells

Myeloid-derived suppressor cells (MDSCs) comprise a heterogeneous population of early-stage (E-MDSC), monocytic (M-MDSC), and polymorphonuclear origin (PMN-MDSCs) that typically arise in chronic inflammatory sites, including cancer [63]. Furthermore, M-MDSCs can promptly differentiate into TAMs in the tumor milieu

[64]. It is widely accepted that MDSCs show their immune-suppressive roles in CRC mostly via inhibiting T-cell proliferation and stimulating regulatory T cells (Tregs) development [65]. Several studies have reported that tumor-infiltrating and circulating MDSCs were significantly increased in primary CRC patients compared to healthy controls and that circulating MDSCs were associated with advanced cancer stages and metastases [66, 67], which indicate the correlation between circulating MDSCs and the disease progression of CRC. Also, Solito et al. [68] found that stage IV CRC patients with high circulating MDSCs had worse OS, and Tada et al. [69] further revealed that circulating M-MDSCs levels of mCRC patients were inversely associated with progression-free survival after receiving the first-line chemotherapy. In addition, high counts of pretreatment circulating MDSCs may indicate poor survival in CRC patients [70]. Mundy et al. also reported that M-MDSCs and PMN-MDSCs were significantly elevated in CRC cases versus normal donors [71]. Whereas there are lacking clinical studies investigating the composition of circulating E-MDSCs in CRC.

1.2.5 Natural Killer and Natural Killer T Cells

Both natural killer (NK) cells and natural killer T (NKT) cells are innate-like lymphocyte populations with cytotoxic function independent of MHC molecular on pathogenic cells and tumor cells in the innate immunity. NK cells can be subdivided into two types according to the expression level of CD56, namely CD56^{bright} and CD56^{dim} NK cells. CD56^{bright} NK cells generally have immunoregulatory functions and produce pro-inflammatory cytokines, while CD56^{dim} NK cells mainly elicit cytotoxic functions [72, 73]. Furthermore, NKT cells are a unique immune cell population with characteristics of NK cells and T cells [74]. In addition, the cytotoxic activity of NK- and NKT cells mainly relies on the delicate balance between inhibitory and activating signals from cell-surface triggering receptors [75]. It is reported that the level of pre-surgery circulating CD16⁺ NKT cells was inversely related with DFS in CRC patients who underwent curative surgical resection [48]. Moreover, a recent retrospective study reported the percentage of total NK cell level

in the peripheral blood as a prognostic marker in CRC patients who received R0 or R1 resection and chemotherapy [76]. Krijgsman et al.[77] also revealed that colon carcinoma could induce immune suppression on NK- and NKT cells, an effect that could be diminished after tumor resection. Although uncommonly found among the intratumor immune infiltrates, the number of tumor-infiltrating NK and NKT cells are positively correlated with better prognosis in patients with CRC [78-80]. Nonetheless, the distribution of NK and NKT cells with the early activation marker (CD69) has not yet been examined in CRC cohorts.

1.2.6 Adaptive Immune System

Meanwhile, the adaptive immune system also played an important role in regulating CRC development. Different subsets of T- and B- lymphocytes have been reported through the years, whereas these subsets with distinct functions could have opposing effects on anti-tumoral immune responses. For example, CD8⁺ T lymphocytes could recognize cancer cells in MHC I-restricted mechanism and produce cytotoxic molecules to eliminate them directly. In contrast, Treg cells could directly secret or promote the synthesis of immunosuppressive mediators and alter the functional status of antigen-presenting cells (APC) [81]. Nowadays, high intratumor infiltration of total T cells, CD8⁺ cytotoxic T cells, and CD45RO⁺ memory T cells in CRC have been widely accepted as good prognostic markers [82]. In addition, several studies also suggested that intratumor Tregs density is associated with better patients' prognosis in CRC[83-85]. PD-L1 expressing tumor cells may inhibit Tregs infiltration in the tumor microenvironment[86], which might explain the above findings of Treg cells. Additionally, tumor-infiltrating Th1 and Th17 cells have been proven to have negative prognostic effects on patients with CRC [87-90]. Apart from the clinical research of T cells in the tumor tissues, a few studies reported the systemic immune response of these cells in CRC. They suggested that circulating Tregs percentage in the peripheral blood was significantly different between CRC patients and healthy control, but they failed to be a prognostic marker [48, 91].

In addition, tumor-infiltrating mature B lymphocytes have the role of inhibiting tumor development via secreting antibodies, facilitating T cell response, and killing tumor cells directly, whereas regulatory B cells (Bregs) could promote tumor growth via secreting immunosuppressive cytokines [92]. A clinical study demonstrated that memory B- and plasma- cells are the main components of tumor-infiltrating B lymphocytes in primary CRC lesions, while advanced tumors have significantly higher infiltration of Bregs than early-stage CRC [93]. Besides, they also indicated that CRC patients have lower levels of naïve B cells and higher levels of memory B cells, plasmablast cells, and Breg cells in the peripheral blood than healthy controls [93]. Two clinical studies[94, 95] found that tumor-infiltrating CD20⁺ B lymphocytes were strongly associated with favorable prognosis in CRC patients. Overall, there is much less research on the prognostic role of B cells than T cells in CRC patients, which requires more future clinical studies to deepen our understanding of the potential immunotherapeutic application of B cells.

1.3 FACS Analysis of Human Immune Cells

Regarding the entity of fresh blood samples, there is no need to use viability dyes to distinguish between live and dead cells in flow cytometric analysis. CD45, type I transmembrane protein, is expressed in virtually all differentiated hematopoietic cells but not in erythrocytes and plasma cells. CD45 is usually the first to be gated in the FACS analysis to identify immune cells from the peripheral blood or tissue samples. Meanwhile, according to the intrinsic differences of immune cells in size and granularity, side-scatter (SSC) and forward-scatter (FSC) are applied to differentiate lymphocytes from non-lymphocytes in the leukocytes population. In addition, SSC-height (SSC-H) versus SSC-width (SSC-W) and FSC-height (FSC-H) versus FSC-width (FSC-W) are sequentially performed to exclude doublets from the targeted cell populations. Afterward, the singlet cell population is gated to identify immune cell subsets of three panels, including T lymphocytes, B lymphocytes, and innate immune cells.

1.3.1 Innate Immune Cells

1.3.1.1 Neutrophils, Monocytes and Dendritic Cells

Acted as the co-receptor of TLR4 for detecting of pathogen-associated molecular patterns, CD14 is the first identified marker of monocytes to induce intracellular responses upon bacterial encounter [96]. And it is broadly recognized that monocytes and macrophages mainly express CD14. In order to exclude the contamination of monocytes in the identification of granulocytes, CD14⁻ phenotype is performed to gate monocytes out from the non-lymphocytes population. CD66b, also known as carcinoembryonic antigen-related cell adhesion molecule 8 (CEACAM8), is only expressed on granulocytes. Thus, granulocytes are gated out from CD14⁻ non-lymphocytes with the phenotype of CD66b⁺ and CD15⁺ acting as the myeloid-derived cells marker. Contaminating CD66b⁺ eosinophils are removed from the granulocytes using the gating strategy based on CD45^{hi}CD16^{-/low} [97]. Due to the heterogeneous populations of circulating neutrophils, both mature and immature neutrophils are characterized by CD11b⁺CD16^{+/-} phenotype [97, 98].

Similarly, CD66b⁻ phenotype is gated on the non-lymphocytes population to exclude the potential mixed neutrophils. HLA-DR, an MHC class II surface receptor, has the main function of presenting foreign peptide antigens to Th cells for eliciting or suppressing the immune response. Accumulating studies have pointed that monocytes have the capacity of presenting antigens *in vivo* [99]. Then targeted cells are identified from CD66b⁻ non-lymphocytes using HLA-DR⁺ phenotype. Multiple subsets of monocytes have been identified according to the differential expression of CD14 and CD16, including classical monocytes, intermediate monocytes, and non-classical monocytes [100]. Among monocytes subsets, classical monocytes have the unique feature enabling them to migrate towards tissues under homeostasis conditions. In contrast to classical monocytes, non-classical monocytes have a longer lifespan in the circulation and show patrolling behavior within the vasculature to scavenge luminal microparticles and monitor endothelial cell integrity [100]. Furthermore, intermediate monocytes represent the bridge linking classical monocytes with subsequently

differentiated non-classical monocytes in the circulation. DCs belong to bone marrow (BM)-derived cells mainly distributed in the blood, epithelial, lymphoid, and intestinal tissues. Acted as the professional antigen-presenting cells, DCs can be further split into classical DC1 (cDC1), classical DC2 (cDC2), and plasmacytoid DCs (pDCs). The gating strategy for three subsets of monocytes and DCs is acquired from flow cytometry guidelines [98]. The immunophenotyping of neutrophils and monocytes is listed in Table 2.

1.3.1.2 Myeloid-derived Suppressor Cells

CD33, a transmembrane receptor, is mainly expressed on myeloid-lineage cells. Due to the reduced expression of CD33 on mature neutrophils [101], the CD33⁺ phenotype is applied to gate lymphocytes and a large proportion of neutrophils out from the non-lymphocytes population. Owing to the immature features of MDSCs in the differentiation level, HLA-DR is used to identify targeted cells without antigen-presenting capacity from CD33⁺ non-lymphocytes. Multiple studies have reported that MDSCs consist of three groups of cells: PMN-MDSCs, M-MDSCs, and early-stage MDSCs [102]. Early-stage MDSCs (E-MDSC) represent a mixed group of immature progenitor cells, which may further differentiate into either M-MDSCs or PMN-MDSCs [103]. Consensus guidelines have defined the immunophenotyping of MDSCs subsets listed in Table 2 [102, 104].

1.3.1.3 Natural Killer and Natural Killer T Cells

To exclude the potential contamination of monocytes, CD14⁻ phenotype is first performed on the population of lymphocytes. CD56, an isoform of the human neural cell adhesion molecule, is mainly expressed on NK and NKT cells. Compared to NK cells, NKT cells have the characteristic features of both conventional T cells and NK cells. Although NKT cells have a cytotoxic function, NKT cells mainly exert an immune regulatory effect upon activation via secreting amounts of pro- or anti-inflammatory cytokines [74]. Thus, NK and NKT cells are characterized by CD56⁺CD3⁻ and CD56⁺CD3⁺ phenotype within CD14⁻ lymphocytes population, respectively [48]. Moreover, NK cells are further divided into CD56^{bright} and CD56^{dim}

NK cells according to the expression level of CD56. In terms of a well-known linear model of NK cell development, CD56^{bright} NK cells could subsequently differentiate into CD56^{dim} NK cells via upregulating CD16 and killer immunoglobulin-like receptors (KIR) [105]. Accumulating studies have demonstrated that the activity of NK and NKT cells largely depends on the balance between inhibitory and stimulatory signals from corresponding membrane receptors [74, 75]. CD16, also referred to as FcγRIIIA, could activate NK cells by promoting its antibody-dependent cellular cytotoxicity (ADCC) [106]. CD8 has an important role in enhancing the cytolytic function of NK cells via acting as the activating cell surface receptor [107]. Furthermore, multiple studies indicated that CD69 is a stimulatory membrane receptor since it could increase NK cytotoxicity [108]. Due to the characteristics similarity between NKT and NK cells [74], it is reasonable to infer that these three markers may also represent the activation receptors of NKT cells. Hence, thirteen subsets of NK and NKT cells are identified from peripheral blood samples. The immunophenotyping of each subset is listed in Table 2.

1.3.2 T lymphocytes

CD3, a multimeric protein complex, is specifically expressed in T cells and stably appears at all subsets of T lymphocytes. CD8 and CD4, transmembrane glycoproteins functioning as co-receptors for the T-cell receptor (TCR), are predominantly expressed in cytotoxic T cells and T helper cells, respectively. Then CD3 marker is used to isolate T cells from lymphocytes, and the latter is subdivided into CD8⁺ cytotoxic T cells (CD8T) and CD4⁺ T helper (Th) cells. CD45RO, one of the CD45 isoforms, is mainly expressed on most thymocytes, activated T cells, memory T cells, granulocytes, and monocytes. CD197, also referred to as CCR7, is a seven-transmembrane G-protein-coupled receptor for C-C chemokines. Through interacting with two ligands, CCL19 and CCL21, CCR7 has an important role in balancing immunity and immune tolerance in the peripheral blood [109]. With the help of CD197, naive T lymphocytes could home to secondary lymphoid organs to be

activated with the antigen presented by DCs. Upon activation, part of naïve T cells will differentiate into effector T cells, and the rest of them persist as circulating memory T cells that can provide long-term enhanced immune responses upon pathogen re-exposure. Furthermore, it is widely accepted that CCR7 could divide memory T cells into two distinct subtypes according to its expression level, central memory (CCR7⁺) T cells (TCMs) and effector memory (CCR7⁻) T cells (TEMs). Compared with TEMs mainly migrated into inflamed tissues to directly exert immune responses to the pathogen, TCMs prone to migrate into secondary lymphoid organs and lack immediate effector function but can differentiate into TEMs upon a secondary challenge [110]. Therefore, Naïve- and central memory-T cells can express CCR7, whereas effector- and effector memory-T cells lack the expression of CCR7. Thus, CCR7 and CD45RO are used to identify four subsets of CD8T cells and Th cells, namely naïve T cells, effector T cells, effector memory T cells, and central memory T cells. CD38, a major NAD⁺ glycohydrolase, could catalyze the cyclization of NAD⁺ to cyclic ADP-ribose (cADPR) that mediates the activation of intracellular Ca²⁺ signaling, and the latter has a fundamental role in activating T cells [111]. HLA-DR, an MHC class II cell surface receptor, has been considered as a marker for the activation of T cells [112, 113]. Then activated CD8T and activated Th cells are gated upon CD38 and HLA-DR markers from CD8T and Th cells, respectively. CD194, also called CCR4, is a chemokine receptor for CC chemokine ligands CCL17 and CCL22. CD196, known as CCR6, is a CC chemokine receptor protein for only one chemokine ligand-CCL20. It is broadly accepted that CCR4 is specifically expressed in helper T type 2 (Th2) cells, Treg cells, and interleukin 17 (IL-17)-producing T helper (Th17) cells, whereas CCR6 is also expressed in Th17 [114]. Upon various immunological challenges, Th cells could develop into a spectrum of polarized, counterbalancing subsets, including Th1, Th2, and Th17 cells. Th1 cells mainly stimulate the cellular immune response against intracellular pathogens via the secretion of IFN- γ . In contrast, through secreting IL-4, IL-5, IL-9, and IL13, Th2 cells

typically initiate diversified immune responses for extracellular pathogens and bacterial infection [115]. Additionally, pro-inflammatory Th17 cells play a vital role in the clearance of extracellular bacterial and fungal infections by producing IL-17A, IL17F, and IL-22. Meanwhile, CCR6 and CCR4 have been proven to identify Th17 cells [116]. According to the different expression patterns of CCR6 and CCR4, Th1 could be identified as CCR6⁻CCR4⁻, while Th2 as CCR6⁻CCR4⁺. To further recognize Tregs from the peripheral blood, low expression of CD127 combined with high expression of CD25 is used to identify Tregs from the Th cells population [117, 118]. Subsequently, Tregs are subdivided into memory Tregs and naïve Tregs according to the expression of CD45RO and CD194 [117]. Activated Tregs are recognized with the positive expression of CCR4 and HLA-DR [117].

1.3.3 B Lymphocytes

CD19, as a co-receptor for the B cell antigen receptor (BCR) signaling pathway, is exclusively expressed on B lymphocytes. Evidence pointed that CD19 is broadly expressed from the early stage of pre-B cells until plasma cell differentiation [119, 120]. In terms of the negative expression of CD3 on non-T cells, B lymphocytes are recognized with the combinational markers of CD3 and CD19 from the leukocytes population. According to the lineage development of B cells, hematopoietic precursor cells (HSC) in the bone marrow differentiate into pro-B, pre-B, and immature B cells in the sequential order via stepwise rearrangement of variable region-encoding gene segments [121]. In terms of the negative expression of CD19 on pro-B cells, circulating pre-B cells could be identified from B lymphocytes with the phenotype of CD10⁺IgM⁻CD24^{hi}CD38^{hi}CD20⁺ [122, 123]. Expressing the prototypic form of BCR, the immature B cell is the first representative of the B-cell lineage to counter against an antigen in a clonotypically restricted manner [124]. After exiting from bone marrow, immature B cells are termed transitional B cells in the peripheral blood [125]. Depending on the interactions between BCR and ligands, transitional B cells will go through a series of positive and negative selections to eventually become mature naïve

B cells [126]. Transitional B cells are commonly characterized by CD24^{hi}CD38^{hi}CD10⁺ phenotype combined with the negative expression of CD27 acting as the memory B cell marker [123]. Furthermore, in T-dependent immune responses, naive B cells could travel to the germinal centers (GC) of secondary lymphoid organs after antigen activation and then differentiate either into plasmablast or class-switched memory (CSM) B cells [127]. On the other hand, non-class switched memory (NCSM) B cells, also known as IgM-only memory B cells, are derived from naïve B cells in the T-cell independent mechanism. In contrast to CSM-B cells expressing multiple types of immunoglobulin, NCSM-B cells represent the first-line defense against foreign pathogens [128]. Besides, both memory B cells carry somatic mutations of their V(D)J rearrangements [128]. According to IgD expression, CD27⁺ memory B cells have been subcategorized as IgD⁺ NCSM-B cells and IgD⁻ CSM-B cells [98]. Acted as the immediate precursor of plasma cells, plasmablast cells have the capability to proliferate and travel to bone marrow parenchyma for long-term survival. According to the guideline for using flow cytometry, plasmablast cells are recognized as CD27⁺CD20^{low/-}CD38^{hi} phenotype [98]. In addition, although the immune suppressive function of Bregs has been widely recognized, there is no unified consensus regarding their phenotype so far [129]. Multiple Bregs subsets of mice have been reported, such as transitional 2 marginal-zone precursors (T2-MZP) cells, B10 cells, and plasma cells. Likewise, in humans, both CD24^{hi}CD27⁺ (B10) cells and CD24^{hi}CD38^{hi} (Immature) cells of B lymphocytes have been identified as the Bregs [129]. Therefore, nine subsets of B lymphocytes are identified from peripheral blood samples.

1.4 Hypothesis and Specific Aims

In terms of the promising future of immunotherapy, it is imperative to decipher the clinical significance of immune subsets in CRC patients. Most publications regarding the systemic immune status of patients with colorectal carcinoma focus on certain cell subtypes and do not consider investigating most blood cell subsets simultaneously.

Meanwhile, there are lacking clinical studies exploring the difference of multiple subsets of T lymphocytes, early-stage MDSCs, monocytes subsets, DCs, neutrophils, CD69⁺ NK, and CD69⁺ NKT cells between CRC patients and healthy controls.

The general hypothesis of this dissertation was that CRC patients have a more pronounced systemic immune suppression than healthy controls. The specific aims were :

- 1) To investigate the difference of circulating immune subsets between CRC subjects and healthy controls.
- 2) To construct the diagnostic model based on the circulating immune cells to discriminate between CRC individuals and healthy controls.
- 3) To explore the underlying molecular mechanism associated with the differential immune subsets in CRC patients.
- 4) To examine the difference of circulating immune subsets between right-sided CRC patients and left-sided ones.

2. Material and Methods

2.1 Materials

2.1.1 Devices

BD LSRFortessa Cell Analyzer	BD Biosciences, USA
Benchtop Centrifuge Rotina 380R	Hettich, Germany
Milli-QR Ultrapure and Pure Lab Water Purification System	Merck, Germany
Single-channel Micropipette Transferpette S	BRAND, Germany
Repetitive Pipettes HandyStep S	BRAND, Germany
Pipette Controllers Accu-jet S	BRAND, Germany
Laboratory Refrigerator LABO 340 Ultimate	Kirsch, Germany
Nalgene Unwire Polypropylene Test Tube Racks	Thermo Fisher Scientific, USA
Vortex Mixer	Scientific industries, Inc., USA
Beakers	DURAN, Germany
Laboratory Bottles	DURAN, Germany

2.1.2 Consumables

Pipette Tips	BRAND, Germany
Filter Tips	BRAND, Germany
Adapter for PD-Tips II	BRAND, Germany
5ml Polystyrene Round-Bottom Tubes	Corning, USA
7.5ml Sterile Heparin Vacutainers	Sarstedt, Germany
Nunc TM Serological Pipettes	Thermo Fisher Scientific, USA
5ml Eppendorf Combitips Plus Pipet Tips	Eppendorf, Germany
50 ml Dispenser-Tips PD-Tips II	BRAND, Germany

2.1.3 Chemicals and Antibodies

Bovine Serum Albumin (BSA), Fraction V	Biomol GmbH, Germany
Sodium Azide	Merck KGaA, Germany
Potassium Dihydrogen Phosphate	Carl Roth, Germany
Potassium Chloride	Merck KGaA, Germany
Sodium Chloride	Merck KGaA, Germany
Di-Sodium Hydrogen Phosphate Dihydrate	Merck KGaA, Germany

Huamn BD Fc Block™	BD Biosciences, USA
Anti-CD45	BD Biosciences, USA
Anti-CD4	BD Biosciences, USA
Anti-CD3	BioLegend, USA
Anti-CD197	BD Biosciences, USA
Anti-CD194	BD Biosciences, USA
Anti-CD38	BD Biosciences, USA
Anti-CD25	BD Biosciences, USA
Anti-CD196	BD Biosciences, USA
Anti-CD127	BD Biosciences, USA
Anti-CD45RO	BD Biosciences, USA
Anti-HLA-DR	BD Biosciences, USA
Anti-CD8	BD Biosciences, USA
Anti-IgM	BD Biosciences, USA
Anti-CD27	BD Biosciences, USA
Anti-CD19	BD Biosciences, USA
Anti-CD10	BD Biosciences, USA
Anti-CD24	BD Biosciences, USA
Anti-IgD	BD Biosciences, USA
Anti-CD20	BD Biosciences, USA
Anti-CD69	BD Biosciences, USA
Anti-CD14	BD Biosciences, USA
Anti-CD33	BD Biosciences, USA
Anti-CD16	BD Biosciences, USA
Anti-CD11c	BD Biosciences, USA
Anti-CD15	BD Biosciences, USA
Anti-CD11b	BD Biosciences, USA
Anti-CD66b	BD Biosciences, USA
Anti-CD56	BD Biosciences, USA
2.1.4 Buffers and Solutions	
BD Anti-Mouse Ig, κ/Negative Control	BD Biosciences, USA
Compensation Particles Set	
Cytometer Setup & Tracking Beads kit	BD Biosciences, USA

1 × PBS Solution	10L Millipore water 80g NaCl 14.4g Na ₂ HPO ₄ * 2H ₂ O 1.92g KH ₂ PO ₄ 2.0g KCl
BD FACST TM Lysing Solution (10×)	BD Biosciences, USA
eBioscience TM Permeabilization Buffer (10×)	Thermo Fisher Scientific, USA
eBioscience TM Intracellular Fixation buffer	Thermo Fisher Scientific, USA
1× Lysing Solution	50ml Lysing Solution (10×) 450ml Millipore water
1× Permeabilization buffer	20ml Permeabilization buffer (10×) 180ml Millipore Water
Flow Cytometry Buffer	1L 1 × PBS Solution 2ml Sodium Azide 5g Bovine Serum Albumin
BD FACSRinse	BD Biosciences, USA
BD FACSClean	BD Biosciences, USA
Millipore Water	Merck, Germany
2.1.5 Software	
BD FACSDiva TM	BD Biosciences, USA
FlowJo TM v10.4	BD Biosciences, USA
R version 4.1.0	Open Source Software, Austria
Microsoft Excel	Microsoft, USA
Adobe Illustrator CC 2019	Adobe Inc., USA

2.2 Methods

2.2.1 Study Population

This study included 12 patients with CRC who were diagnosed according to the 2019 World Health Organization classification and underwent curative surgical resection at the Ludwig-Maximilians-University Munich (LMU) hospital (Munich, Germany) between September 2020 and September 2021. Blood samples were collected within 4 hours prior to surgery for these patients. The inclusion criteria were surgical R0 resection, Tumor Node Metastasis (TNM) stage 0-III, histologically confirmed colorectal carcinoma, and the provision of written informed consent. The exclusion criteria were a history of chemoradiotherapy treatment, concomitant immune-associated disorders and other carcinomas, and the use of immunomodulating drugs or oral steroids within the past three years. In addition, the pre-operative clinical data of CRC patients were also collected. Peripheral blood samples from 11 healthy donors were obtained from LMU hospital after obtaining written consent, and these samples were considered healthy controls. This study was approved by the local review board.

2.2.2 Flow Cytometry Antibody Staining

Venous blood samples were collected from each recruited subject using sterile heparin vacutainers. Moreover, all peripheral blood (PB) specimens were directly measured within 12 hours after harvesting. Immunophenotyping of circulating B lymphocytes, T lymphocytes, and innate immune subsets from whole blood samples was detected using multiparametric flow cytometry with fluorescent-labeled mouse monoclonal antibodies (mAbs) (Table 1). Thus, three multicolor flow cytometry panels were designed to identify these three cell populations, respectively (Table 1). Briefly, 0.2 ml anticoagulated-PB (around 1×10^6 cells) was blocked with 2.5ul Fc block (Fc1.3216, BD Biosciences) for 10 min in the dark, then incubated with extracellular staining antibodies in the dark for 15 min, including all mAbs of flow panel 2 and 3, and most mAbs of panel 1 (except for CD20 antibody). Then 2ml lysing solution (BD Biosciences) was used to lyse red blood cells following direct

immunofluorescence staining of peripheral blood cells. Due to the freshly PB samples' entity, there is no need to apply viability dyes to exclude dead cells from the analysis. Due to the intracellular staining of CD20 in flow panel 1, there were two distinct methods to treat the cells of three panels. As for flow panels 2 and 3, the cells were washed once in flow cytometry buffer consisting of PBS/0.5% BSA (Biomol GmbH, Hamburg, Germany)/0.2% sodium azide (Merck KGaA, Darmstadt, Germany). As for flow panel 1, permeabilization buffer (eBioscience) was used to treat the cells two times following the 20 min fixation step using the intracellular fixation buffer (eBioscience) in the dark according to the manufacturer's instruction. Next, the CD20 antibody of panel 1 was incubated with the cells for 30 min in the dark. Then the permeabilization buffer and flow cytometry buffer were sequentially used to wash the cells of panel 1. Lastly, all processed cells were kept in flow cytometry buffer before measurement. All procedures were performed at room temperature.

Table 1 Flow cytometry panels applied to identify peripheral blood B-, T-, and Innate immune subsets

Flow panel 1				
B lymphocytes subsets				
Marker	Fluorochrome	Clone	Catalog number	Source
IgM	BV510	G20-127	563113	BD Biosciences
CD38	BV605	HB7	562665	BD Biosciences
CD45	BV650	HI30	563717	BD Biosciences
CD27	BV786	L128	563327	BD Biosciences
CD19	FITC	HIB19	555412	BD Biosciences
CD3	PerCP Cy5.5	UCHT1	300430	BioLegend
CD10	PE	HI10a	555375	BD Biosciences
CD24	PE-CF594	ML5	562405	BD Biosciences
IgD	PE-Cy7	IA6-2	561314	BD Biosciences
CD20*	APC-H7	H1	561172	BD Biosciences
Flow panel 2				
T lymphocytes subsets				
CD4	BUV395	SK3	563550	BD Biosciences
CD197	BV421	150503	562555	BD Biosciences
CD194	BV510	1G1	563066	BD Biosciences
CD38	BV605	HB7	562665	BD Biosciences
CD45	BV650	HI30	563717	BD Biosciences
CD25	BB515	2A3	564467	BD Biosciences
CD3	PerCP Cy5.5	UCHT1	300430	BioLegend
CD196	PE	11A9	559562	BD Biosciences
CD127	PE-CF594	HIL-7R-M21	562397	BD Biosciences
CD45RO	PE-Cy7	UCHL1	560608	BD Biosciences
HLA-DR	APC	G46-6	559866	BD Biosciences
CD8	APC-H7	SK1	560179	BD Biosciences
Flow panel 3				
Innate Immune subsets				
CD69	BUV395	FN50	564364	BD Biosciences

HLA-DR	BV421	G46-6	562804	BD Biosciences
CD14	BV510	MφP9	563079	BD Biosciences
CD45	BV650	HI30	563717	BD Biosciences
CD33	BV786	WM53	740974	BD Biosciences
CD16	FITC	B73.1	561308	BD Biosciences
CD3	PerCP Cy5.5	UCHT1	300430	BioLegend
CD11c	PE	B-ly6	555392	BD Biosciences
CD15	PE-CF594	W6D3	562372	BD Biosciences
CD11b	PE-Cy7	ICRF44	557743	BD Biosciences
CD66b	AF647	G10F5	561645	BD Biosciences
CD56	APC-R700	NCAM16.2	565139	BD Biosciences
CD8	APC-H7	SK1	560179	BD Biosciences

*, represent the intracellular staining antibody.

Abbreviations: AF, Alexa fluor; APC, allophycocyanin; BV, brilliant violet; FITC, fluorescein isothiocyanate; PE, phycoerythrin; PE-Cy7, phycoerythrin-cyanine7; PerCP, peridinin chlorophyll protein complex; V500, violet500. BUUV, brilliant ultraviolet.

2.2.3 Flow Cytometry Data Analysis

At least 1×10^5 events per sample were acquired promptly after staining by 18-color flow cytometry using the LSR Fortessa (BD Biosciences) with BD FACSDiva™ software version 8.0.1 (BD Biosciences). For each experiment, the optimal cytometer values were maintained by this software. The flow cytometer setup and performance tracking were conducted using cytometer setup and tracking beads (BD Biosciences). According to the manufacturer's protocol, the compensation control was carried out with the CompBeads set (BD Biosciences). Positive staining cells were identified using fluorescence minus one (FMO) control when necessary [130]. FMO controls were used for IgM, CD38, CD27, CD10, CD24, IgD, and CD20 in flow panel 1. Eight FMO controls were set for flow panel 2, including CD197, CD194, CD38, CD25, CD196, CD127, CD45RO, and HLA-DR. Furthermore, FMO controls were separately prepared for CD69, HLA-DR, CD14, CD33, CD16, CD11c, CD15, CD11b, CD66b, and CD56 in flow panel 3. The immunophenotyping of circulating B

lymphocytes, T lymphocytes, and innate immune subsets was listed in Table 2. In addition, the sequential gating strategy for each panel was depicted in Fig. 1, 2, and 3, respectively. The expression levels of immune markers on circulating B cells, T cells, and innate immune subsets were evaluated by the percentage of targeted cells or the median fluorescence intensity (MFI) or the absolute number of immune cells. FlowJo software version 10.4 (Tree Star) was applied to analyze the datasets, and the data were displayed in dot plots.

Table 2 Immunophenotyping of B lymphocytes, T lymphocytes, and Innate immune subsets

Immune cells	Immunophenotyping
B lymphocytes subsets	
B lymphocytes	CD45 ⁺ CD3 ⁻ CD19 ⁺
Pre-B cells	CD45 ⁺ CD3 ⁻ CD19 ⁺ CD10 ⁺ IgM ⁻ CD24 ^{high} CD38 ^{high} CD20 ⁺
Transitional B cells	CD45 ⁺ CD3 ⁻ CD19 ⁺ CD24 ^{high} CD38 ^{high} CD10 ⁺ CD27 ⁻
Breg-Immature cells	CD45 ⁺ CD3 ⁻ CD19 ⁺ CD24 ^{high} CD38 ^{high} CD27 ⁻
Breg-B10 cells	CD45 ⁺ CD3 ⁻ CD19 ⁺ CD24 ^{high} CD27 ⁺
Naïve B cells	CD45 ⁺ CD3 ⁻ CD19 ⁺ CD27 ⁺ IgD ⁺
Non-Classic switched memory B cells	CD45 ⁺ CD3 ⁻ CD19 ⁺ CD27 ⁺ IgD ⁺
Class switched memory B cells	CD45 ⁺ CD3 ⁻ CD19 ⁺ CD27 ⁺ IgD ⁻
Plasmablasts	CD45 ⁺ CD3 ⁻ CD19 ⁺ CD27 ⁺ CD20 ^{low/-} CD38 ^{high}
T lymphocytes subsets	
T lymphocytes	CD45 ⁺ CD3 ⁺
CD8T cells	CD45 ⁺ CD3 ⁺ CD8 ⁺
Activated CD8T cells	CD45 ⁺ CD3 ⁺ CD8 ⁺ CD38 ⁺ HLA ⁻ DR ⁺
Effector CD8T cells	CD45 ⁺ CD3 ⁺ CD8 ⁺ CD197 ⁻ CD45RO ⁻
Effector memory CD8T cells	CD45 ⁺ CD3 ⁺ CD8 ⁺ CD197 ⁻ CD45RO ⁺

Naïve CD8T cells	CD45 ⁺ CD3 ⁺ CD8 ⁺ CD197 ⁺ CD45RO ⁻
Central memory CD8T cells	CD45 ⁺ CD3 ⁺ CD8 ⁺ CD197 ⁺ CD45RO ⁺
Th cells	CD45 ⁺ CD3 ⁺ CD4 ⁺
Activated Th cells	CD45 ⁺ CD3 ⁺ CD4 ⁺ CD38 ⁺ HLA-DR ⁺
Effector Th cells	CD45 ⁺ CD3 ⁺ CD4 ⁺ CD197 ⁻ CD45RO ⁻
Effector memory Th cells	CD45 ⁺ CD3 ⁺ CD4 ⁺ CD197 ⁻ CD45RO ⁺
Naïve Th cells	CD45 ⁺ CD3 ⁺ CD4 ⁺ CD197 ⁺ CD45RO ⁻
Central memory Th cells	CD45 ⁺ CD3 ⁺ CD4 ⁺ CD197 ⁺ CD45RO ⁺
Th17 cells	CD45 ⁺ CD3 ⁺ CD4 ⁺ CD194 ⁺ CD196 ⁺
Th1 cells	CD45 ⁺ CD3 ⁺ CD4 ⁺ CD194 ⁻ CD196 ⁻
Th2 cells	CD45 ⁺ CD3 ⁺ CD4 ⁺ CD194 ⁺ CD196 ⁻
Treg cells	CD45 ⁺ CD3 ⁺ CD4 ⁺ CD25 ^{high} CD127 ^{low}
Memory Treg cells	CD45 ⁺ CD3 ⁺ CD4 ⁺ CD25 ^{high} CD127 ^{low} CD194 ⁺ CD45RO ⁺
Naive Treg cells	CD45 ⁺ CD3 ⁺ CD4 ⁺ CD25 ^{high} CD127 ^{low} CD194 ⁺ CD45RO ⁻
Activated Treg cells	CD45 ⁺ CD3 ⁺ CD4 ⁺ CD25 ^{high} CD127 ^{low} CD194 ⁺ HLA-DR ⁺
Innate immune subsets	
Neutrophils	CD45 ⁺ CD14 ⁻ CD66b ⁺ CD15 ⁺ CD11b ⁺ CD16 ^{+/-}
Classical Monocytes	CD45 ⁺ CD66b ⁻ HLA-DR ⁺ CD14 ^{high} CD16 ⁻
Non-Classical Monocytes	CD45 ⁺ CD66b ⁻ HLA-DR ^{low/+} CD14 ^{low/+} CD16 ⁺
Intermediate Monocytes	CD45 ⁺ CD66b ⁻ HLA-DR ^{high} CD14 ^{high} CD16 ⁺
Dendritic cells	CD45 ⁺ CD66b ⁻ HLA-DR ⁺ CD14 ^{-/low} CD16 ⁻
MDSCs	CD45 ⁺ CD33 ⁺ HLA-DR ^{-/low} CD11b ⁺
PMN-MDSCs	CD45 ⁺ CD33 ⁺ HLA-DR ^{-/low} CD11b ⁺ CD14 ⁻ CD15 ⁺
M-MDSCs	CD45 ⁺ CD33 ⁺ HLA-DR ^{-/low} CD11b ⁺ CD14 ⁺ CD15 ⁻
Early stage-MDSCs	CD45 ⁺ CD33 ⁺ HLA-DR ^{-/low} CD11b ⁺ CD14 ⁻ CD15 ⁻ CD56 ⁻
NK cells	CD45 ⁺ CD14 ⁻ CD3 ⁻ CD56 ⁺
CD56 ^{bright} NK cells	CD45 ⁺ CD14 ⁻ CD3 ⁻ CD56 ^{high}
CD8 ⁺ CD56 ^{bright} NK cells	CD45 ⁺ CD14 ⁻ CD3 ⁻ CD56 ^{high} CD8 ⁺

CD16 ⁺ CD56 ^{bright} NK cells	CD45 ⁺ CD14 ⁻ CD3 ⁻ CD56 ^{high} CD16 ⁺
CD69 ⁺ CD56 ^{bright} NK cells	CD45 ⁺ CD14 ⁻ CD3 ⁻ CD56 ^{high} CD69 ⁺
CD56 ^{dim} NK cells	CD45 ⁺ CD14 ⁻ CD3 ⁻ CD56 ^{+/Low}
CD8 ⁺ CD56 ^{dim} NK cells	CD45 ⁺ CD14 ⁻ CD3 ⁻ CD56 ^{dim} CD8 ⁺
CD16 ⁺ CD56 ^{dim} NK cells	CD45 ⁺ CD14 ⁻ CD3 ⁻ CD56 ^{dim} CD16 ⁺
CD69 ⁺ CD56 ^{dim} NK cells	CD45 ⁺ CD14 ⁻ CD3 ⁻ CD56 ^{dim} CD69 ⁺
NKT cells	CD45 ⁺ CD14 ⁻ CD3 ⁺ CD56 ⁺
CD8 ⁺ NKT cells	CD45 ⁺ CD14 ⁻ CD3 ⁺ CD56 ⁺ CD8 ⁺
CD16 ⁺ NKT cells	CD45 ⁺ CD14 ⁻ CD3 ⁺ CD56 ⁺ CD16 ⁺
CD69 ⁺ NKT cells	CD45 ⁺ CD14 ⁻ CD3 ⁺ CD56 ⁺ CD69 ⁺

Abbreviations: Breg, regulatory B; Th, T helper; Treg, regulatory T; MDSCs, myeloid-derived suppressor cells; PMN-MDSCs, polymorphonuclear MDSCs; M-MDSCs, Monocytic MDSCs; NK, Natural killer; NKT, Natural killer T.

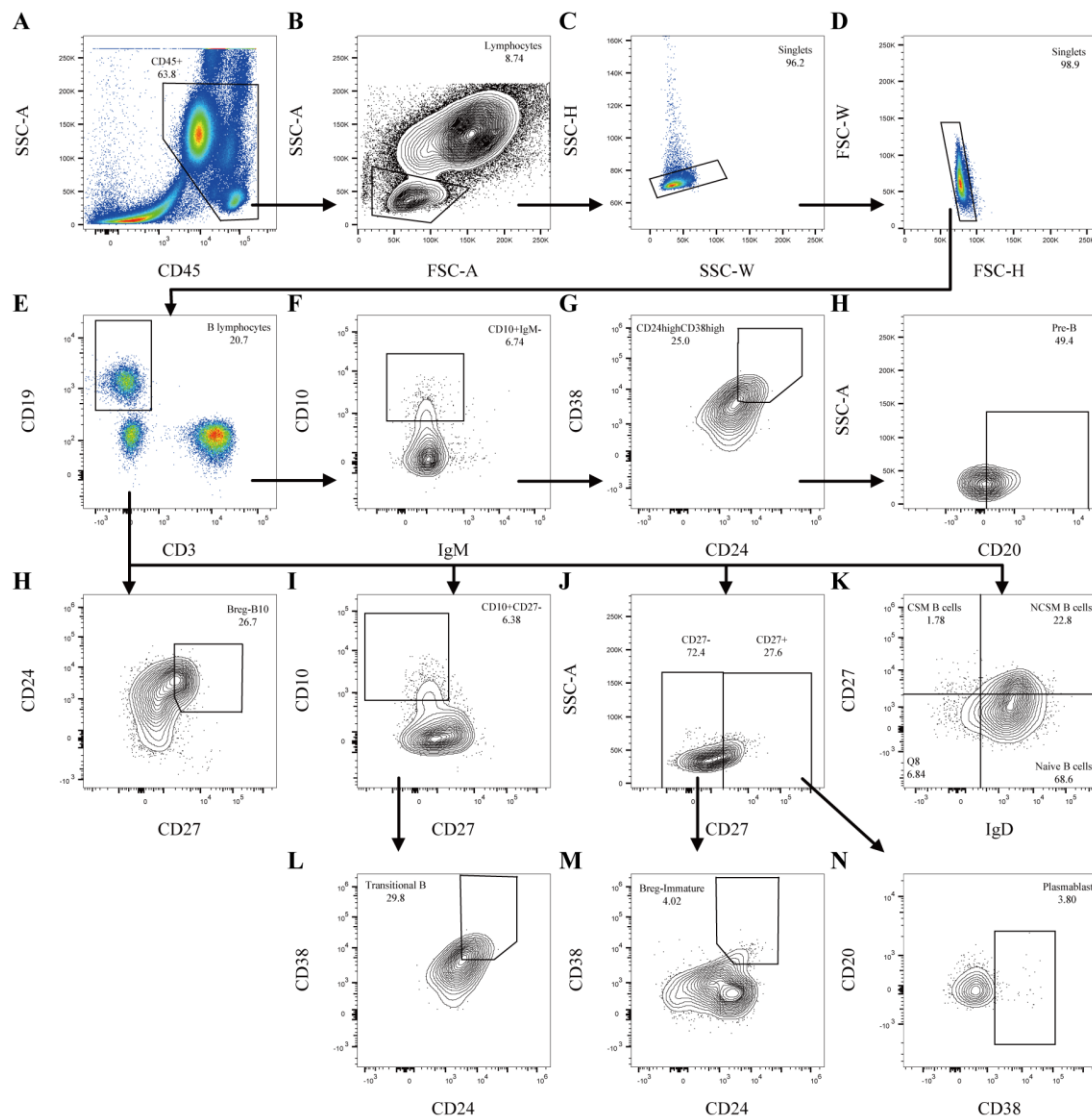


Figure 1: Flow cytometry gating strategy applied for the identification of circulating B lymphocyte subsets

The standardized gating strategy was used for flow cytometry panel 1. A) Leukocytes (excluding debris with SSC^{low}/FSC^{low}). B) Lymphocytes (excluding monocytes and granulocytes). C, D) Single lymphocytes (excluding doublets). E) B lymphocytes ($CD3^{-}CD19^{+}$ cells). F-H) Pre-B cells. H) Breg (regulatory B)-B10 cells ($CD24^{high}CD27^{+}$). I, L) Transitional B cells ($CD10^{+}CD27^{-}CD24^{high}CD38^{high}$). J, M) Breg-immature cells ($CD27^{-}CD24^{high}CD38^{high}$). J, N) Plasmablast ($CD27^{+}CD20^{low/-}CD38^{high}$). K) CSM (Class-switched memory) B cells, NCSM (Non-class switched memory) B cells, and naive B cells.

Abbreviation: SSC, side scatter; FSC, forward scatter.

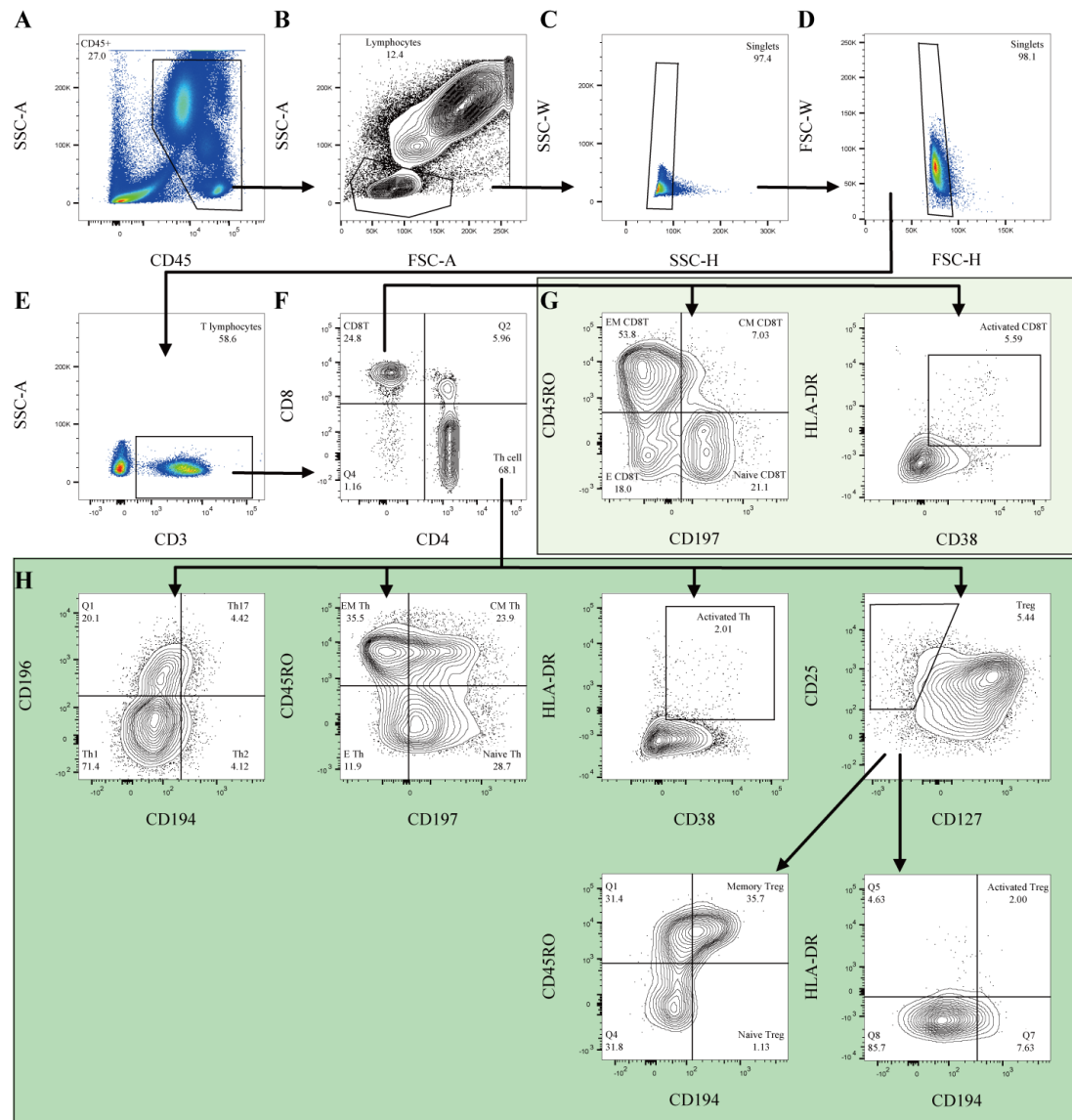


Figure 2: Flow cytometry gating strategy applied for the identification of circulating T lymphocyte subsets

The standardized gating strategy was used for flow cytometry panel 2. A) Leukocytes (excluding debris with SSC^{low}/FSC^{low}). B) Lymphocytes (excluding monocytes and granulocytes). C, D) Single lymphocytes (excluding doublets). E) T lymphocytes ($CD3^+$ cells). F) Th (T helper) cells ($CD4^+$ cells) and $CD8T$ ($CD8^+T$) cells. G) $CD8T$ subsets, including EM (effector memory) $CD8T$ cells, CM (central memory) $CD8T$ cells, Naïve $CD8T$ cells, E (effector) $CD8T$ cells, and activated $CD8T$ cells. H) Th cells subsets, including Th1, Th2, Th17, EM (effector memory) Th cells, CM (central memory) Th cells, Naïve Th cells, E (effector) Th cells, activated Th cells, Tregs (regulatory T cells), memory Tregs, naïve Tregs, and activated Tregs. Abbreviation: SSC, side scatter; FSC, forward scatter.

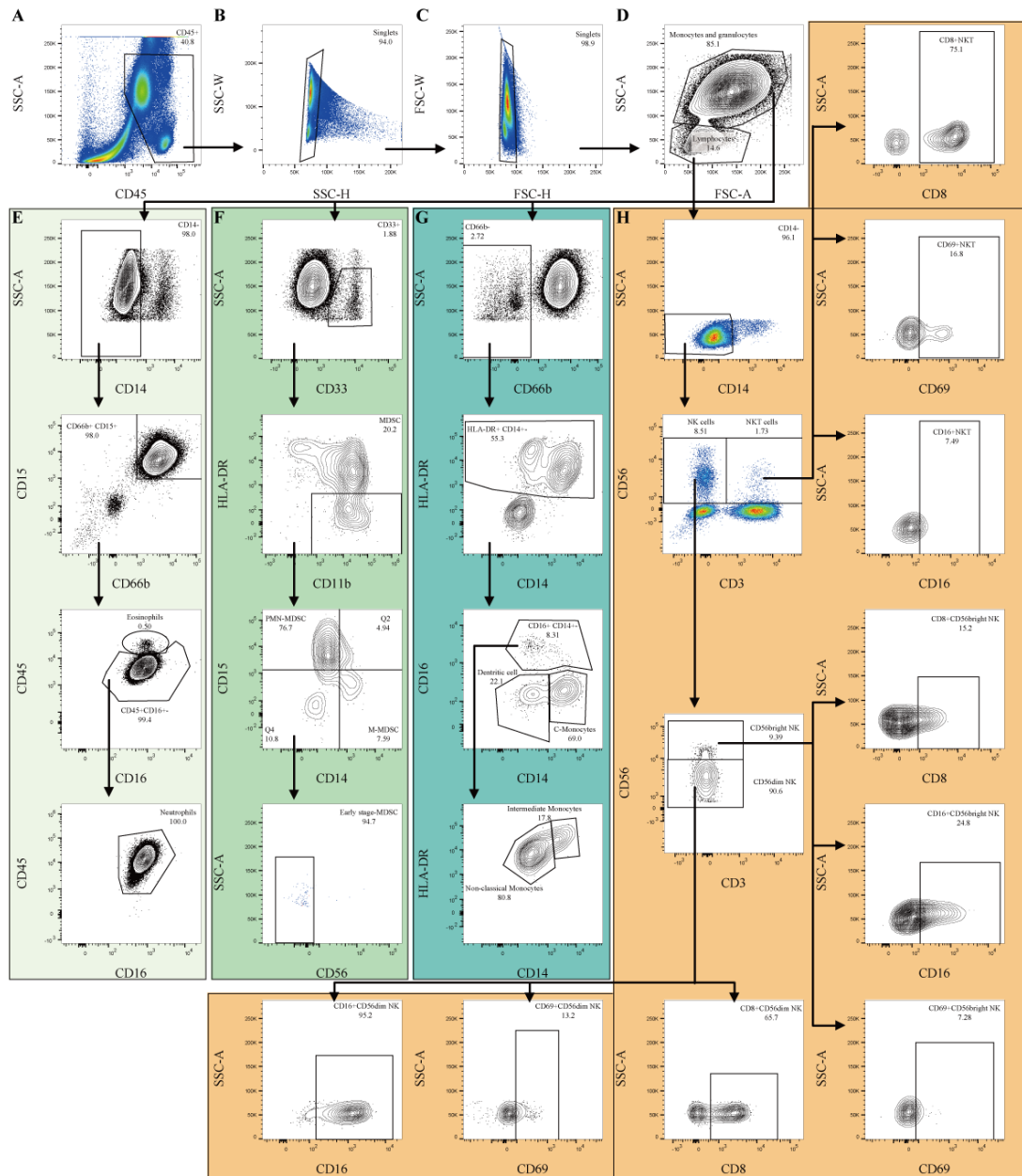


Figure 3: Flow cytometry gating strategy applied for the identification of circulating innate immune cell subsets

The standardized gating strategy was used for flow cytometry panel 3. A) Leukocytes (excluding debris with SSC^{low}/FSC^{low}). B, C) Single leukocytes (excluding doublets). D) Lymphocytes and non-lymphocytes. E) Neutrophils. F) MDSC (Myeloid-derived suppressor cell) and its subsets, including M-MDSC (monocytic MDSC), PMN-MDSC (polymorphonuclear MDSC), and early-stage MDSC. G) Dendritic cells, C-Monocytes (classical monocytes), intermediate monocytes, and non-classical monocytes. H) NK (natural killer) and NKT (natural killer T) cells population, including $CD8^{+}CD56^{dim}$ cells, $CD16^{+}CD56^{dim}$ cells, $CD69^{+}CD56^{dim}$ cells, $CD8^{+}CD56^{bright}$ cells, $CD16^{+}CD56^{bright}$ cells, $CD69^{+}CD56^{bright}$ cells, $CD8^{+}NKT$ cells,

CD16⁺NKT cells, and CD69⁺NKT cells.

Abbreviation: SSC, side scatter; FSC, forward scatter.

2.2.4 Construction of Diagnostic Model

The univariable logistic regression was conducted to evaluate the predictive ability of each immune subset on two cohorts. In order to obtain immune subsets that displayed relatively higher accuracy with the prediction, we kept those immune subsets with *p*-values less than 0.05. The support vector machine (SVM) learning model was performed to identify the optimal parameters from the above immune subsets to discriminate CRC from healthy controls. To ensure the stability and reliability of our prediction method, tenfold cross-validation was applied by the SVM model. The best parameters were identified from maximum cross-validation results. The above best parameters were fitted into a multivariable logistic regression analysis to construct the diagnostic model. Each parameter would be assigned with a logistic regression coefficient, and an immune score was generated using the following formula:

$$\mathbf{Immune\ Score} = \sum_{n=1}^{\mathbf{Num}} (\mathbf{Composition}_n * \mathbf{LC}_n)$$

Where Num refers to the number of immune subset, $\mathbf{Composition}_n$ represents the percentage of immune subset_n, and \mathbf{LC}_n is the logistic coefficient of immune subset_n.

Furthermore, a nomogram was constructed to visualize this diagnostic model in our cohort. The calibration curve and the Hosmer-Lemeshow test were performed to evaluate the goodness-of-fit of the nomogram model. Decision curve analysis (DCA) was used to assess the model's reliability by calculating the clinical net benefit for patients at each threshold probability. The receiver operating characteristic (ROC) curve was applied to evaluate the discrimination performance of the nomogram.

Logistic regression analysis was performed using the *stats* R package [131]. SVM model analysis was conducted using the *e1071* R package [132]. *pROC* and *ggplot2* R package were used to draw the diagnostic ROC curves [133, 134].

2.2.5 Gene Expression Profile Collection and Processing

Gene Expression Omnibus (GEO) database was thoroughly searched to find eligible GEO datasets with the following searching strategy (“colon” or “colorectal” or “rectal”) and (“cancer*” or “neoplas*” or “dysplasia”) and (“homo sapiens”) and (“gse”). The inclusion criteria of the datasets were listed in Fig. 4. A total of two datasets (GSE164191 and GSE46703) representing different independent studies of CRC were enrolled, of which GSE164191 contained 59 CRC and 62 normal samples, and GSE46703 included 14 CRC samples without prior treatment. Moreover, GSE164191 and GSE46703 were derived from GPL570 and GPL6884, respectively. *GEOquery* R package was used to download the expression matrixes of the above datasets [135]. The probes were annotated into gene symbols based on the corresponding annotation files. When multiple probes matched one gene, the median was calculated as its expression values. Besides, since GSE164191 and GSE46703 were hybridized into two distinct platforms, the *combat* function of the *sva* R package was applied to integrate two normalized datasets into a meta-cohort to remove batch effects (Fig. 5A, B) [136]. Next, the merging datasets were quantile normalized with the *normalizeBetweenArrays* function of *limma* R package (Fig. 5C, D) [137]. Therefore, the merged GEO datasets were considered the normalized expression profiles of blood samples for CRC and healthy controls.

Due to the potential interaction between colorectal tumor and the peripheral blood, the sequencing data of CRC tissue samples was also obtained from public repository. The Cancer Genome Atlas (TCGA) projects deposited the largest tissue expression matrixes of CRC on the single dataset level. Then gene expression profiles of 568 CRC patients and 51 non-cancerous samples were downloaded from TCGA through the GDC data portal.

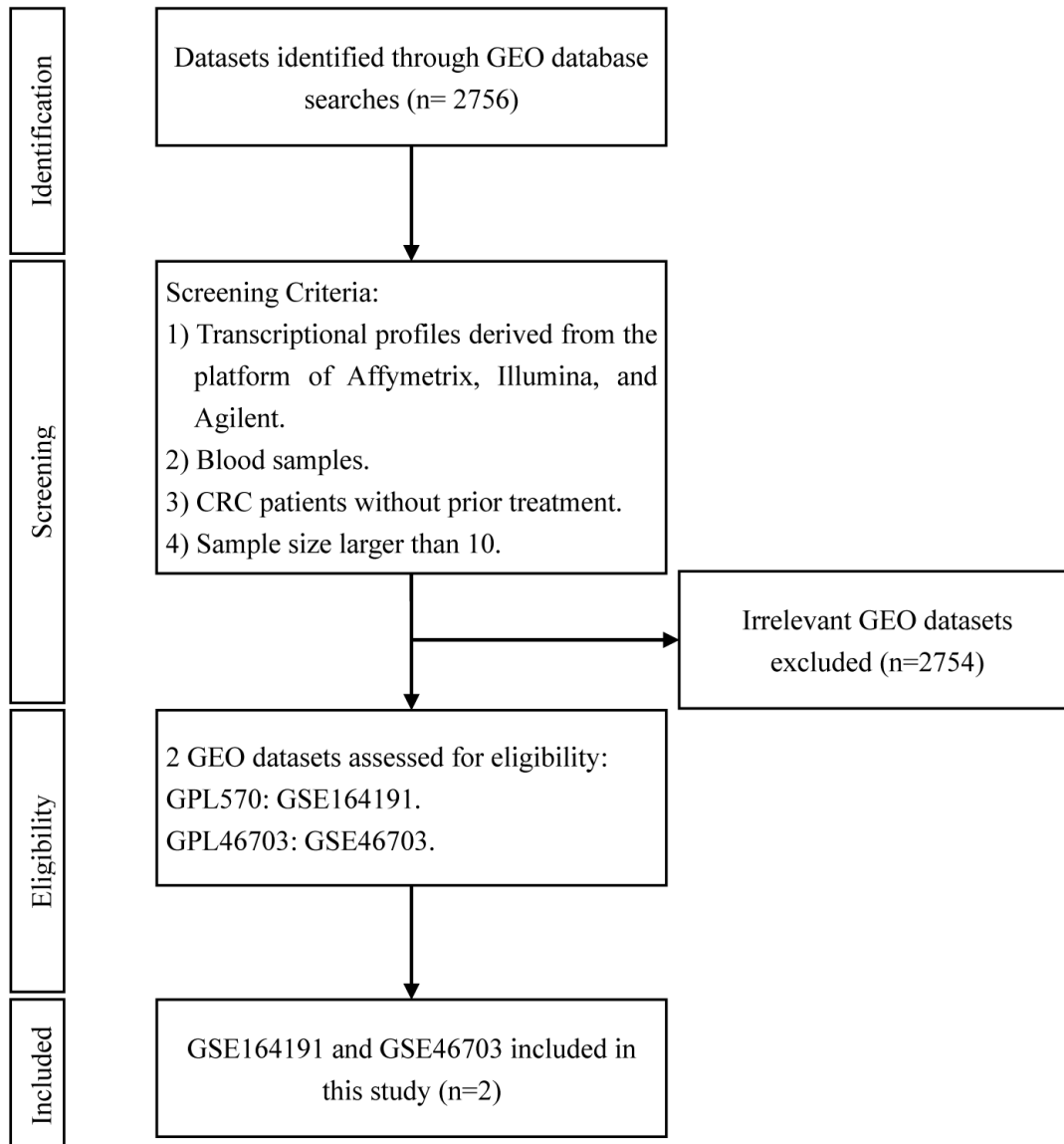


Figure 4: Flow diagram of identifying and selecting eligible GEO datasets

Abbreviation: GEO, Gene Expression Omnibus; CRC, colorectal cancer.

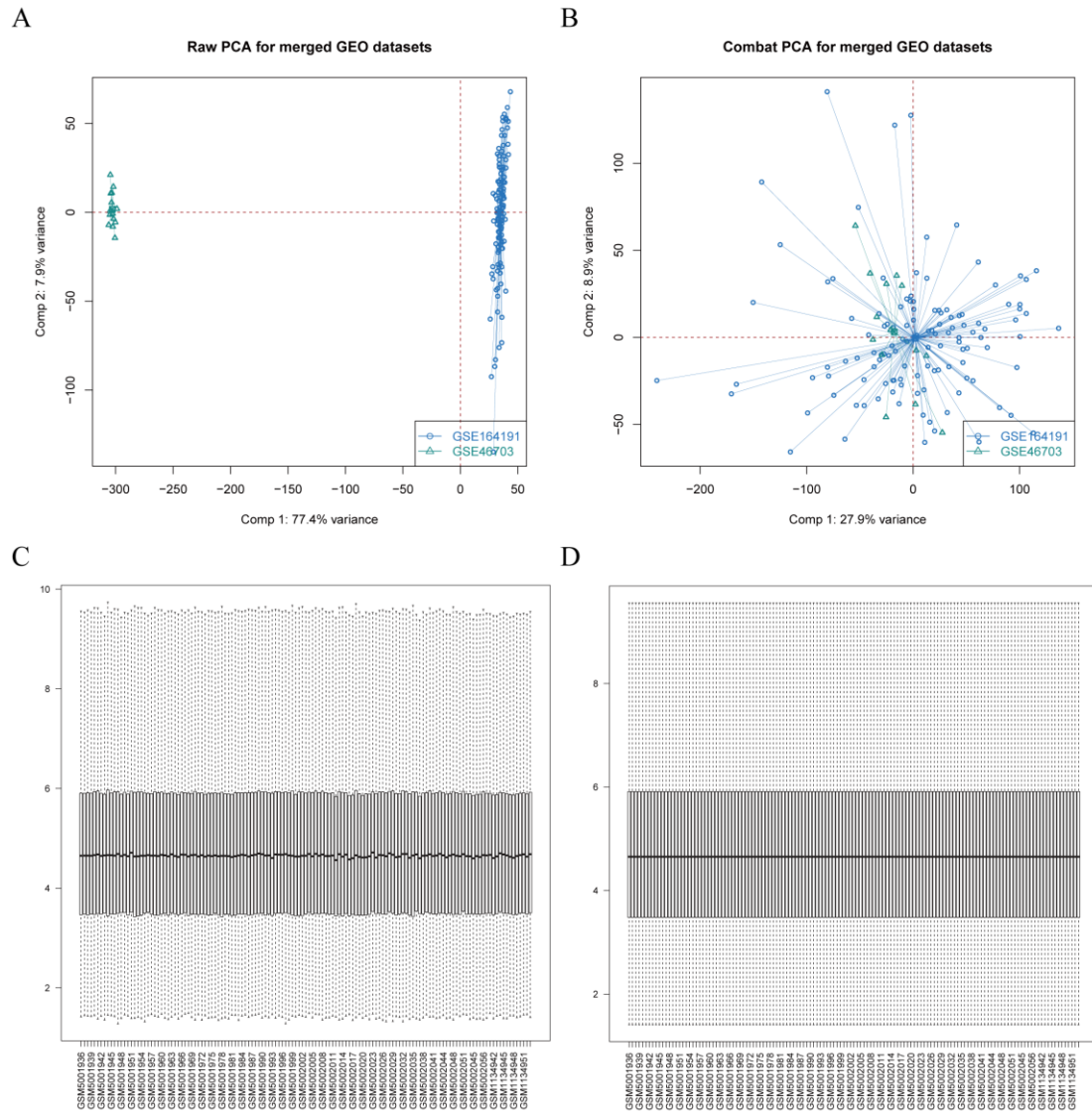


Figure 5: The pre-processing of merged GEO datasets

A) PCA graph of the merged GEO datasets without the removal of batch effects. B) PCA graph of the merged GEO datasets with the removal of batch effects. C) The boxplot of merged GEO datasets without quantile normalization. D) The boxplot of merged GEO datasets with quantile normalization.

Abbreviation: GEO, Gene Expression Omnibus. PCA, principal component analysis.

2.2.6 xCell Algorithm

The *xCell* R package was used to deconvolute peripheral blood mononuclear cell types based on the merged GEO datasets. By applying a novel gene signature-based method, the xCell algorithm could reliably estimate enrichment of 64 stromal and immune cell types from gene expression data derived from tissue or blood samples, among which 34 cell types are immune subsets [138]. According to the validation results on the extensive in-silico simulations and cytometry immune profiling, xCell was proven to outperform other digital dissection methodologies, including CIBERSORT [138].

2.2.7 Differential Expression Analysis

To identify the differential expression genes (DEGs) in blood and tissue samples between CRC and normal subjects, we performed the differential expression analysis on the merged GEO and TCGA datasets using the *limma* and *DESeq2* R package, respectively [137, 139]. In GEO dataset, any gene with adjusted P values of < 0.05 and $|\log_2(\text{Foldchange})| > 0.25$ was regarded as the DEGs. Owing to the entity of colorectal carcinoma, the DEGs of the TCGA dataset were defined as genes with adjusted P values of < 0.05 and $|\log_2(\text{Foldchange})| > 1$. Furthermore, DEGs consistently changed in the above two datasets were identified as the common DEGs.

2.2.8 Gene Ontology Enrichment Analysis

Gene Ontology (GO) enrichment analysis was performed to determine the potential biological function of identified common DEGs using *ClusterProfiler* R package [140]. GO analysis contained three categories: biological process, molecular function, and cellular components. The cutoff criteria of P values of < 0.05 and the false discovery rate (FDR) < 0.1 was regarded as statistically significant differences for all analyses.

2.2.9 Correlation Analysis

Correlation analysis was performed to explore the association between immune cell compositions and genetic expression and investigate the underlying relationship between immune cell subsets and clinical test parameters using *hmisc* and *corrplot* R

package. The correlation coefficients and corresponding p values were used to select the significantly correlated pairs.

2.2.10 Statistical Analysis

Correlation analysis was performed using the Pearson method. The statistical difference between continuous variables was calculated using the two-sample t-test or the Wilcoxon rank-sum test depending on normal distribution. P -values of multiple testing were corrected using the Benjamini-Hochberg method. Comparisons between categorical variables were conducted by applying Fisher's exact test. All statistical analyses were completed using R software (version 4.1.0). P -value < 0.05 was regarded as statistically significant.

3. Results

3.1 Patients with CRC Exhibiting Systemic Immune Suppression

The study has been conducted as depicted in Fig. 6. Since chemoradiotherapy could affect the systemic immune system, the blood samples were only collected from patients without any neoadjuvant therapy. Table 3 summarizes the clinicopathological characteristics of 12 CRC patients and 11 healthy controls included in the analyses. The detailed data of the immune distributional comparison between these two groups are shown in Table 4.

At first, compared to healthy controls, the proportion of B lymphocytes was significantly ($P = 0.0421$) lower in CRC patients (Fig. 7A, C). There was no distributional difference of two Breg subsets between CRC patients and healthy controls (Fig. 7A). No differences of other B lymphocytes subsets were detected between CRC patients and healthy controls (Fig. 7A).

Secondly, the distribution of seven subsets belonging to the T lymphocyte population was statistically different in the two cohorts (Fig. 7A, C): remarkably lower proportions of circulating T lymphocytes ($P = 0.0184$), and Th cells ($P = 0.0243$) were observed in CRC patients. In contrast, the percentage of activated CD8T ($P = 0.0107$) and activated Th ($P = 0.0107$) cells was significantly higher in CRC patients compared to healthy controls. Furthermore, CRC patients presented with an increased percentage of naïve ($P = 0.0088$) and central memory Th ($P = 0.0088$) cells, but with a decreased proportion of effector Th ($P = 0.0088$) cells compared to healthy controls. In addition, the percentage of Tregs and its subsets was comparable between CRC patients and healthy controls (Fig. 7A).

Thirdly, among four monocytes subsets, only non-classical monocytes were significantly ($P = 0.0125$) lower in CRC patients compared to healthy controls. Meanwhile, there was no difference in the percentage of neutrophils between these two groups (Fig. 7A).

Fourthly, similar percentages of circulating NK and NKT cells were observed in

CRC patients and healthy controls (Fig. 7A). No differences were detected in CD56^{bright} and CD56^{dim} NK cells (% of NK). Although CRC patients have the similar distribution of CD69⁺CD56^{dim} and CD69⁺CD56^{bright} NK cells with healthy controls, the expression level (MFI) of CD69 on these two NK subsets was significantly ($P = 0.0277$) lower in CRC patients than healthy controls (Fig. 8). No differences in other phenotypic markers on NK and NKT cells were observed between CRC patients and healthy controls (Fig. 8).

Lastly, in contrast to healthy controls, CRC patients have also an increased percentage of PMN-MDSC ($P = 0.0107$) population (Fig. 7C). Moreover, a lower percentage of DCs was detected in CRC patients than in healthy controls (Fig. 7C).

Furthermore, we applied the digital dissection method of the xCell algorithm on the merged GEO dataset consisting of 73 CRC patients and 62 healthy controls to estimate the distribution of circulating immune cells. In total, sixty-four subsets, including thirty-four immune subsets, were calculated for CRC patients and healthy controls (Fig. 7B). Although thirteen immune cell subsets showed a significant difference between CRC patients and healthy controls (Fig. 7D), only Th cells cells were consistently changed in the flow cytometry analysis and bioinformatics analysis (Fig. 7C, D).

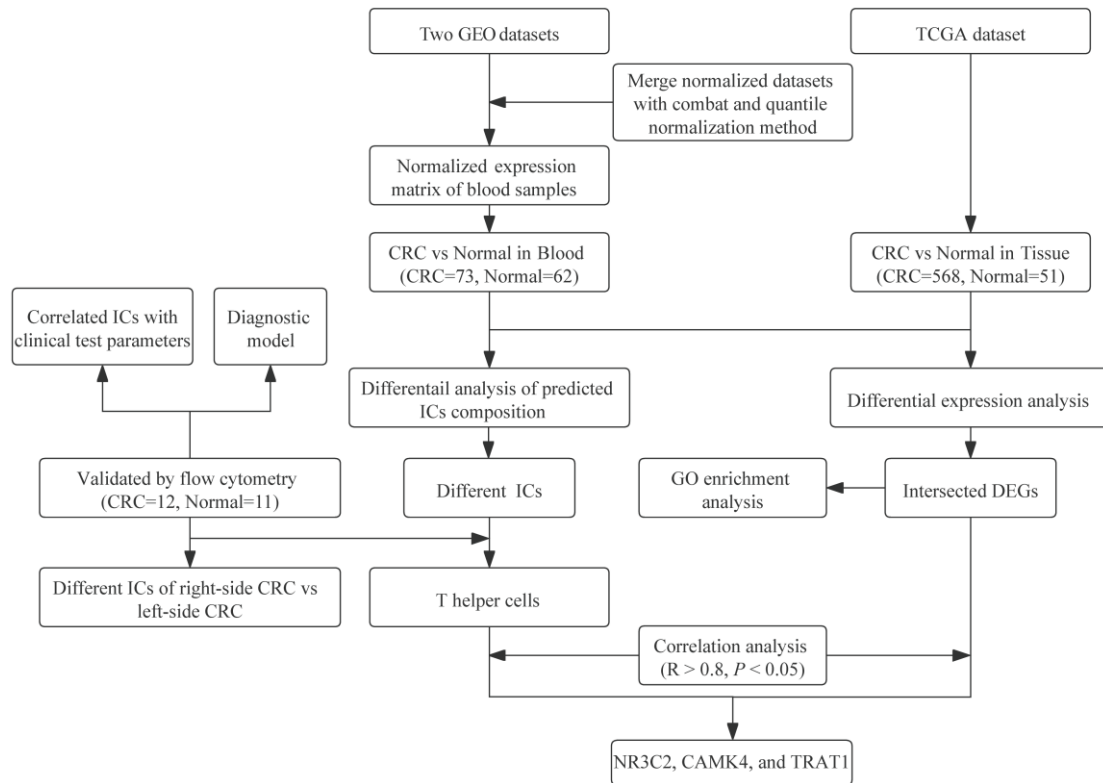


Figure 6: Analysis flow diagram of the study

Abbreviation: GEO, Gene Expression Omnibus; TCGA, the Cancer Genome Atlas; CRC, colorectal cancer; ICs, immune cells; GO, gene ontology; DEGs, differential expression genes.

Table 3 Clinical characteristics of healthy controls and CRC patients

Variables	CRC (n = 12)	Healthy control (n = 11)	P-value
Age, year*	72.5 ± 10.26	61.6 ± 11	0.0600
Gender			0.6800
Female	6 (50.0%)	4 (36.4%)	
Male	6 (50.0%)	7 (63.6%)	
Sideness			
Left side	5 (41.7%)		
Right side	6 (50.0%)		
whole colon	1 (8.3%)		
Surgery Type			
Open surgery	9 (75%)		
Laparoscopic Surgery	2 (16.7%)		
Robot-assisted surgery	1 (8.3%)		
T (AJCC 7 th)			
T1	1 (8.3%)		
T2	6 (50.0%)		
T3	3 (25.0%)		
T4a	2 (16.7%)		
N (AJCC 7 th)			
N0	11 (91.7%)		
N1b	1 (8.3%)		
M (AJCC 7 th)			
M0	12 (100.0%)		
Tumor Stage (AJCC 7 th)			
I	7 (58.4%)		
II	4 (33.3%)		
III	1 (8.3%)		

Abbreviations: CRC, colorectal cancer; AJCC, American Joint Committee on Cancer; T, tumor; N, lymph node; M, metastasis.

Data were represented as n (%) unless otherwise annotated. * Age was presented as mean ± standard deviation.

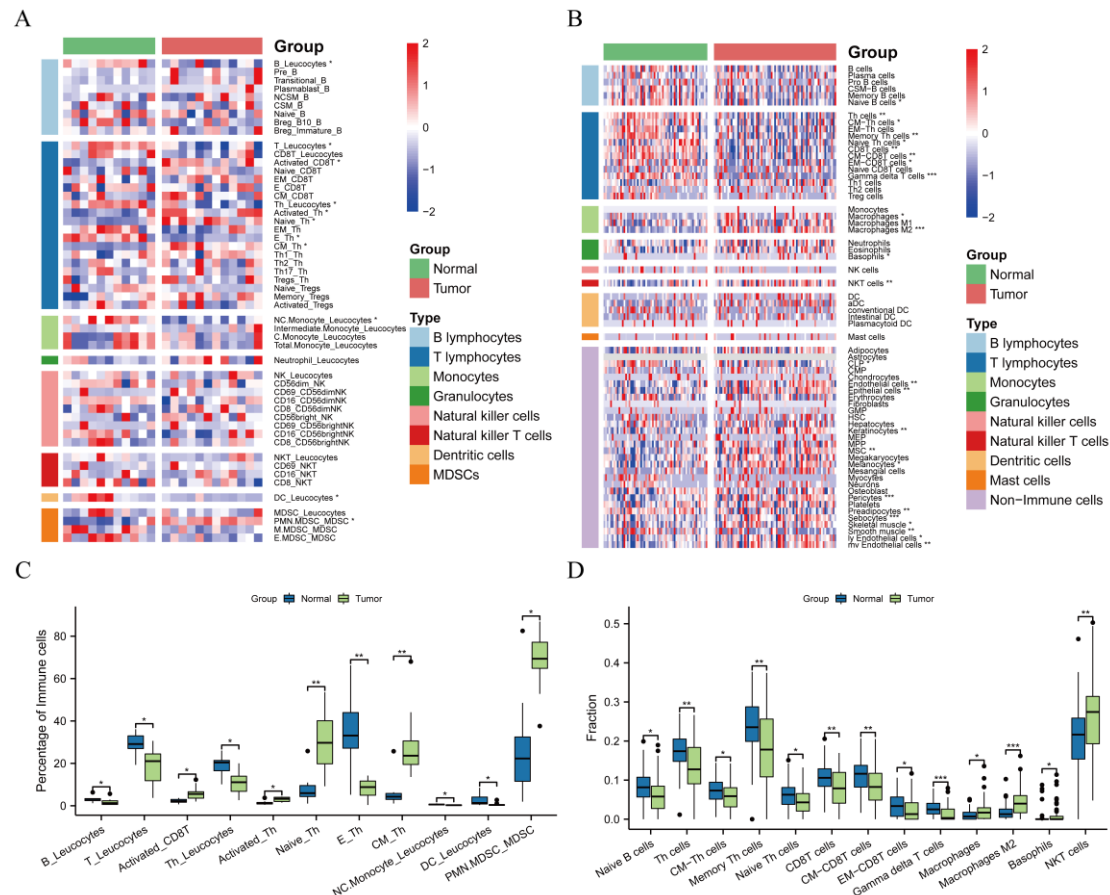


Figure 7: The circulating immune subsets distribution in CRC patients compared to healthy controls

A) The heatmap of immune subsets from flow cytometry analysis. Each immune subset was expressed as the percentage of source cells annotated following the underscore. B) The heatmap of immune and stromal cells computed from merged GEO datasets using the xCell algorithm. C, D) The boxplot of significantly different immune subsets from flow cytometry analysis and xCell algorithm, respectively. The bars show median values of each immune cell subset and the corresponding 95% confidence interval. Corrected *P*-values were calculated for each comparison using Benjamini-Hochberg method. *, *P* < 0.05; **, *P* < 0.01; ***, *P* < 0.001.

Abbreviation: NCSM: non-class switched memory; CSM: class switched memory; Breg, regulatory B cells; EM, effector memory; E, effector; CM, central memory; Tregs, regulatory T cells; NC.Monocyte, non-classical monocytes; C.Monocytes, classical monocytes; NK, natural killer; NKT, natural killer T; DC, Dendritic cell; PMN.MDSC, polymorphonuclear MDSC; M.MDSC, mononuclear MDSC; E.MDSC, early-stage MDSC; CLP, common lymphoid progenitors; CMP, common myeloid progenitors; GMP, granulocyte-monocyte progenitor; HSC, hematopoietic stem cells; MEP, megakaryocyte-erythroid progenitor cell; MPP, multipotent progenitors; MSC, mesenchymal stem cell; ly, lymphatic; mv, microvascular.

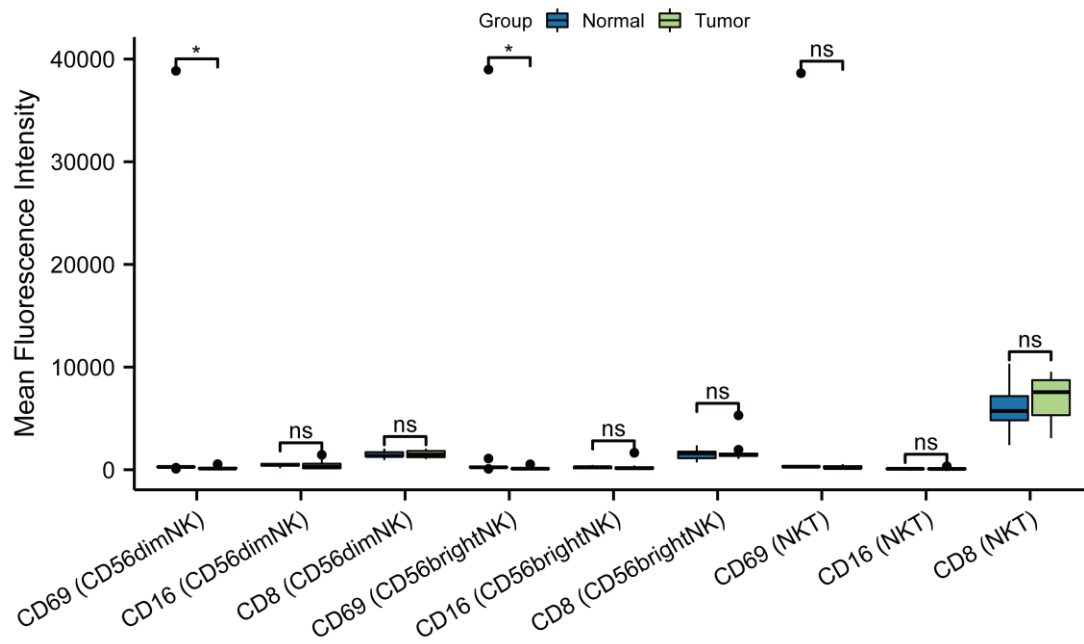


Figure 8: The peripheral blood immunophenotype of NK and NKT cells in CRC patients compared to healthy controls

The bars showed the median MFI of the respective immune cell subset and the corresponding 95% confidence interval. Corrected *P*-values were calculated for each comparison using Benjamini-Hochberg method. *, $P < 0.05$; **, $P < 0.01$; ***, $P < 0.001$.

Abbreviation: NK, natural killer; NKT, natural killer T.

Table 4 Comparison of circulating immune subsets between CRC patients and healthy controls

Immune cells	Healthy controls (N = 11)	CRC patients (N = 12)	Corrected <i>P</i> -value [#]
B % Leukocytes	3.10 ± 1.21	1.72 ± 1.43	0.0421
Pre % B	0.53 ± 0.34	1.39 ± 1.70	0.5772
Transitional % B	1.28 ± 0.70	3.43 ± 3.61	0.2850
Plasmablast % B	1.16 ± 1.17	5.31 ± 10.52	0.0503
NCSM % B	9.14 ± 5.63	8.73 ± 6.28	0.8650
CSM % B	16.84 ± 13.02	16.20 ± 9.96	0.9509
Naive % B	59.95 ± 20.35	53.50 ± 21.90	0.6556
Breg-B10 % B	20.63 ± 12.38	12.09 ± 8.09	0.2326
Breg-Immature % B	4.24 ± 1.89	5.54 ± 5.03	0.9889
T % Leukocytes	29.15 ± 4.96	18.10 ± 8.03	0.0184
CD8T % Leukocytes	8.76 ± 3.93	5.45 ± 3.44	0.1391
Activated % CD8T	2.23 ± 0.96	5.84 ± 2.97	0.0107
Naive % CD8T	16.79 ± 14.84	15.59 ± 7.17	0.7963
EM % CD8T	32.96 ± 17.28	36.54 ± 12.93	0.6556
E % CD8T	44.32 ± 20.54	39.18 ± 17.30	0.5692
CM % CD8T	5.92 ± 3.82	8.69 ± 4.57	0.3331
Th % Leukocytes	18.84 ± 4.43	11.13 ± 5.17	0.0243
Activated % Th	1.40 ± 0.87	3.00 ± 1.08	0.0107
Naive % Th	7.87 ± 6.43	30.04 ± 14.88	0.0088
EM % Th	51.07 ± 15.45	33.67 ± 15.60	0.0507
E % Th	35.16 ± 15.95	8.20 ± 4.13	0.0088
CM % Th	5.92 ± 6.46	28.11 ± 14.64	0.0088
Th1 % Th	62.77 ± 10.55	64.51 ± 13.81	0.4574
Th2 % Th	8.71 ± 3.59	10.03 ± 6.68	1.0000
Th17 % Th	10.37 ± 5.53	10.95 ± 8.74	0.9831
Tregs % Th	6.94 ± 3.17	8.91 ± 3.95	0.4574
Naive % Tregs	6.47 ± 7.71	1.70 ± 1.47	0.2140
Memory % Tregs	41.36 ± 20.09	58.28 ± 14.31	0.2140

Activated % Tregs	14.30 ± 6.66	12.83 ± 8.30	0.6118
Neutrophil % Leukocytes	54.16 ± 7.93	61.41 ± 14.75	0.0125
Non-Classical- Monocyte % Leukocytes	0.60 ± 0.26	0.24 ± 0.15	0.6621
Intermediate- Monocyte % Leukocytes	0.04 ± 0.02	0.06 ± 0.09	0.9946
Classical-Monocyte % Leukocytes	2.24 ± 1.95	1.91 ± 1.37	0.7087
Monocyte % Leukocytes	2.93 ± 1.95	2.21 ± 1.46	0.5359
DC % Leukocytes	2.93 ± 2.82	0.59 ± 0.69	0.0265
MDSC % Leukocytes	0.37 ± 0.27	0.28 ± 0.16	0.7266
PMN-MDSC % MDSC	26.04 ± 22.18	68.27 ± 12.84	0.0107
M-MDSC % MDSC	38.53 ± 27.40	17.11 ± 12.60	0.2065
E-MDSC % MDSC	24.00 ± 14.37	11.29 ± 7.91	0.1096
NK % Leukocytes	3.38 ± 1.85	4.09 ± 4.46	0.8650
CD56 ^{dim} % NK	92.64 ± 4.89	90.08 ± 5.39	0.2787
CD69 ⁺ % CD56 ^{dim} NK	12.93 ± 27.45	19.39 ± 25.30	0.0662
CD69 (CD56 ^{dim} NK) *	279.00 (269.50, 297.00)	116.5 (105.58, 201.00)	0.0277
CD16 ⁺ % CD56 ^{dim} NK	93.96 ± 4.74	80.19 ± 21.89	0.2004
CD16 (CD56 ^{dim} NK) *	480.00 (394.50, 585.50)	284.00 (145.00, 591.50)	0.4222
CD8 ⁺ % CD56 ^{dim} NK	30.59 ± 18.38	32.61 ± 15.86	0.7266
CD8 (CD56 ^{dim} NK) *	1345.00 (1302.00, 1712.00)	1482.50 (1226.75, 1827.25)	0.9264
CD56 ^{bright} % NK	7.35 ± 4.89	9.86 ± 5.22	0.2912
CD69 ⁺ % CD56 ^{bright} NK	14.35 ± 27.99	15.15 ± 25.91	0.4574
CD69 (CD56 ^{bright} NK) *	245.00 (223.50, 296.50)	112.00 (76.38, 145.00)	0.0277

CD16 ⁺ % CD56 ^{bright} NK	40.71 ± 13.95	29.48 ± 21.38	0.2737
CD16 (CD56 ^{bright} NK) *	255.00 (137.00, 304.00)	150.00 (90.70, 256.25)	0.4180
CD8 ⁺ % CD56 ^{bright} NK	24.70 ± 22.80	21.66 ± 10.74	0.7087
CD8 (CD56 ^{bright} NK) *	1601.00 (1129.5, 1775.00)	1441.50 (1346.50, 1586.00)	0.8795
NKT % Leukocytes	2.27 ± 2.54	1.37 ± 1.35	0.2065
CD69 ⁺ % NKT	14.28 ± 27.71	20.19 ± 24.09	0.1002
CD69 (NKT) *	303.00 (285.50, 352.50)	178.00 (152.75, 356.75)	0.1815
CD16 ⁺ % NKT	6.48 ± 7.15	5.51 ± 4.32	0.7877
CD16 (NKT) *	97.70 (85.15, 110.00)	86.45 (72.33, 131.50)	0.8795
CD8 ⁺ % NKT	67.57 ± 19.76	55.18 ± 12.64	0.2737
CD8 (NKT) *	5726.00 (4821.00, 7183.00)	7563.00 (5321.25, 8728.75)	0.4222

*, represent the MFI value expressed as the median with 95% confidence interval. All other data were presented with the Mean ± SD (%). The Benjamini-Hochberg method was used to correct *P*-value for multiple testing, which was indicated by *P*-value[#]. *P*-value[#] < 0.05 was regarded as statistically different.

Abbreviation: NCSM: non-class switched memory; CSM: class switched memory; Breg, regulatory B; EM, effector memory; E, effector; CM, central memory; Treg, regulatory T cells; NK, natural killer; NKT, natural killer T; DC, dendritic cell; PMN-MDSC, polymorphonuclear MDSC; M-MDSC, mononuclear MDSC; E-MDSC, early-stage MDSC.

3.2 Diagnostic Model allowed Differentiation of CRC Patients from Healthy Controls

Eleven immune subsets were identified from the univariable logistic regression on fifty-two immune subsets (Table 8 in the Appendix). When SVM was applied to evaluate the accuracy of different combinations of the above immune subsets in discriminating between CRC individuals and healthy controls, the combination of seven immune subsets was optimal, with an accuracy of 0.936 (Fig. 9A), including NC.Monocyte_Leukocytes, E_Th, T_Leukocytes, Activated_Th, Activated_CD8T, Th_Leukocytes, and Naïve_Th (Table 5). Therefore, these seven immune subsets were chosen to construct a diagnostic model using a logistic regression algorithm. The diagnostic formula was determined as follows:

$$\left[\begin{array}{l} 112.9468 - 44.5381 \times \text{Non-Classical Monocyte (\% of Leukocytes)} - 3.1629 \\ \times \text{Effector Th (\% of Th cells)} - 5.8056 \times \text{T (\% of Leukocytes)} - 6.0697 \times \\ \text{Activated Th (\% of Th cells)} + 8.9753 \times \text{Activated CD8T (\% of CD8T cells)} \\ + 5.7387 \times \text{Th (\% of Leukocytes)} + 0.0072 \times \text{Naïve Th (\% of Th cells)}. \end{array} \right]$$

Moreover, a nomogram incorporating the above immune subsets was constructed to visualize this diagnostic model and efficiently predict the risk of malignancy (Fig. 9B). This study used 12 CRC and 11 normal samples as the training set. The calibration curve of the nomogram confirmed that the predictive probability of CRC nearly matched the actual probability, which was also supported by the Hosmer-Lemeshow test result ($P = 1.0000$) (Fig. 9C). According to the DCA curve, we observed that the diagnostic model acquired the most clinical benefit with the entire range of threshold probabilities compared to the individual immune subset (Fig. 9D). Furthermore, ROC analysis in our training cohort suggested that the nomogram model accurately distinguished CRC and normal subjects with an AUC of 1.000 (95% CI 1.000-1.000), the sensitivity of 1.000, specificity of 1.000, positive predictive value of 1.000, and negative predictive value of 1.000 at the cut-off point of -0.038 (Fig. 9E). In addition, each immune cell subset of the model has a good diagnostic performance in distinguishing these two groups with an AUC greater than 0.850 (Fig. 9F-H).

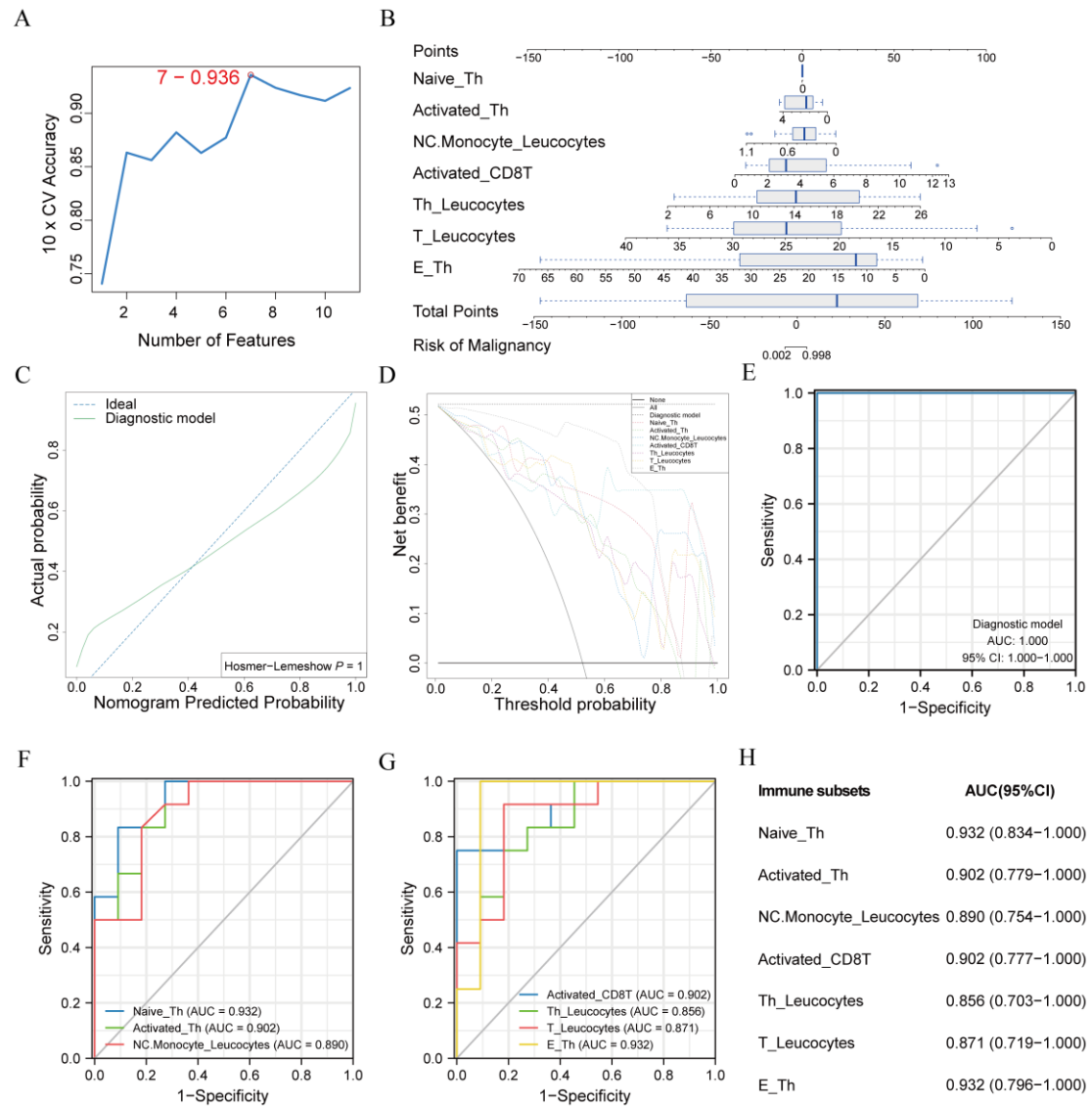


Figure 9: Diagnostic model for differentiating CRC patients from healthy controls

A) Tenfold cross-validation accuracy plot of SVM algorithm. B) Diagnostic nomogram model to predict the risk probability of CRC. C) Calibration curve of the nomogram model. D) DCA curve of the nomogram model and corresponding seven predictive risk factors. E) ROC analysis of the nomogram model. F, G) ROC analysis of seven predictive immun subsets in the model. H) The forest plot of the AUC value and 95% CI for each immune subset. Each immune subset was expressed as the percentage of source cells annotated following the underscore.

Abbreviation: Naïve_Th, naïve Th (% of Th); Activated_Th, activated Th (% of Th); NC.Monocyte_Leukocytes, non-classical monocyte (% of Leukocytes); Activated_CD8T, activated CD8T (% of CD8T); Th_Leukocytes, Th (% of Leukocytes); T_Leukocytes, T (% of Leukocytes); E_Th, effector Th (% of Th); Th, T helper, CD8T, CD8⁺ T; ROC, receiver operating curve; AUC, area under curve; 95% CI, 95% confidence interval.

Table 5 The accuracy of individual immune subset or the combination of different immune subsets as the classifier to distinguish CRC patients from healthy controls by Support Vector Machine learning algorithm

Feature Combinations	10 × CV Accuracy
NC.Monocyte_Leukocytes	0.741
NC.Monocyte_Leukocytes and E_Th	0.863
NC.Monocyte_Leukocytes, E_Th, and T_Leukocytes	0.856
NC.Monocyte_Leukocytes, E_Th, T_Leukocytes, and Activated_Th	0.882
NC.Monocyte_Leukocytes, E_Th, T_Leukocytes, Activated_Th, and Activated_CD8T	0.863
NC.Monocyte_Leukocytes, E_Th, T_Leukocytes, Activated_Th, Activated_CD8T, and Th_Leukocytes	0.877
NC.Monocyte_Leukocytes, E_Th, T_Leukocytes, Activated_Th, Activated_CD8T, Th_Leukocytes, and Naïve_Th	0.936
NC.Monocyte_Leukocytes, E_Th, T_Leukocytes, Activated_Th, Activated_CD8T, Th_Leukocytes, Naïve_Th, and PMN.MDSC_MDSC	0.924
NC.Monocyte_Leukocytes, E_Th, T_Leukocytes, Activated_Th, Activated_CD8T, Th_Leukocytes, Naïve_Th, PMN.MDSC_MDSC, and EM_Th	0.917
NC.Monocyte_Leukocytes, E_Th, T_Leukocytes, Activated_Th, Activated_CD8T, Th_Leukocytes, Naïve_Th, PMN.MDSC_MDSC, EM_Th, and CM_Th	0.911
NC.Monocyte_Leukocytes, E_Th, T_Leukocytes, Activated_Th, Activated_CD8T, Th_Leukocytes, Naïve_Th, PMN.MDSC_MDSC, EM_Th, CM_Th, and E.MDSC_MDSC	0.924

Abbreviation: 10 × CV, ten-fold cross validation; NC.Monocyte_Leukocytes; non-classical monocyte (% of Leukocytes); E_Th, effector Th (% of Th); Activated_Th, activated Th (% of Th); T_Leukocytes, T (% of Leukocytes); Activated_CD8T, activated CD8T (% of CD8T); Th_Leukocytes, Th (% of Leukocytes); Naïve_Th,

naïve Th (% of Th); PMN.MDSC_MDSC, polymorphonuclear MDSC (% of MDSC); EM_Th, effector memory Th (% of Th); CM_Th, central memory Th (% of Th); E.MDSC_MDSC, early-stage MDSC (% of MDSC); MDSC, myeloid-derived suppressor cell; Th, T helper, CD8T, CD8⁺ T.

3.3 NR3C2, CAMK4, and TRAT1 Associated with the Composition of Th cells

To further elucidate the underlying molecular mechanism associated with the distinct circulating immune subsets between CRC cases and healthy controls, we performed the differential expression analysis on GEO and TCGA datasets. In the GEO dataset, we identified 398 DEGs in blood samples of CRC patients compared to healthy controls, of which 38 genes and 360 genes were up-regulated and down-regulated, respectively (Fig. 10A). Meanwhile, 5245 DEGs were obtained from the gene expression analysis on CRC and non-cancerous tissue samples in the TCGA dataset, including 2594 up-regulated genes and 2651 down-regulated genes (Fig. 10B). We performed the intersection of DEGs between GEO and TCGA datasets to identify the consistently changed genes in both blood and tissue samples regarding the potential interaction between colorectal carcinoma and the systemic immune system. In total, 39 DEGs consisting of 1 up-regulated gene and 38 down-regulated genes were identified as the common DEGs (Fig. 10C, D). Next, the GO enrichment analysis indicated that these genes were mainly involved in lymphocyte differentiation and purinergic receptor signaling pathway (Fig. 10E).

In order to study the relationship between different distributional immune subsets and regulated genes, the correlation analysis between immune cell subsets and common DEGs was conducted in healthy controls and CRC patients, respectively (Fig. 11A, B). Furthermore, details of the correlation results are depicted in the appendix (Table 9 and Table 10). To ensure the robustness of the selection on potential genes associated with the composition of Th cells, correlation pairs between immune cell subsets and DEGs were used to filter genes with the coefficient greater than 0.8 and *p*-value less than 0.05 in both healthy controls and CRC patients. Three genes: NR3C2,

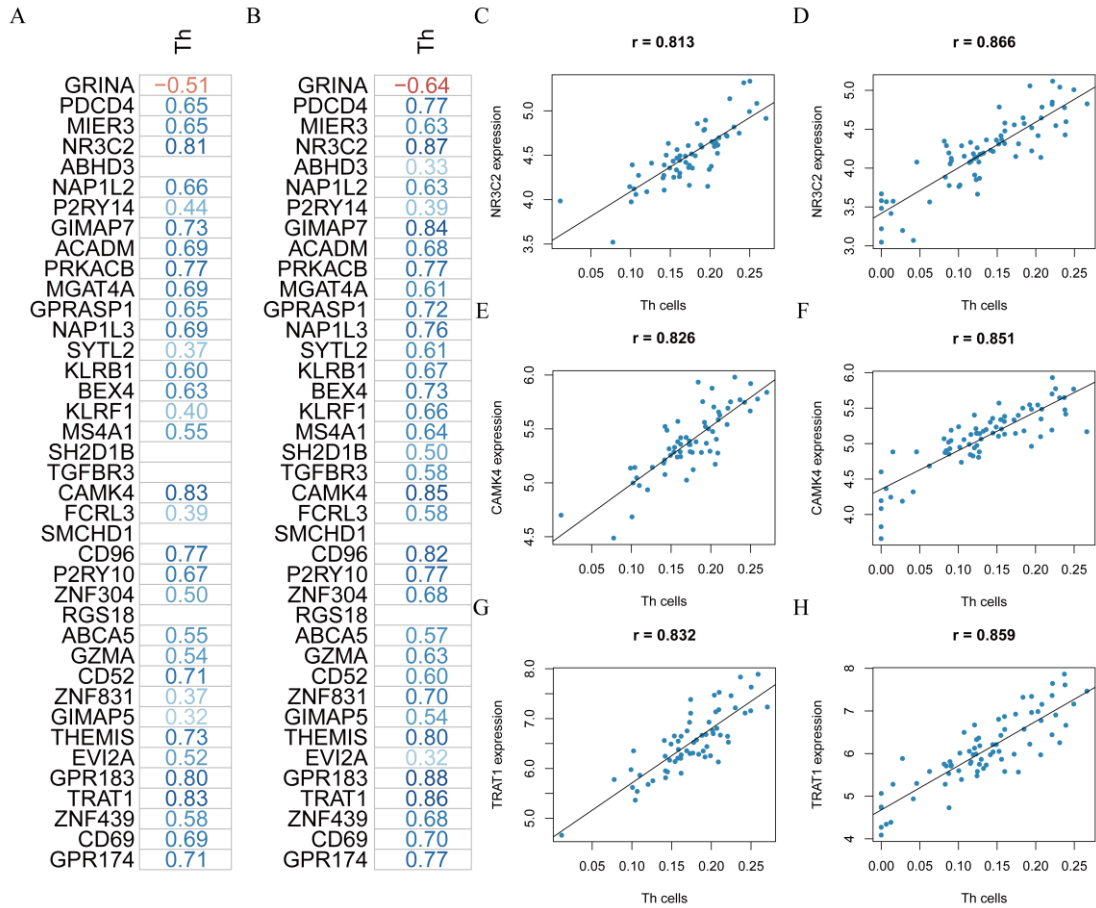


Figure 11: Identification of candidate genes associated with the composition of circulating Th cells

A, B) The heatmap of the correlation coefficient between common DEGs and Th cells in healthy controls and CRC patients, respectively. Blank cells represented the *p*-value of the correlation greater than 0.05. Blue color and red color referred to positive and negative correlation, respectively. C, D) Correlation plot of NR3C2 with Th cells in healthy controls and CRC patients, respectively. E, F) Correlation plot of CAMK4 with Th cells in healthy controls and CRC patients, respectively. G, H) Correlation plot of TRAT1 with Th cells in healthy controls and CRC patients, respectively.

Abbreviation: Th, T helper.

3.4 Right-sided CRC Patients demonstrating Similar Systemic Immune Landscape with Left-sided Ones

To further characterize the systemic immune status in different sidedness of CRC, we compared the distribution of circulating fifty-two immune subsets between RSC and LSC patients (Fig. 12A). These two cohorts have a similar pattern of age, gender, TNM classification, tumor stage, residual tumor classification, and concomitant diseases (Table 6). Meanwhile, the absolute number of each immune subset was calculated based on distributional percentage and leukocytes counts of clinical test to maximize the accuracy of cell compositional estimates. However, no differences were detected in the distribution of fifty-two immune subsets and phenotypic markers expression on NK and NKT cells between RSC patients and LSC ones (Fig. 12A, B).

Annotation for Table 6:

Abbreviations: CRC, colorectal cancer; AJCC, American Joint Committee on Cancer; T, tumor; N, lymph node; M, metastasis. COPD, chronic obstructive pulmonary disease.

Data were represented as n (%) unless otherwise annotated. * Age was presented as mean \pm standard deviation.

Table 6 Clinical characteristics of left-sided CRC patients and right-sided ones

Variables	Left-sided CRC (n=5)	Right-sided CRC (n=6)	P-value
Age, year*	66.20 ± 11.82	75.83 ± 6.37	0.1500
Gender			0.5671
Female	2 (40%)	4 (66.67%)	
Male	3 (60%)	2 (33.33%)	
T (AJCC 7 th)			0.5455
T1/T2	4 (80%)	3 (50%)	
T3/T4	1 (20%)	3 (50%)	
N (AJCC 7 th)			1.0000
N0	5 (100%)	5 (83%)	
N1	0 (0%)	1 (17%)	
M (AJCC 7 th)			1.0000
M0	5 (100%)	6 (100%)	
Tumor Stage (AJCC 7 th)			0.5455
I	4 (80%)	3 (50%)	
II/III	1 (20%)	3 (50%)	
Residual tumor classification			1.0000
R0	5 (100%)	6 (100%)	
Diabetes mellitus			1.0000
No	4 (80%)	4 (66.67%)	
Yes	1 (20%)	2 (33.33%)	
Coronary heart disease			0.5455
No	4 (80%)	3 (50%)	
Yes	1 (20%)	3 (50%)	
Heart failure			0.4545
No	5 (100%)	4 (66.67%)	
Yes	0 (0%)	2 (33.33%)	
COPD			1.0000
No	5 (100%)	5 (83.33%)	
Yes	0 (0%)	1 (16.67%)	

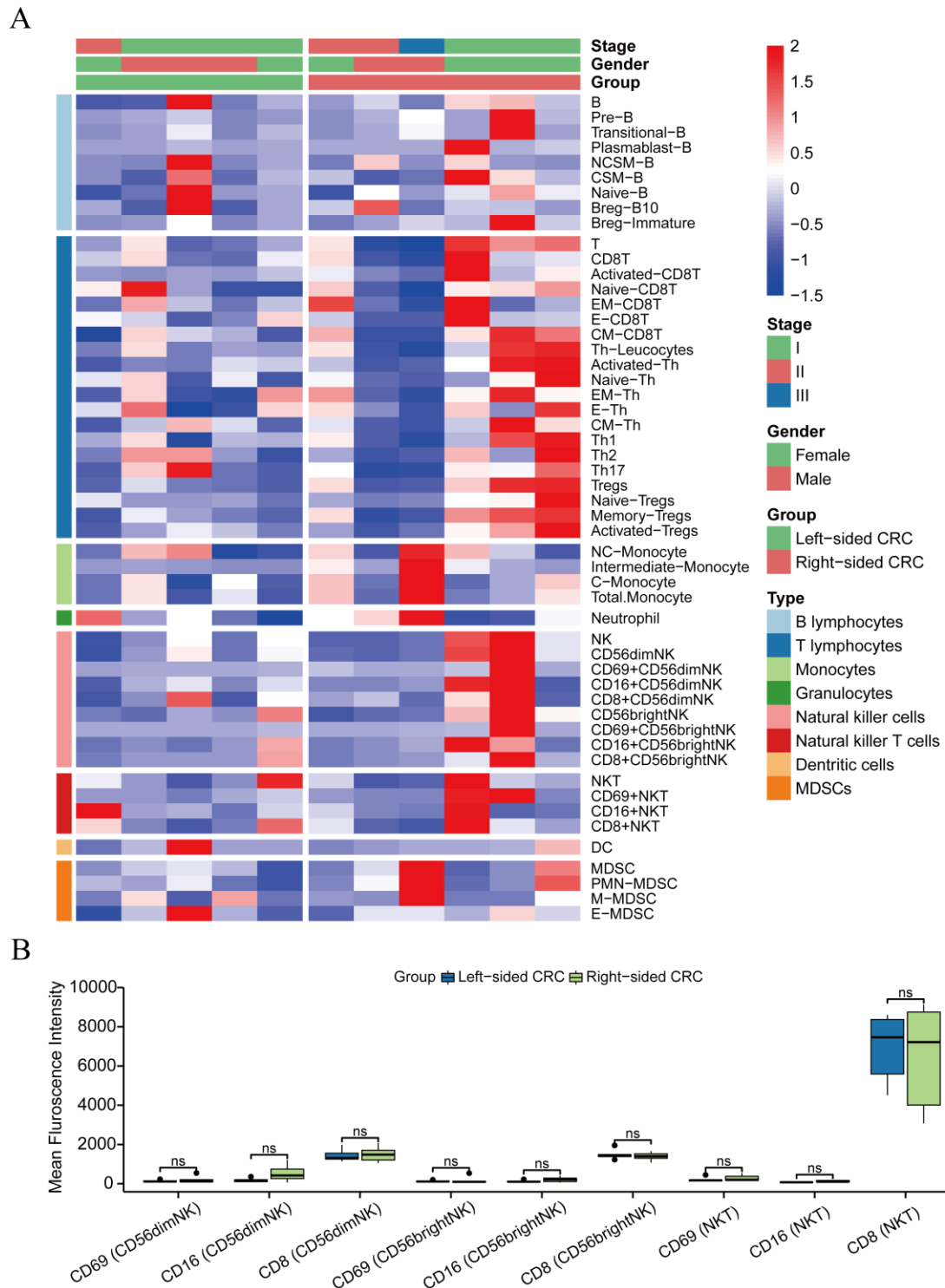


Figure 12: The circulating immune subsets distribution in right-sided CRC patients compared to left-sided ones

A) The heatmap of circulating immune subsets. B) The boxplot of the expression of phenotypic markers on NK and NKT cells. Each immune cell subset was expressed as the absolute cell number in 200ul peripheral blood. The bars show median values of each immune cell subset and the corresponding 95% confidence interval. Corrected *P*-

values were calculated for each comparison using Benjamini-Hochberg method. *, $P < 0.05$; **, $P < 0.01$; ***, $P < 0.001$; ns, not significant.

Abbreviation: NCSM: non-class switched memory; CSM: class switched memory; Breg, regulatory B cells; EM, effector memory; E, effector; CM, central memory; Tregs, regulatory T cells; NC.Monocyte, non-classical monocytes; C.Monocytes, classical monocytes; NK, natural killer; NKT, natural killer T; DC, dendritic cell; PMN.MDSC, polymorphonuclear MDSC; M.MDSC, mononuclear MDSC; E-MDSC, early-stage MDSC.

3.5 Correlation of Clinical Test Parameters with Immune Subsets in CRC Patients

To further study the relationship between fifty-two immune cell subsets and twelve clinical test parameters, the correlation analysis was performed for CRC patients using the absolute number of the respective immune subsets (Fig. 13). In order to find reliable biomarkers associated with the immune cell composition in the peripheral blood, correlated pairs with the coefficient greater than 0.8 and p -value less than 0.05 were selected from the above analysis. In total, three parameters were proved to be strongly associated with the distribution of immune subsets in CRC patients (Table 7). Firstly, gamma-glutamyltransferase was positively correlated with the level of circulating DCs. Five positively correlated pairs involving aspartate aminotransferase (AST) were identified, including plasmablasts, activated CD8T cells, effector CD8T cells, class-switched memory B cells, and CD8T cells. In contrast to AST, only two immune subsets, T lymphocytes and memory Treg cells, were positively associated with the alanine aminotransferase (ALT).

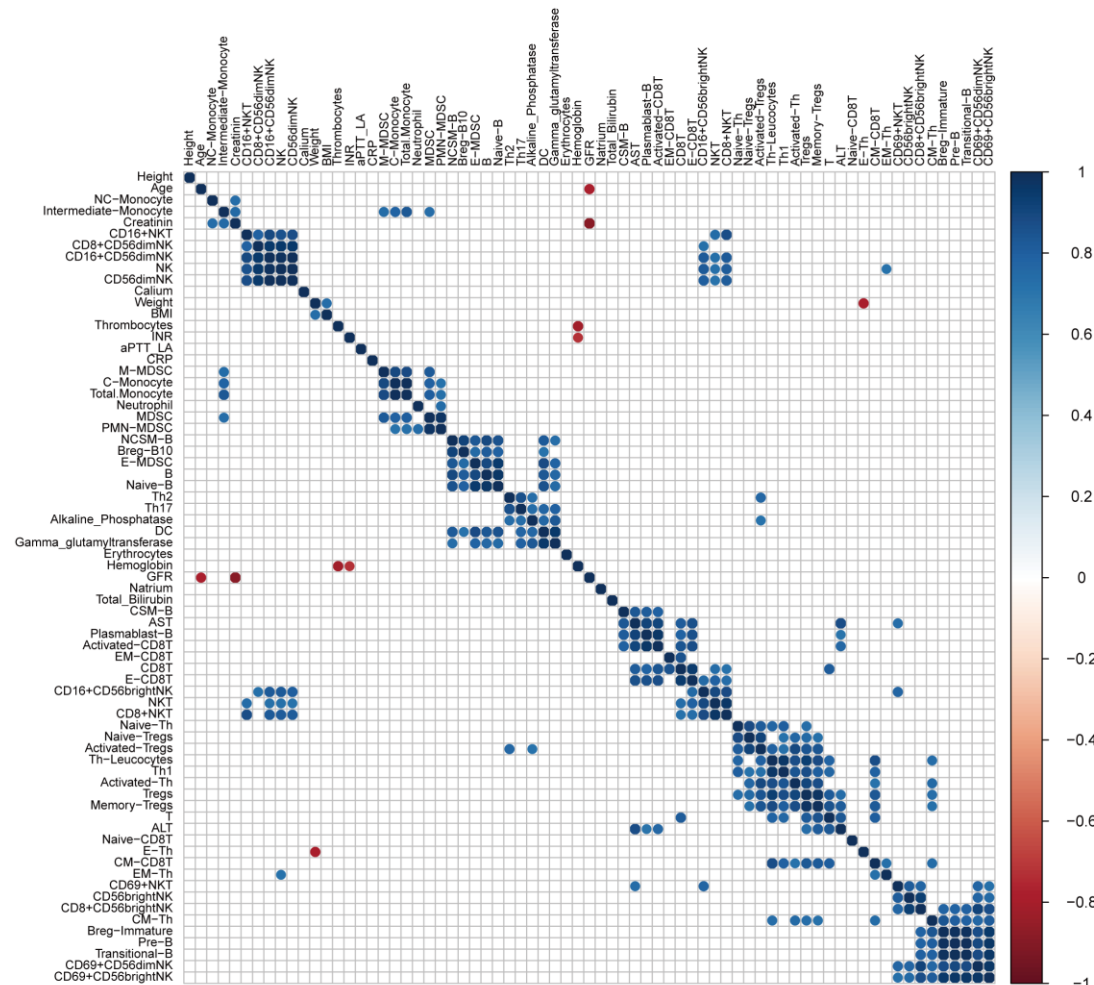


Figure 13: Correlation analysis between circulating immune subsets and clinical test parameters

Each immune subset was expressed as the absolute cell number in 200ul peripheral blood. Blank cells represented the p -value of the correlation greater than 0.05. Blue circles and red circles referred to positive and negative correlations, respectively.

Abbreviation: NCSM: non-class switched memory; CSM: class switched memory; Breg, regulatory B cells; EM, effector memory; E, effector; CM, central memory; Tregs, regulatory T cells; NC.Monocyte, non-classical monocytes; C.Monocytes, classical monocytes; NK, natural killer; NKT, natural killer T; DC, Dendritic cell; PMN.MDSC, polymorphonuclear MDSC; M.MDSC, mononuclear MDSC; E-MDSC, early-stage MDSC.

Table 7 Clinical test parameters correlated with immune subsets

Clinical parameters	Immune cells	Coefficient	<i>P</i> -value
Gamma-glutamyltransferase	Dendritic cells	0.96	1.31E-06
AST	Plasmablasts	0.95	1.55E-06
AST	Activated CD8T cells	0.91	4.91E-05
AST	Effector CD8T cells	0.87	2.60E-04
ALT	T lymphocytes	0.84	6.60E-04
AST	CSM-B cells	0.83	7.29E-04
ALT	Memory Treg cells	0.82	1.19E-03
AST	CD8T cells	0.81	1.34E-03

Abbreviation: AST, aspartate aminotransferase; ALT, alanine aminotransferase; CSM, class-switched memory; Treg, regulatory T; CD8T, CD8⁺ T.

4. Discussion

The immunoscore, based on the quantification of CD3⁺ and CD8⁺ tumor-infiltrating lymphocytes (TILs) at the invasive margin and at the core of the carcinoma, has been proven to be more reliable than tumor-node-metastasis (TNM) staging as a prognostic marker in patients with CRC [45, 46]. Meanwhile, cancer immunity is considered a combination of the intratumoral immune events and the systemic immune response [47]. Although most studies focus on the TILs, immune subsets in the peripheral blood are the main resources for intratumoral immune components. Therefore, the composition and phenotype of circulating immune cell subsets may be linked to the immune response inside the tumor, potentially playing a significant role in predicting the tumor progression and drug responses in CRC. In addition, the impact of CRC on the systemic immunity remains to be elucidated. To characterize peripheral blood immune features of CRC patients, we analyzed fifty-two subsets of circulating immune cells, including B and T lymphocytes, monocytes, neutrophils, NK cells, NKT cells, DCs, and MDSCs. Furthermore, these immune subsets were used to construct the diagnostic model to differentiate CRC patients from healthy controls and further correlated with the clinical test data.

4.1 Distributional Characteristics of Circulating Immune Subsets in CRC patients

Even though acting as the main effector cell of humoral immunity, B lymphocytes are poorly investigated in the TME because of their controversial role in regulating tumor progression [141]. Conversely, T cells infiltration of TME has been widely researched in CRC patients [82, 87-90]. Innate immune cells that principally comprise neutrophils, monocytes, dendritic cells (DCs), myeloid-derived suppressor cells (MDSCs), NK, and NKT cells, are also involved in the interplay with tumor cells. Neutrophils are indispensable immune cells in defending against invading microorganisms and facilitating wound healing [49]. Moreover, monocytes are considered critical regulators of cancer development and metastasis, with different subsets performing opposing roles in enabling tumor growth and preventing

metastatic spread of tumor cells [52]. DCs, one of the essential antigen-presenting cells, could initiate adaptive immune responses and secret costimulatory molecules to drive cytotoxic T cells clonal expansion [58]. Besides, MDSCs consist of a heterogeneous population of early-stage (E-MDSC), monocytic (M-MDSC), and polymorphonuclear origin (PMN-MDSCs) that typically arise in chronic inflammatory sites, including cancer [142]. NK and NKT cells are innate-like lymphocyte populations with cytotoxic functions independent of MHC molecular on pathogenic cells and tumor cells in the innate immunity. It is worth noting that the composition of the above immune subsets is seldomly reported in the peripheral blood of CRC patients.

We first demonstrated that CRC patients have a lower percentage of B lymphocytes than healthy controls. This finding contradicted Shimabukuro-Vornhagen et al., which showed a comparable proportion of B lymphocytes in peripheral blood of CRC patients compared to healthy controls [93]. Since chemoradiotherapy prior to surgery can potentially change the circulating immune landscape by stimulating the systemic immune response, this discrepancy may attribute to the different inclusion criteria of patients with CRC. Meanwhile, we observed that multiple subsets of T lymphocytes have different compositional features in CRC patients than healthy controls. T lymphocytes, Th cells, and effector Th cells have decreased proportion in CRC patients, whereas activated CD8T cells, activated Th cells, naïve Th cells, and central memory Th cells were significantly increased in those patients. Although evidence reported that CRC patients have a similar distribution of naïve T cells, central memory T cells, and effector memory T cells with healthy controls [48], they failed to discriminate between the two major subpopulations of T cell, namely CD8T and Th cells. Conflicting results have been reported on the level of circulating Treg cells in CRC patients. Dylag-Trojanowska et al. indicated that Treg cells were significantly decreased in CRC patients [143], whereas the opposite trend of Treg cells was reported in another study [48]. Interestingly, our results showed that Treg cells have

similar distributional characteristics in CRC patients and healthy controls. In addition, Krijgsman et al. reported no statistical difference in the distribution of T lymphocytes and Th cells between CRC patients and healthy controls, which is not in line with our study [49]. Due to the critical role of T lymphocytes in the systemic immune reaction, it is fundamental to focus on the dynamic distributional changes of circulating T cells in the context of leukocytes. Compared to leukocytes as the denominator for T lymphocytes and Th cells in our study, Krijgsman et al. [49] used the lymphocytes or T lymphocytes as the denominator of the above immune cell subsets, partially explaining the discrepant results between the two studies. Due to the low percentage of B and T lymphocytes, and Th cells in the leukocyte population of the peripheral blood, CRC patients may have immune suppression on the adaptive immune response.

To our knowledge, this is the first study comparing circulating DCs of CRC patients and healthy controls. We found that those were significantly less frequent than healthy controls. Furthermore, we demonstrated that CRC patients presented altered distribution of monocytes compared to healthy controls, characterized by reduced proportions of circulating non-classical monocytes. These findings are partially consistent with one clinical study that showed no significant compositional differences in total monocytes, classical monocytes, intermediate monocytes, and non-classical monocytes between CRC patients and healthy controls [144]. The explanation for the difference was that in their study $CD14^+CD16^{++}$ was used to identify non-classical monocytes, whereas we regarded $CD14^{low/+}CD16^+$ as the immunophenotype of these cells. Also, previous reports indicated that non-classical monocytes could reduce metastatic lung burden in a mouse model via NK cell recruitment and activation [145, 146]. Regarding DCs and non-classical monocytes belonging to antigen-presenting cells, CRC patients may have impaired immune activation on the adaptive immune response due to the low number of these two immune cell subsets in the peripheral blood.

Neutrophils are regarded as critical effector cells in the innate arm of the immune

system by counting against invading microorganisms [147]. Nevertheless, studies on circulating neutrophils are virtually scarce. Our study showed that CRC patients have a similar proportion of circulating neutrophils to healthy controls. Furthermore, it is widely accepted that MDSCs exert immune suppressive effects mostly via inhibiting T-cell proliferation and stimulating Treg development [65]. In contrast to several studies that reported circulating MDSCs were significantly increased in CRC patients [67, 68], we found no difference in the distribution of MDSCs between CRC patients and healthy controls. Besides, our study explicitly indicated that CRC patients had an increased percentage of PMN-MDSCs compared to healthy controls. Accumulating studies have reported that PMN-MDSCs are the main components of circulating MDSCs and have a more prominent immune suppressive function than M-MDSC [65]. Hence, high proportions of PMN-MDSCs within the MDSCs population could present stronger immune suppression on the systemic immune response of CRC patients than healthy controls.

Additionally, compared to healthy controls, we demonstrated that CRC patients have an altered phenotype of circulating CD56^{dim} and CD56^{bright} NK cells characterizing with reduced expression of CD69. Due to CD69 being widely regarded as the stimulatory membrane receptor of NK cells [108], both CD56^{dim} and CD56^{bright} NK cells may have compromised cytotoxic activity in patients with CRC. These findings are in line with a recent study that showed reduced expression of activating receptors on NK cells in CRC patients [48]. Furthermore, Krijgsman et al. proved that the immune suppression on circulating NK cells could be removed by tumor resection in patients with colon carcinoma [77]. Therefore, we could infer that CRC could inhibit the immune function of circulating NK cells via downregulating the expression of cytotoxic activation receptors.

4.2 Construction of a Diagnostic Model based on the Circulating Immune Subsets

Regarding the different distribution of circulating immune subsets in CRC patients compared to healthy controls, we intended to construct a diagnostic model based on

these immune subsets to differentiate these two cohorts. Accumulating diagnostic models have been proposed to identify CRC patients from the population. Most of them are based on clinicopathological characteristics, clinical test parameters, and molecular-based biomarkers. To our knowledge, this study is probably the first clinical research using flow cytometry data to build a diagnostic model for CRC diagnosis. SVM, a machine learning algorithm, is a robust and flexible type of supervised algorithm for both classification and regression. Due to the advantages of high accuracy with less computer power and effectiveness in high dimensional spaces in the classification, SVM was conducted to select the best combination from eleven circulating immune subsets identified from univariable logistic regression. Then seven immune subsets selected from SVM were used to construct our diagnostic model.

In this study, we established a 7-immune subsets classifier to differentiate CRC patients from healthy controls in our cohort. This 7-immune subsets classifier has a great performance in diagnosing patients with CRC according to the corresponding AUC value and the Hosmer-Lemeshow test result. Furthermore, we used nomogram to visualize this diagnostic model to facilitate its potential application in the clinics. DCA plot also proved that 7-immune subsets classifier-based nomogram have the biggest diagnostic capability than each immune subset, which strengthen the reliability of our diagnostic model. In the clinical setting, physicians could collect the peripheral blood sample from suspected patients and further use flow cytometry to detect these samples to infer the risk of CRC. Besides, each of 7-immune subsets also has a great performance in the diagnosis of CRC with the AUC value above 0.85. It is worth noting that the distribution of these immune subsets was significantly different between CRC patients and healthy controls. Due to the limited number of subjects in our study, a large cohort study is needed to validate the diagnostic accuracy of this classifier in the diagnosis of CRC.

4.3 Prediction of Molecular Mechanism Regulating the Level of Circulating Th cells using Bioinformatics Analysis

Bioinformatics is widely applied in biological and medical research ranging from laboratory tests to diagnosing and treating diseases. With the help of bioinformatics analysis, the researcher could predict an array of potential molecules which may play a critical role in certain disorders. Due to the lack of transcriptional profiles from our samples, we intended to obtain the public available sequencing data based on similar cohorts. GEO is an international public functional genomics data repository under the support of the USA National Center for Biotechnology Information (NCBI). To guarantee the inclusion of all available GEO datasets, we applied the methodology of meta-analysis to select the suitable datasets from GEO manually. As depicted in Fig. 4, 2756 records were identified from the above database. A dozen sequencing platforms have performed RNA sequencing in the past two decades. In terms of the dramatic difference in the sequencing coverage among platforms, we decided only to select the GEO datasets from three widely used platforms to minimize the missing of genes, namely Affymetrix, Illumina, and Agilent. Secondly, to exclude the potential impact of therapy on the genetic expression of blood, the GEO datasets should be sequenced from the peripheral blood samples of CRC patients without the prior treatment. Thirdly, to maximize the merging credibility of multiple datasets, a sample size larger than ten was used to select the suitable GEO datasets. We included two GEO datasets as the gene expression profiles of blood samples from CRC and healthy controls according to the above three screening criteria. Also, tissue-based RNA expression profiles were obtained to explore the potential interaction between the peripheral blood and carcinoma in CRC patients. TCGA, as a landmark cancer genomic program, deposited the largest number of primary cancer and matched normal samples' sequencing profiles spanning 33 cancer types. Therefore, we considered the CRC profiles from TCGA as the transcriptional matrixes of colorectal carcinoma.

Through bioinformatics analyses on the gene expression profiles of the peripheral blood samples, only Th cells were consistently identified as the differential immune cells in CRC patients between flow cytometry detection and xCell algorithm analysis.

To explore the underlying molecular mechanism involving the regulation of the Th cells in the peripheral blood, we identified genes differentially expressed not only in blood samples but also in tissue samples of CRC patients compared to normal controls with the consideration of the potential effects of the colorectal tumor on the systemic immune system. Next, we pinpointed three genes that have a strong positive correlation with the level of Th cells in the peripheral blood of both healthy controls and CRC patients, namely NR3C2, CAMK4, and TRAT1. NR3C2, also known as mineralocorticoid receptor (MR), has a critical role in mediating cardiovascular injury induced by the activation of MR. Recent studies revealed that MR activation could facilitate the inflammation by inducing T lymphocytes differentiation into the pro-inflammatory Th1 and Th17 subsets while inhibiting the formation of anti-inflammatory Tregs [148]. CAMK4, a member of the serine/threonine kinase family, could regulate gene expression via activating transcription factors in cells of immune systems [149]. Previous studies reported that CAMK4, highly expressed in T cells, was an essential molecule mediating the differentiation of Th17 cells from T lymphocytes [150, 151]. TRAT1, also referred to as TRIM, can stabilize the T cell receptor (TCR) levels via working as the integral component of TCR [152]. Although lacking studies reported the influence of TRAT1 on the proliferation of T cells, TRAT1 could elevate the expression level of surface CTLA-4 via accelerating its transport from cytoplasm [153], which may result in the inhibition of Th cell proliferation. Therefore, we confer that NR3C2, CAMK4, and TRAT1 have the potential to be candidate genes involving regulating the number of Th cells in the peripheral blood.

4.4 Distributional Comparison of Circulating Immune Subsets between Right-sided CRC patients and Left-sided ones

Primary tumor location has an essential role in predicting the prognosis and the drug responses for patients with CRC [154]. In the clinical settings, CRC was commonly sub-divided as right-sided CRC (RSC) and left-sided CRC (LSC) according to the

proximity to the splenic flexure [154, 155]. There are widely recognized different features between RSC and LSC. Clinicopathologically, RSC tend to have older age, female, high TNM at diagnosis, poor differentiation, mucinous contingent, and inflammation in the comparison with LSC [155]. In terms of the metastatic sites of CRC, liver and lung are more common positions in LSC, while RSC is more frequently metastasis to peritoneum [156, 157]. Genetically, RSC is characterized with high MSI and elevated frequency of KRAS proto-oncogene (KRAS)/ B-Raf proto-oncogene (BRAF)/ phosphatidylinositol-4,5-bisphosphate 3-kinase (PI3KCA) mutation, whereas CIN and mutations in APC, tumor protein p53 (TP53), SMAD family member 4 (SMAD4) and KRAS genes have commonly occurred in LSC [158-160]. In addition, as opposed to RSC, LSC is associated with higher expression of the epidermal growth factor receptor (EGFR) and their ligands, including epiregulin (EREG) and amphiregulin (AREG)[156, 161], which is also the main reason why the NCCN guidelines only recommend the use of anti-EGFR drugs for the treatment of LSC with wild type of RAS [162]. Lastly, several studies demonstrated that LSC has a much better prognosis than RSC for patients with metastatic CRC (mCRC) [163, 164]. However, the effects of primary tumor location on the immune landscape of the peripheral blood remain poorly understood in CRC patients.

Among fifty-two immune subsets, similar distribution of circulating immune subsets and phenotypic markers expression was detected between RSC patients and LSC ones. Thus, RSC patients may have comparable systemic immune landscape with LSC patients, which may indicate that the primary tumor location has no impact on the systemic immune responses.

4.5 Correlation Analysis between Clinical Test Parameters and Circulating Immune Subsets in CRC Patients

When investigating the associations between circulating immune cell subsets and clinical test parameters, eight positively correlated pairs involving three parameters were identified in CRC patients. Firstly, AST was correlated with five immune cell

subsets, including plasmablasts, activated CD8T cells, effector CD8T cells, class-switched memory B cells, and CD8T cells. Besides, ALT was associated with T lymphocytes and memory Treg cells, and gamma-glutamyltransferase was strongly related to DCs. Multiple studies pointed out that T cell subsets, Breg cells, and DCs have a positive or negative correlation with AST and ALT in hepatitis patients [165-169]. Although there were scarcely reports about these relationships in CRC, the above clinical parameters could indirectly reflect the status of the systemic immune profiles, which may contribute to predict the occurrence of surgery-related complications.

4.6 Research Significance

Our study has prominent significance by characterizing the distribution of a broad spectrum of circulating immune subsets and opening new avenues to underlying molecular mechanisms regulating the composition of Th cells in the peripheral blood of CRC patients. Until now, this study is also the first clinical study to simultaneously characterize fifty-two circulating immune subsets in CRC patients.

4.7 Limitations and Future Directions

The primary limitation of this study is that the number of patients is low, which may compromise the validity of our diagnostic model. However, recently several robust studies constructed the diagnostic model based on a comparable size of subjects [170-172]. Although tenfold cross-validation was performed to guarantee the predictive accuracy of the diagnostic model, our study failed to find external flow cytometry datasets to validate this model. Furthermore, the gene expression profiles of peripheral blood samples were not derived from the recruited patients in this study, which may weaken the credibility of the predicted genes. But, with the help of bioinformatics analysis on the public available datasets, our study could predict the most potential molecular which may participate in the regulation of the distribution of circulating immune cells.

In the future, our research group will carry on this project by expanding the number

of recruited patients and starting the follow-up to investigate the prognostic role of circulating immune subsets on CRC patients. Also, it will be interesting to examine the effect of therapeutic strategies on the systemic immune landscape of patients with CRC. Regarding the significant systemic immune suppression of CRC patients compared to normal controls, it is imperative to develop new drugs to reverse the inhibition of the immune status in the peripheral blood of CRC patients.

5. Conclusion

In summary, we found that CRC patients displayed profound distinctions in the immune cell subset distribution and their phenotype compared to healthy controls, showing that CRC patients have evident immune suppression on the systemic immune response. Moreover, NR3C2, CAMK4, and TRAT1 were identified as the candidate genes regulating the level of circulating Th cells in CRC patients. Furthermore, RSC patients have the similar systemic immune response with LSC ones. These findings are of importance for deciphering the unique features of circulating immune cell subsets in CRC, which could complement the regional immune status of the TME and contribute to the discovery of immune-related biomarkers for the diagnosis of CRC.

6. References

1. Keum N, Giovannucci E. Global burden of colorectal cancer: emerging trends, risk factors and prevention strategies. *Nat Rev Gastroenterol Hepatol*. 2019;16(12):713-32.
2. Dekker E, Tanis PJ, Vleugels JLA, Kasi PM, Wallace MB. Colorectal cancer. *Lancet*. 2019;394(10207):1467-80.
3. Shah SC, Itzkowitz SH. Colorectal Cancer in Inflammatory Bowel Disease: Mechanisms and Management. *Gastroenterology*. 2021.
4. Schlesinger S, Aleksandrova K, Abar L, Vieria AR, Vingeliene S, Polemiti E, Stevens CAT, Greenwood DC, Chan DSM, Aune D, Norat T. Adult weight gain and colorectal adenomas-a systematic review and meta-analysis. *Ann Oncol*. 2017;28(6):1217-29.
5. Okabayashi K, Ashrafian H, Hasegawa H, Yoo JH, Patel VM, Harling L, Rowland SP, Ali M, Kitagawa Y, Darzi A, Athanasiou T. Body mass index category as a risk factor for colorectal adenomas: a systematic review and meta-analysis. *Am J Gastroenterol*. 2012;107(8):1175-85; quiz 86.
6. Harriss DJ, Atkinson G, George K, Cable NT, Reilly T, Haboubi N, Zwahlen M, Egger M, Renehan AG. Lifestyle factors and colorectal cancer risk (1): systematic review and meta-analysis of associations with body mass index. *Colorectal Dis*. 2009;11(6):547-63.
7. Kerr J, Anderson C, Lippman SM. Physical activity, sedentary behaviour, diet, and cancer: an update and emerging new evidence. *Lancet Oncol*. 2017;18(8):e457-e71.
8. Seiwert N, Heylmann D, Hasselwander S, Fahrer J. Mechanism of colorectal carcinogenesis triggered by heme iron from red meat. *Biochim Biophys Acta Rev Cancer*. 2020;1873(1):188334.
9. Henrikson NB, Webber EM, Goddard KA, Scrol A, Piper M, Williams MS, Zallen DT, Calonge N, Ganiats TG, Janssens AC, Zauber A, Lansdorp-Vogelaar I, van Ballegooijen M, Whitlock EP. Family history and the natural history of colorectal cancer: systematic review. *Genet Med*. 2015;17(9):702-12.
10. John SK, George S, Primrose JN, Fozard JB. Symptoms and signs in patients with colorectal cancer. *Colorectal Dis*. 2011;13(1):17-25.
11. Carethers JM, Jung BH. Genetics and Genetic Biomarkers in Sporadic Colorectal Cancer. *Gastroenterology*. 2015;149(5):1177-90.e3.
12. Stoffel EM, Boland CR. Genetics and Genetic Testing in Hereditary Colorectal Cancer. *Gastroenterology*. 2015;149(5):1191-203.e2.
13. Nguyen LH, Goel A, Chung DC. Pathways of Colorectal Carcinogenesis. *Gastroenterology*. 2020;158(2):291-302.
14. Rosen MJ, Dhawan A, Saeed SA. Inflammatory Bowel Disease in Children and Adolescents. *JAMA Pediatr*. 2015;169(11):1053-60.
15. Munkholm P. Review article: the incidence and prevalence of colorectal cancer in inflammatory bowel disease. *Aliment Pharmacol Ther*. 2003;18 Suppl 2:1-5.

16. Fornaro R, Caratto M, Caratto E, Caristo G, Fornaro F, Giovinazzo D, Sticchi C, Casaccia M, Andorno E. Colorectal Cancer in Patients With Inflammatory Bowel Disease: The Need for a Real Surveillance Program. *Clin Colorectal Cancer*. 2016;15(3):204-12.
17. Lu C, Schardey J, Zhang T, Crispin A, Wirth U, Karcz KW, Bazhin AV, Andrassy J, Werner J, Kühn F. Survival Outcomes and Clinicopathological Features in Inflammatory Bowel Disease-Associated Colorectal Cancer: A Systematic Review and Meta-Analysis. *Ann Surg*. 2021.
18. Axelrad JE, Shah SC. Diagnosis and management of inflammatory bowel disease-associated neoplasia: considerations in the modern era. *Therapeutic advances in gastroenterology*. 2020;13:1756284820920779-.
19. Rogler G. Chronic ulcerative colitis and colorectal cancer. *Cancer Lett*. 2014;345(2):235-41.
20. Choi CR, Bakir IA, Hart AL, Graham TA. Clonal evolution of colorectal cancer in IBD. *Nat Rev Gastroenterol Hepatol*. 2017;14(4):218-29.
21. Xie Y-H, Chen Y-X, Fang J-Y. Comprehensive review of targeted therapy for colorectal cancer. *Signal Transduct Target Ther*. 2020;5(1):22.
22. Cassidy J, Tabernero J, Twelves C, Brunet R, Butts C, Conroy T, Debraud F, Figuer A, Grossmann J, Sawada N, Schöffski P, Sobrero A, Van Cutsem E, Díaz-Rubio E. XELOX (capecitabine plus oxaliplatin): active first-line therapy for patients with metastatic colorectal cancer. *J Clin Oncol*. 2004;22(11):2084-91.
23. Goldberg RM, Sargent DJ, Morton RF, Fuchs CS, Ramanathan RK, Williamson SK, Findlay BP, Pitot HC, Alberts SR. A randomized controlled trial of fluorouracil plus leucovorin, irinotecan, and oxaliplatin combinations in patients with previously untreated metastatic colorectal cancer. *J Clin Oncol*. 2004;22(1):23-30.
24. Gill S, Thomas RR, Goldberg RM. Colorectal cancer chemotherapy. *Aliment Pharmacol Ther*. 2003;18(7):683-92.
25. Van Cutsem E, Cervantes A, Nordlinger B, Arnold D. Metastatic colorectal cancer: ESMO Clinical Practice Guidelines for diagnosis, treatment and follow-up. *Annals of Oncology*. 2014;25(suppl 3):iii1-iii9.
26. Siegel RL, Miller KD, Jemal AJCajfc. Cancer statistics, 2019. 2019;69(1):7-34.
27. Vecchione L, Jacobs B, Normanno N, Ciardiello F, Tejpar S. EGFR-targeted therapy. *Exp Cell Res*. 2011;317(19):2765-71.
28. Roskoski R. Small molecule inhibitors targeting the EGFR/ErbB family of protein-tyrosine kinases in human cancers. *Pharmacol Res*. 2019;139:395-411.
29. Price TJ, Peeters M, Kim TW, Li J, Cascinu S, Ruff P, Suresh AS, Thomas A, Tjulandin S, Zhang K, Murugappan S, Sidhu R. Panitumumab versus cetuximab in patients with chemotherapy-refractory wild-type KRAS exon 2 metastatic colorectal cancer (ASPECCT): a randomised, multicentre, open-label, non-inferiority phase 3 study. *Lancet Oncol*. 2014;15(6):569-79.
30. Passardi A, Nanni O, Tassinari D, Turci D, Cavanna L, Fontana A, Ruscelli S, Mucciarini C, Lorusso V, Ragazzini A, Frassinetti GL, Amadori D. Effectiveness of

bevacizumab added to standard chemotherapy in metastatic colorectal cancer: final results for first-line treatment from the ITACa randomized clinical trial. *Ann Oncol.* 2015;26(6):1201-7.

31. Cremolini C, Loupakis F, Antoniotti C, Lupi C, Sensi E, Lonardi S, Mezi S, Tomasello G, Ronzoni M, Zaniboni A, Tonini G, Carlomagno C, Allegrini G, Chiara S, D'Amico M, Granetto C, Cazzaniga M, Boni L, Fontanini G, Falcone A. FOLFOXIRI plus bevacizumab versus FOLFIRI plus bevacizumab as first-line treatment of patients with metastatic colorectal cancer: updated overall survival and molecular subgroup analyses of the open-label, phase 3 TRIBE study. *Lancet Oncol.* 2015;16(13):1306-15.

32. Cunningham D, Lang I, Marcuello E, Lorusso V, Ocvirk J, Shin DB, Jonker D, Osborne S, Andre N, Waterkamp D, Saunders MP. Bevacizumab plus capecitabine versus capecitabine alone in elderly patients with previously untreated metastatic colorectal cancer (AVEX): an open-label, randomised phase 3 trial. *Lancet Oncol.* 2013;14(11):1077-85.

33. Venook AP, Niedzwiecki D, Lenz HJ, Innocenti F, Fruth B, Meyerhardt JA, Schrag D, Greene C, O'Neil BH, Atkins JN, Berry S, Polite BN, O'Reilly EM, Goldberg RM, Hochster HS, Schilsky RL, Bertagnolli MM, El-Khoueiry AB, Watson P, Benson AB, 3rd, Mulkerin DL, Mayer RJ, Blanke C. Effect of First-Line Chemotherapy Combined With Cetuximab or Bevacizumab on Overall Survival in Patients With KRAS Wild-Type Advanced or Metastatic Colorectal Cancer: A Randomized Clinical Trial. *JAMA.* 2017;317(23):2392-401.

34. Heinemann V, von Weikersthal LF, Decker T, Kiani A, Vehling-Kaiser U, Al-Batran SE, Heintges T, Lerchenmüller C, Kahl C, Seipelt G, Kullmann F, Stauch M, Scheithauer W, Hielscher J, Scholz M, Müller S, Link H, Niederle N, Rost A, Höffkes HG, Moehler M, Lindig RU, Modest DP, Rossius L, Kirchner T, Jung A, Stintzing S. FOLFIRI plus cetuximab versus FOLFIRI plus bevacizumab as first-line treatment for patients with metastatic colorectal cancer (FIRE-3): a randomised, open-label, phase 3 trial. *Lancet Oncol.* 2014;15(10):1065-75.

35. Khattak MA, Martin H, Davidson A, Phillips M. Role of first-line anti-epidermal growth factor receptor therapy compared with anti-vascular endothelial growth factor therapy in advanced colorectal cancer: a meta-analysis of randomized clinical trials. *Clin Colorectal Cancer.* 2015;14(2):81-90.

36. Arnold D, Lueza B, Douillard JY, Peeters M, Lenz HJ, Venook A, Heinemann V, Van Cutsem E, Pignon JP, Tabernero J, Cervantes A, Ciardiello F. Prognostic and predictive value of primary tumour side in patients with RAS wild-type metastatic colorectal cancer treated with chemotherapy and EGFR directed antibodies in six randomized trials. *Ann Oncol.* 2017;28(8):1713-29.

37. Tejpar S, Stintzing S, Ciardiello F, Tabernero J, Van Cutsem E, Beier F, Esser R, Lenz HJ, Heinemann V. Prognostic and Predictive Relevance of Primary Tumor Location in Patients With RAS Wild-Type Metastatic Colorectal Cancer: Retrospective Analyses of the CRYSTAL and FIRE-3 Trials. *JAMA Oncol.*

2017;3(2):194-201.

38. Casak SJ, Marcus L, Fashoyin-Aje L, Mushti SL, Cheng J, Shen YL, Pierce WF, Her L, Goldberg KB, Theoret MR, Kluetz PG, Pazdur R, Lemery SJ. FDA Approval Summary: Pembrolizumab for the First-line Treatment of Patients with MSI-H/dMMR Advanced Unresectable or Metastatic Colorectal Carcinoma. *Clin Cancer Res.* 2021;27(17):4680-4.

39. Jamal-Hanjani M, Huebner A, McGranahan N, Swanton C. Defining the lethal subclone in metastatic lung cancer. *Annals of Oncology.* 2018;29:viii702.

40. Ganesh K, Stadler ZK, Cercek A, Mendelsohn RB, Shia J, Segal NH, Diaz LA, Jr. Immunotherapy in colorectal cancer: rationale, challenges and potential. *Nat Rev Gastroenterol Hepatol.* 2019;16(6):361-75.

41. Van Cutsem E, Cervantes A, Adam R, Sobrero A, Van Krieken JH, Aderka D, Aranda Aguilar E, Bardelli A, Benson A, Bodoky G, Ciardiello F, D'Hoore A, Diaz-Rubio E, Douillard JY, Ducreux M, Falcone A, Grothey A, Gruenberger T, Haustermans K, Heinemann V, Hoff P, Kohne CH, Labianca R, Laurent-Puig P, Ma B, Maughan T, Muro K, Normanno N, Osterlund P, Oyen WJG, Papamichael D, Pentheroudakis G, Pfeiffer P, Price TJ, Punt C, Ricke J, Roth A, Salazar R, Scheithauer W, Schmoll HJ, Tabernero J, Taieb J, Tejpar S, Wasan H, Yoshino T, Zaanan A, Arnold D. ESMO consensus guidelines for the management of patients with metastatic colorectal cancer. *Annals of Oncology.* 2016;27(8):1386-422.

42. Markman JL, Shiao SL. Impact of the immune system and immunotherapy in colorectal cancer. *Journal of Gastrointestinal Oncology.* 2015;6(2):208-23.

43. Ferrone C, Dranoff G. Dual roles for immunity in gastrointestinal cancers. *J Clin Oncol.* 2010;28(26):4045-51.

44. Fletcher R, Wang Y-J, Schoen RE, Finn OJ, Yu J, Zhang L. Colorectal cancer prevention: Immune modulation taking the stage. *Biochim Biophys Acta Rev Cancer.* 2018;1869(2):138-48.

45. Pages F, Mlecnik B, Marliot F, Bindea G, Ou FS, Bifulco C, Lugli A, Zlobec I, Rau TT, Berger MD, Nagtegaal ID, Vink-Borger E, Hartmann A, Geppert C, Kolwelter J, Merkel S, Grutzmann R, Van den Eynde M, Jouret-Mourin A, Kartheuser A, Leonard D, Remue C, Wang JY, Bavi P, Roehrl MHA, Ohashi PS, Nguyen LT, Han S, MacGregor HL, Hafezi-Bakhtiari S, Wouters BG, Masucci GV, Andersson EK, Zavadova E, Vocka M, Spacek J, Petruzella L, Konopasek B, Dundr P, Skalova H, Nemejcova K, Botti G, Tatangelo F, Delrio P, Ciliberto G, Maio M, Laghi L, Grizzi F, Fredriksen T, Buttard B, Angelova M, Vasaturo A, Maby P, Church SE, Angell HK, Lafontaine L, Bruni D, El Sissy C, Haicheur N, Kirilovsky A, Berger A, Lagorce C, Meyers JP, Paustian C, Feng Z, Ballesteros-Merino C, Dijkstra J, van de Water C, van Lent-van Vliet S, Knijn N, Musina AM, Scripcariu DV, Popivanova B, Xu M, Fujita T, Hazama S, Suzuki N, Nagano H, Okuno K, Torigoe T, Sato N, Furuhashi T, Takemasa I, Itoh K, Patel PS, Vora HH, Shah B, Patel JB, Rajvik KN, Pandya SJ, Shukla SN, Wang Y, Zhang G, Kawakami Y, Marincola FM, Ascierto PA, Sargent DJ, Fox BA, Galon J. International validation of the consensus

Immunoscore for the classification of colon cancer: a prognostic and accuracy study. *Lancet*. 2018;391(10135):2128-39.

46. Anitei MG, Zeitoun G, Mlecnik B, Marliot F, Haicheur N, Todosi AM, Kirilovsky A, Lagorce C, Bindea G, Ferariu D, Danciu M, Bruneval P, Scripcariu V, Chevallier JM, Zinzindohoué F, Berger A, Galon J, Pagès F. Prognostic and predictive values of the immunoscore in patients with rectal cancer. *Clin Cancer Res*. 2014;20(7):1891-9.

47. Choi J, Maeng HG, Lee SJ, Kim YJ, Kim DW, Lee HN, Namgung JH, Oh HM, Kim TJ, Jeong JE, Park SJ, Choi YM, Kang YW, Yoon SG, Lee JK. Diagnostic value of peripheral blood immune profiling in colorectal cancer. *Ann Surg Treat Res*. 2018;94(6):312-21.

48. Krijgsman D, de Vries NL, Skovbo A, Andersen MN, Swets M, Bastiaannet E, Vahrmeijer AL, van de Velde CJH, Heemskerk MHM, Hokland M, Kuppen PJK. Characterization of circulating T-, NK-, and NKT cell subsets in patients with colorectal cancer: the peripheral blood immune cell profile. *Cancer Immunol Immunother*. 2019;68(6):1011-24.

49. Coffelt SB, Wellenstein MD, de Visser KE. Neutrophils in cancer: neutral no more. *Nature Reviews Cancer*. 2016;16(7):431-46.

50. Governa V, Trella E, Mele V, Tornillo L, Amicarella F, Cremonesi E, Muraro MG, Xu H, Drosler R, Däster SR, Bolli M, Rosso R, Oertli D, Eppenberger-Castori S, Terracciano LM, Iezzi G, Spagnoli GC. The Interplay Between Neutrophils and CD8⁺ T Cells Improves Survival in Human Colorectal Cancer. 2017;23(14):3847-58.

51. Rao HL, Chen JW, Li M, Xiao YB, Fu J, Zeng YX, Cai MY, Xie D. Increased intratumoral neutrophil in colorectal carcinomas correlates closely with malignant phenotype and predicts patients' adverse prognosis. *PLoS One*. 2012;7(1):e30806.

52. Olingy CE, Dinh HQ, Hedrick CC. Monocyte heterogeneity and functions in cancer. *J Leukoc Biol*. 2019;106(2):309-22.

53. Engblom C, Pfirschke C, Pittet MJ. The role of myeloid cells in cancer therapies. *Nat Rev Cancer*. 2016;16(7):447-62.

54. Pinto ML, Rios E, Durães C, Ribeiro R, Machado JC, Mantovani A, Barbosa MA, Carneiro F, Oliveira MJ. The Two Faces of Tumor-Associated Macrophages and Their Clinical Significance in Colorectal Cancer. *Front Immunol*. 2019;10:1875.

55. Rossi S, Basso M, Strippoli A, Schinzari G, D'Argento E, Larocca M, Cassano A, Barone C. Are Markers of Systemic Inflammation Good Prognostic Indicators in Colorectal Cancer? *Clin Colorectal Cancer*. 2017;16(4):264-74.

56. Tan D, Fu Y, Tong W, Li F. Prognostic significance of lymphocyte to monocyte ratio in colorectal cancer: A meta-analysis. *Int J Surg*. 2018;55:128-38.

57. Shibutani M, Maeda K, Nagahara H, Fukuoka T, Nakao S, Matsutani S, Hirakawa K, Ohira M. The peripheral monocyte count is associated with the density of tumor-associated macrophages in the tumor microenvironment of colorectal cancer: a retrospective study. *BMC Cancer*. 2017;17(1):404-.

58. Banchereau J, Steinman RM. Dendritic cells and the control of immunity. *Nature*. 1998;392(6673):245-52.
59. Anguille S, Smits EL, Lion E, van Tendeloo VF, Berneman ZN. Clinical use of dendritic cells for cancer therapy. *Lancet Oncol*. 2014;15(7):e257-67.
60. Subbiah V, Murthy R, Hong DS, Prins RM, Hosing C, Hendricks K, Kolli D, Noffsinger L, Brown R, McGuire M, Fu S, Piha-Paul S, Naing A, Conley AP, Benjamin RS, Kaur I, Bosch ML. Cytokines Produced by Dendritic Cells Administered Intratumorally Correlate with Clinical Outcome in Patients with Diverse Cancers. *Clin Cancer Res*. 2018;24(16):3845-56.
61. Palucka K, Ueno H, Fay J, Banchereau J. Dendritic cells and immunity against cancer. 2011;269(1):64-73.
62. Malietzis G, Lee GH, Jenkins JT, Bernardo D, Moorghen M, Knight SC, Al-Hassi HO. Prognostic Value of the Tumour-Infiltrating Dendritic Cells in Colorectal Cancer: A Systematic Review. *Cell Communication & Adhesion*. 2015;22(1):9-14.
63. Baumann T, Dunkel A, Schmid C, Schmitt S, Hiltensperger M, Lohr K, Laketa V, Donakonda S, Ahting U, Lorenz-Depiereux B, Heil JE, Schredelseker J, Simeoni L, Fecher C, Körber N, Bauer T, Hüser N, Hartmann D, Laschinger M, Eyerich K, Eyerich S, Anton M, Streeter M, Wang T, Schraven B, Spiegel D, Assaad F, Misgeld T, Zischka H, Murray PJ, Heine A, Heikenwälder M, Korn T, Dawid C, Hofmann T, Knolle PA, Höchst B. Regulatory myeloid cells paralyze T cells through cell–cell transfer of the metabolite methylglyoxal. *Nature Immunology*. 2020;21(5):555-66.
64. Kumar V, Patel S, Tcyganov E, Gabrilovich DI. The Nature of Myeloid-Derived Suppressor Cells in the Tumor Microenvironment. *Trends Immunol*. 2016;37(3):208-20.
65. Gabrilovich DI, Nagaraj S. Myeloid-derived suppressor cells as regulators of the immune system. *Nat Rev Immunol*. 2009;9(3):162-74.
66. OuYang LY, Wu XJ, Ye SB, Zhang RX, Li ZL, Liao W, Pan ZZ, Zheng LM, Zhang XS, Wang Z, Li Q, Ma G, Li J. Tumor-induced myeloid-derived suppressor cells promote tumor progression through oxidative metabolism in human colorectal cancer. *J Transl Med*. 2015;13:47.
67. Zhang B, Wang Z, Wu L, Zhang M, Li W, Ding J, Zhu J, Wei H, Zhao K. Circulating and tumor-infiltrating myeloid-derived suppressor cells in patients with colorectal carcinoma. *PLoS One*. 2013;8(2):e57114.
68. Solito S, Falisi E, Diaz-Montero CM, Doni A, Pinton L, Rosato A, Francescato S, Basso G, Zanovello P, Onicescu G, Garrett-Mayer E, Montero AJ, Bronte V, Mandruzzato S. A human promyelocytic-like population is responsible for the immune suppression mediated by myeloid-derived suppressor cells. *Blood*. 2011;118(8):2254-65.
69. Tada K, Kitano S, Shoji H, Nishimura T, Shimada Y, Nagashima K, Aoki K, Hiraoka N, Honma Y, Iwasa S, Okita N, Takashima A, Kato K, Yamada Y, Katayama N, Boku N, Heike Y, Hamaguchi T. Pretreatment Immune Status Correlates with Progression-Free Survival in Chemotherapy-Treated Metastatic Colorectal Cancer

- Patients. *Cancer Immunol Res.* 2016;4(7):592-9.
70. Wang P-F, Song S-Y, Wang T-J, Ji W-J, Li S-W, Liu N, Yan C-X. Prognostic role of pretreatment circulating MDSCs in patients with solid malignancies: A meta-analysis of 40 studies. *Oncoimmunology.* 2018;7(10):e1494113-e.
71. Mundy-Bosse BL, Young GS, Bauer T, Binkley E, Bloomston M, Bill MA, Bekaii-Saab T, Carson WE, 3rd, Lesinski GB. Distinct myeloid suppressor cell subsets correlate with plasma IL-6 and IL-10 and reduced interferon-alpha signaling in CD4⁺ T cells from patients with GI malignancy. *Cancer Immunol Immunother.* 2011;60(9):1269-79.
72. Cooper MA, Fehniger TA, Caligiuri MA. The biology of human natural killer-cell subsets. *Trends Immunol.* 2001;22(11):633-40.
73. Jonges LE, Albertsson P, van Vlierberghe RL, Ensink NG, Johansson BR, van de Velde CJ, Fleuren GJ, Nannmark U, Kuppen PJ. The phenotypic heterogeneity of human natural killer cells: presence of at least 48 different subsets in the peripheral blood. *Scand J Immunol.* 2001;53(2):103-10.
74. Krijgsman D, Hokland M, Kuppen PJK. The Role of Natural Killer T Cells in Cancer—A Phenotypical and Functional Approach. 2018;9(367).
75. Biassoni R, Cantoni C, Pende D, Sivori S, Parolini S, Vitale M, Bottino C, Moretta A. Human natural killer cell receptors and co-receptors. *Immunol Rev.* 2001;181:203-14.
76. Tang YP, Xie MZ, Li KZ, Li JL, Cai ZM, Hu BL. Prognostic value of peripheral blood natural killer cells in colorectal cancer. *BMC Gastroenterol.* 2020;20(1):31.
77. Krijgsman D, De Vries NL, Andersen MN, Skovbo A, Tollenaar RAEM, Bastiaannet E, Kuppen PJK, Hokland M. The effects of tumor resection and adjuvant therapy on the peripheral blood immune cell profile in patients with colon carcinoma. *Cancer Immunology, Immunotherapy.* 2020;This one will be the writing model of non-health control studies.
78. Coca S, Perez-Piqueras J, Martinez D, Colmenarejo A, Saez MA, Vallejo C, Martos JA, Moreno M. The prognostic significance of intratumoral natural killer cells in patients with colorectal carcinoma. *Cancer.* 1997;79(12):2320-8.
79. Melero I, Rouzaut A, Motz GT, Coukos G. T-cell and NK-cell infiltration into solid tumors: a key limiting factor for efficacious cancer immunotherapy. *Cancer Discov.* 2014;4(5):522-6.
80. Tachibana T, Onodera H, Tsuruyama T, Mori A, Nagayama S, Hiai H, Imamura M. Increased intratumor V α 24-positive natural killer T cells: a prognostic factor for primary colorectal carcinomas. *Clin Cancer Res.* 2005;11(20):7322-7.
81. Giraldo NA, Sanchez-Salas R, Peske JD, Vano Y, Becht E, Petitprez F, Validire P, Ingels A, Cathelineau X, Fridman WH, Sautès-Fridman C. The clinical role of the TME in solid cancer. *Br J Cancer.* 2019;120(1):45-53.
82. Fridman WH, Pagès F, Sautès-Fridman C, Galon J. The immune contexture in human tumours: impact on clinical outcome. *Nature Reviews Cancer.* 2012;12(4):298-306.

83. Frey DM, Drosner RA, Viehl CT, Zlobec I, Lugli A, Zingg U, Oertli D, Kettelhack C, Terracciano L, Tornillo L. High frequency of tumor-infiltrating FOXP3(+) regulatory T cells predicts improved survival in mismatch repair-proficient colorectal cancer patients. *Int J Cancer*. 2010;126(11):2635-43.
84. Correale P, Rotundo MS, Del Vecchio MT, Remondo C, Migali C, Ginanneschi C, Tsang KY, Licchetta A, Mannucci S, Loiacono L, Tassone P, Francini G, Tagliaferri P. Regulatory (FoxP3+) T-cell tumor infiltration is a favorable prognostic factor in advanced colon cancer patients undergoing chemo or chemoimmunotherapy. *J Immunother*. 2010;33(4):435-41.
85. Salama P, Phillips M, Grieco F, Morris M, Zeps N, Joseph D, Platell C, Iacopetta B. Tumor-infiltrating FOXP3+ T regulatory cells show strong prognostic significance in colorectal cancer. *J Clin Oncol*. 2009;27(2):186-92.
86. Masugi Y, Nishihara R, Yang J, Mima K, da Silva A, Shi Y, Inamura K, Cao Y, Song M, Nowak JA, Liao X, Noshio K, Chan AT, Giannakis M, Bass AJ, Hodi FS, Freeman GJ, Rodig S, Fuchs CS, Qian ZR, Ogino S. Tumour CD274 (PD-L1) expression and T cells in colorectal cancer. *Gut*. 2017;66(8):1463-73.
87. Tosolini M, Kirilovsky A, Mlecnik B, Fredriksen T, Mamer S, Bindea G, Berger A, Bruneval P, Fridman W-H, Pagès F, Galon J. Clinical Impact of Different Classes of Infiltrating T Cytotoxic and Helper Cells (Th1, Th2, Treg, Th17) in Patients with Colorectal Cancer. 2011;71(4):1263-71.
88. Galon J, Costes A, Sanchez-Cabo F, Kirilovsky A, Mlecnik B, Lagorce-Pagès C, Tosolini M, Camus M, Berger A, Wind P, Zinzindohoué F, Bruneval P, Cugnenc PH, Trajanoski Z, Fridman WH, Pagès F. Type, density, and location of immune cells within human colorectal tumors predict clinical outcome. *Science*. 2006;313(5795):1960-4.
89. Liu J, Duan Y, Cheng X, Chen X, Xie W, Long H, Lin Z, Zhu B. IL-17 is associated with poor prognosis and promotes angiogenesis via stimulating VEGF production of cancer cells in colorectal carcinoma. *Biochem Biophys Res Commun*. 2011;407(2):348-54.
90. Yoshida N, Kinugasa T, Miyoshi H, Sato K, Yuge K, Ohchi T, Fujino S, Shiraiwa S, Katagiri M, Akagi Y, Ohshima K. A High ROR γ T/CD3 Ratio is a Strong Prognostic Factor for Postoperative Survival in Advanced Colorectal Cancer: Analysis of Helper T Cell Lymphocytes (Th1, Th2, Th17 and Regulatory T Cells). *Ann Surg Oncol*. 2016;23(3):919-27.
91. Dylag-Trojanowska K, Rogala J, Pach R, Siedlar M, Baran J, Sierzega M, Zybaczynska J, Lenart M, Rutkowska-Zapala M, Szczepanik AM. T Regulatory CD4(+)CD25(+)FoxP3(+) Lymphocytes in the Peripheral Blood of Left-Sided Colorectal Cancer Patients. *Medicina (Kaunas)*. 2019;55(6).
92. Tokunaga R, Naseem M, Lo JH, Battaglin F, Soni S, Puccini A, Berger MD, Zhang W, Baba H, Lenz H-J. B cell and B cell-related pathways for novel cancer treatments. *Cancer treatment reviews*. 2019;73:10-9.
93. Shimabukuro-Vornhagen A, Schlosser HA, Gryschock L, Malcher J, Wennhold K,

Garcia-Marquez M, Herbold T, Neuhaus LS, Becker HJ, Fiedler A, Scherwitz P, Koslowsky T, Hake R, Stippel DL, Holscher AH, Eidt S, Hallek M, Theurich S, von Bergwelt-Baildon MS. Characterization of tumor-associated B-cell subsets in patients with colorectal cancer. *Oncotarget*. 2014;5(13):4651-64.

94. Edin S, Kaprio T, Hagström J, Larsson P, Mustonen H, Böckelman C, Strigård K, Gunnarsson U, Haglund C, Palmqvist R. The Prognostic Importance of CD20(+) B lymphocytes in Colorectal Cancer and the Relation to Other Immune Cell subsets. *Sci Rep*. 2019;9(1):19997-.

95. Bindea G, Mlecnik B, Tosolini M, Kirilovsky A, Waldner M, Obenauf AC, Angell H, Fredriksen T, Lafontaine L, Berger A, Bruneval P, Fridman WH, Becker C, Pagès F, Speicher MR, Trajanoski Z, Galon J. Spatiotemporal dynamics of intratumoral immune cells reveal the immune landscape in human cancer. *Immunity*. 2013;39(4):782-95.

96. Wu Z, Zhang Z, Lei Z, Lei P. CD14: Biology and role in the pathogenesis of disease. *Cytokine Growth Factor Rev*. 2019;48:24-31.

97. Marini O, Costa S, Bevilacqua D, Calzetti F, Tamassia N, Spina C, De Sabata D, Tinazzi E, Lunardi C, Scupoli MT, Cavallini C, Zoratti E, Tinazzi I, Marchetta A, Vassanelli A, Cantini M, Gandini G, Ruzzenente A, Guglielmi A, Missale F, Vermi W, Tecchio C, Cassatella MA, Scapini P. Mature CD10⁺ and immature CD10⁻ neutrophils present in G-CSF-treated donors display opposite effects on T cells. *Blood*. 2017;129(10):1343-56.

98. Cossarizza A, Chang HD, Radbruch A, Acs A, Adam D, Adam-Klages S, Agace WW, Aghaepour N, Akdis M, Allez M, Almeida LN, Alvisi G, Anderson G, Andrä I, Annunziato F, Anselmo A, Bacher P, Baldari CT, Bari S, Barnaba V, Barros-Martins J, Battistini L, Bauer W, Baumgart S, Baumgarth N, Baumjohann D, Baying B, Bebawy M, Becher B, Beisker W, Benes V, Beyaert R, Blanco A, Boardman DA, Bogdan C, Borger JG, Borsellino G, Boulais PE, Bradford JA, Brenner D, Brinkman RR, Brooks AES, Busch DH, Büscher M, Bushnell TP, Calzetti F, Cameron G, Cammarata I, Cao X, Cardell SL, Casola S, Cassatella MA, Cavani A, Celada A, Chatenoud L, Chattopadhyay PK, Chow S, Christakou E, Čičin-Šain L, Clerici M, Colombo FS, Cook L, Cooke A, Cooper AM, Corbett AJ, Cosma A, Cosmi L, Coulie PG, Cumano A, Cvetkovic L, Dang VD, Dang-Heine C, Davey MS, Davies D, De Biasi S, Del Zotto G, Dela Cruz GV, Delacher M, Della Bella S, Dellabona P, Deniz G, Dessing M, Di Santo JP, Diefenbach A, Dieli F, Dolf A, Dörner T, Dress RJ, Dudziak D, Dustin M, Dutertre CA, Ebner F, Eckle SBG, Edinger M, Eede P, Ehrhardt GRA, Eich M, Engel P, Engelhardt B, Erdei A, Esser C, Everts B, Evrard M, Falk CS, Fehniger TA, Felipe-Benavent M, Ferry H, Feuerer M, Filby A, Filkor K, Fillatreau S, Follo M, Förster I, Foster J, Foulds GA, Frehse B, Frenette PS, Frischbutter S, Fritzsche W, Galbraith DW, Gangaev A, Garbi N, Gaudilliere B, Gazzinelli RT, Geginat J, Gerner W, Gherardin NA, Ghoreschi K, Gibellini L, Ginhoux F, Goda K, Godfrey DI, Goettlinger C, González-Navajas JM, Goodyear CS, Gori A, Grogan JL, Grummitt D, Grützkau A, Haftmann C, Hahn J, Hammad H,

Hämmerling G, Hansmann L, Hansson G, Harpur CM, Hartmann S, Hauser A, Hauser AE, Haviland DL, Hedley D, Hernández DC, Herrera G, Herrmann M, Hess C, Höfer T, Hoffmann P, Hogquist K, Holland T, Höllt T, Holmdahl R, Hombrink P, Houston JP, Hoyer BF, Huang B, Huang FP, Huber JE, Huehn J, Hundemer M, Hunter CA, Hwang WYK, Iannone A, Ingelfinger F, Ivison SM, Jäck HM, Jani PK, Jávega B, Jonjic S, Kaiser T, Kalina T, Kamradt T, Kaufmann SHE, Keller B, Ketelaars SLC, Khalilnezhad A, Khan S, Kisielow J, Klenerman P, Knopf J, Koay HF, Kobow K, Kolls JK, Kong WT, Kopf M, Korn T, Kriegsmann K, Kristyanto H, Kroneis T, Krueger A, Kühne J, Kukat C, Kunkel D, Kunze-Schumacher H, Kurosaki T, Kurts C, Kvistborg P, Kwok I, Landry J, Lantz O, Lanuti P, LaRosa F, Lehuen A, LeibundGut-Landmann S, Leipold MD, Leung LYT, Levings MK, Lino AC, Liotta F, Litwin V, Liu Y, Ljunggren HG, Lohoff M, Lombardi G, Lopez L, López-Botet M, Lovett-Racke AE, Lubberts E, Luche H, Ludewig B, Lugli E, Lunemann S, Maecker HT, Maggi L, Maguire O, Mair F, Mair KH, Mantovani A, Manz RA, Marshall AJ, Martínez-Romero A, Martrus G, Marventano I, Maslinski W, Matarese G, Mattioli AV, Maueröder C, Mazzoni A, McCluskey J, McGrath M, McGuire HM, McInnes IB, Mei HE, Melchers F, Melzer S, Mielenz D, Miller SD, Mills KHG, Minderman H, Mjösberg J, Moore J, Moran B, Moretta L, Mosmann TR, Müller S, Multhoff G, Muñoz LE, Münz C, Nakayama T, Nasi M, Neumann K, Ng LG, Niedobitek A, Nourshargh S, Núñez G, O'Connor JE, Ochel A, Oja A, Ordonez D, Orfao A, Orłowski-Oliver E, Ouyang W, Oxenius A, Palankar R, Panse I, Pattanapanyasat K, Paulsen M, Pavlinic D, Penter L, Peterson P, Peth C, Petriz J, Piancone F, Pickl WF, Piconese S, Pinti M, Pockley AG, Podolska MJ, Poon Z, Pracht K, Prinz I, Pucillo CEM, Quataert SA, Quatrini L, Quinn KM, Radbruch H, Radstake T, Rahmig S, Rahn HP, Rajwa B, Ravichandran G, Raz Y, Rebhahn JA, Recktenwald D, Reimer D, Reis e Sousa C, Remmerswaal EBM, Richter L, Rico LG, Riddell A, Rieger AM, Robinson JP, Romagnani C, Rubartelli A, Ruland J, Saalmüller A, Saeys Y, Saito T, Sakaguchi S, Sala-de-Oyanguren F, Samstag Y, Sanderson S, Sandrock I, Santoni A, Sanz RB, Saresella M, Sautes-Fridman C, Sawitzki B, Schadt L, Scheffold A, Scherer HU, Schiemann M, Schildberg FA, Schimisky E, Schlitzer A, Schlosser J, Schmid S, Schmitt S, Schober K, Schraivogel D, Schuh W, Schüler T, Schulte R, Schulz AR, Schulz SR, Scottá C, Scott-Algara D, Sester DP, Shankey TV, Silva-Santos B, Simon AK, Sitnik KM, Sozzani S, Speiser DE, Spidlen J, Stahlberg A, Stall AM, Stanley N, Stark R, Stehle C, Steinmetz T, Stockinger H, Takahama Y, Takeda K, Tan L, Tárnok A, Tiegs G, Toldi G, Tornack J, Traggiai E, Trebak M, Tree TIM, Trotter J, Trowsdale J, Tsoumakidou M, Ulrich H, Urbanczyk S, van de Veen W, van den Broek M, van der Pol E, Van Gassen S, Van Isterdael G, van Lier RAW, Veldhoen M, Vento-Asturias S, Vieira P, Voehringer D, Volk HD, von Borstel A, von Volkman K, Waisman A, Walker RV, Wallace PK, Wang SA, Wang XM, Ward MD, Ward-Hartstonge KA, Warnatz K, Warnes G, Warth S, Waskow C, Watson JV, Watzl C, Wegener L, Weisenburger T, Wiedemann A, Wienands J, Wilharm A, Wilkinson RJ, Willmsky G, Wing JB, Winkelmann R, Winkler TH, Wirz OF, Wong A, Wurst P,

Yang JHM, Yang J, Yazdanbakhsh M, Yu L, Yue A, Zhang H, Zhao Y, Ziegler SM, Zielinski C, Zimmermann J, Zychlinsky A. Guidelines for the use of flow cytometry and cell sorting in immunological studies (second edition). *Eur J Immunol*. 2019;49(10):1457-973.

99. Jakubzick CV, Randolph GJ, Henson PM. Monocyte differentiation and antigen-presenting functions. *Nature Reviews Immunology*. 2017;17(6):349-62.

100. Guillemins M, Mildner A, Yona S. Developmental and Functional Heterogeneity of Monocytes. *Immunity*. 2018;49(4):595-613.

101. Ssemaganda A, Kindinger L, Bergin P, Nielsen L, Mpendo J, Ssetaala A, Kiwanuka N, Munder M, Teoh TG, Kropf P, Müller I. Characterization of neutrophil subsets in healthy human pregnancies. *PLoS One*. 2014;9(2):e85696-e.

102. Veglia F, Perego M, Gabrilovich D. Myeloid-derived suppressor cells coming of age. *Nature Immunology*. 2018;19(2):108-19.

103. Dumitru CA, Moses K, Trellakis S, Lang S, Brandau S. Neutrophils and granulocytic myeloid-derived suppressor cells: immunophenotyping, cell biology and clinical relevance in human oncology. *Cancer Immunology, Immunotherapy*. 2012;61(8):1155-67.

104. Bronte V, Brandau S, Chen S-H, Colombo MP, Frey AB, Greten TF, Mandruzzato S, Murray PJ, Ochoa A, Ostrand-Rosenberg S, Rodriguez PC, Sica A, Umansky V, Vonderheide RH, Gabrilovich DI. Recommendations for myeloid-derived suppressor cell nomenclature and characterization standards. *Nature communications*. 2016;7(1):12150.

105. Cichocki F, Grzywacz B, Miller JS. Human NK Cell Development: One Road or Many? *Frontiers in immunology*. 2019;10:2078-.

106. Dutertre C-A, Bonnin-Gélizé E, Pulford K, Bourel D, Fridman W-H, Teillaud J-L. A novel subset of NK cells expressing high levels of inhibitory FcγRIIB modulating antibody-dependent function. *J Leukoc Biol*. 2008;84(6):1511-20.

107. Addison EG, North J, Bakhsh I, Marden C, Haq S, Al-Sarraj S, Malayeri R, Wickremasinghe RG, Davies JK, Lowdell MW. Ligation of CD8α on human natural killer cells prevents activation-induced apoptosis and enhances cytolytic activity. *Immunology*. 2005;116(3):354-61.

108. Borrego F, Robertson MJ, Ritz J, Peña J, Solana R. CD69 is a stimulatory receptor for natural killer cell and its cytotoxic effect is blocked by CD94 inhibitory receptor. *Immunology*. 1999;97(1):159-65.

109. Förster R, Davalos-Misslitz AC, Rot A. CCR7 and its ligands: balancing immunity and tolerance. *Nat Rev Immunol*. 2008;8(5):362-71.

110. Sallusto F, Lenig D, Förster R, Lipp M, Lanzavecchia A. Two subsets of memory T lymphocytes with distinct homing potentials and effector functions. *Nature*. 1999;401(6754):708-12.

111. Kar A, Mehrotra S, Chatterjee S. CD38: T Cell Immuno-Metabolic Modulator. *Cells*. 2020;9(7):1716.

112. Viallard J-F, Blanco P, André M, Etienne G, Liferman F, Neau D, Vidal E,

Moreau J-F, Pellegrin J-LJCI. CD8⁺ HLA-DR⁺ T lymphocytes are increased in common variable immunodeficiency patients with impaired memory B-cell differentiation. 2006;119(1):51-8.

113. Baecher-Allan C, Wolf E, Hafler DAJTJoI. MHC class II expression identifies functionally distinct human regulatory T cells. 2006;176(8):4622-31.

114. Yoshie O. CCR4 as a Therapeutic Target for Cancer Immunotherapy. *Cancers (Basel)*. 2021;13(21):5542.

115. Walker JA, McKenzie ANJ. TH2 cell development and function. *Nature Reviews Immunology*. 2018;18(2):121-33.

116. Acosta-Rodriguez EV, Rivino L, Geginat J, Jarrossay D, Gattorno M, Lanzavecchia A, Sallusto F, Napolitani G. Surface phenotype and antigenic specificity of human interleukin 17-producing T helper memory cells. *Nat Immunol*. 2007;8(6):639-46.

117. Finak G, Langweiler M, Jaimes M, Malek M, Taghiyar J, Korin Y, Raddassi K, Devine L, Obermoser G, Pekalski ML, Pontikos N, Diaz A, Heck S, Villanova F, Terrazzini N, Kern F, Qian Y, Stanton R, Wang K, Brandes A, Ramey J, Aghaeepour N, Mosmann T, Scheuermann RH, Reed E, Palucka K, Pascual V, Blomberg BB, Nestle F, Nussenblatt RB, Brinkman RR, Gottardo R, Maecker H, McCoy JP. Standardizing Flow Cytometry Immunophenotyping Analysis from the Human Immunophenotyping Consortium. *Sci Rep*. 2016;6(1):20686.

118. Banham AH. Cell-surface IL-7 receptor expression facilitates the purification of FOXP3(+) regulatory T cells. *Trends Immunol*. 2006;27(12):541-4.

119. Sato S, Steeber DA, Jansen PJ, Tedder TF. CD19 expression levels regulate B lymphocyte development: human CD19 restores normal function in mice lacking endogenous CD19. *J Immunol*. 1997;158(10):4662-9.

120. Sato S, Ono N, Steeber DA, Pisetsky DS, Tedder TF. CD19 regulates B lymphocyte signaling thresholds critical for the development of B-1 lineage cells and autoimmunity. *J Immunol*. 1996;157(10):4371-8.

121. Pieper K, Grimbacher B, Eibel HJTJoa, immunology c. B-cell biology and development. 2013;131(4):959-71.

122. Schoenberg MB, Zhu T, Hao J, Bucher JN, Li X, Li X, Han Y, Koliogiannis D, Svihla M, Guba MO, Werner J, Bazhin AV. Highly differential count of circulating and tumor infiltrating immune cells in patients with non-HCV/non-HBV hepatocellular carcinoma. *Cancer Immunol Immunother*. 2021.

123. Sims GP, Ettinger R, Shirota Y, Yarboro CH, Illei GG, Lipsky PE. Identification and characterization of circulating human transitional B cells. *Blood*. 2005;105(11):4390-8.

124. King LB, Monroe JG. Immunobiology of the immature B cell: plasticity in the B-cell antigen receptor-induced response fine tunes negative selection. *Immunol Rev*. 2000;176:86-104.

125. Carsetti R, Köhler G, Lamers MC. Transitional B cells are the target of negative selection in the B cell compartment. *The Journal of experimental medicine*.

- 1995;181(6):2129-40.
126. Bemark M. Translating transitions - how to decipher peripheral human B cell development. *Journal of biomedical research*. 2015;29(4):264-84.
127. Pieper K, Grimbacher B, Eibel H. B-cell biology and development. *J Allergy Clin Immunol*. 2013;131(4):959-71.
128. Capolunghi F, Rosado M, Sinibaldi M, Aranburu A, Carsetti RJII. Why do we need IgM memory B cells? 2013;152(2):114-20.
129. Elizabeth, Mauri C. Regulatory B Cells: Origin, Phenotype, and Function. *Immunity*. 2015;42(4):607-12.
130. Maecker HT, Trotter J. Flow cytometry controls, instrument setup, and the determination of positivity. *Cytometry Part A*. 2006;69A(9):1037-42.
131. R Core Team. R: A Language and Environment for Statistical Computing. R Foundation for Statistical Computing, Vienna, Austria. 2021; URL <https://www.R-project.org/>.
132. Meyer D, Dimitriadou E, Hornik K, Weingessel A, Leisch F. e1071: Misc Functions of the Department of Statistics, Probability Theory Group (Formerly: E1071), TU Wien. R package version 17-9. 2021; <https://CRAN.R-project.org/package=e1071>.
133. Robin X, Turck N, Hainard A, Tiberti N, Lisacek F, Sanchez J-C, Müller M. pROC: an open-source package for R and S+ to analyze and compare ROC curves. *BMC Bioinformatics*. 2011;12(1):77.
134. Wickham H. *ggplot2: Elegant Graphics for Data Analysis*. Springer-Verlag New York. 2016; <https://ggplot2.tidyverse.org>.
135. Davis S, Meltzer PS. GEOquery: a bridge between the Gene Expression Omnibus (GEO) and BioConductor. *Bioinformatics*. 2007;23(14):1846-7.
136. Leek JT, Johnson WE, Parker HS, Jaffe AE, Storey JD. The sva package for removing batch effects and other unwanted variation in high-throughput experiments. *Bioinformatics*. 2012;28(6):882-3.
137. Ritchie ME, Phipson B, Wu D, Hu Y, Law CW, Shi W, Smyth GK. limma powers differential expression analyses for RNA-sequencing and microarray studies. *Nucleic acids research*. 2015;43(7):e47-e.
138. Aran D, Hu Z, Butte AJ. xCell: digitally portraying the tissue cellular heterogeneity landscape. *Genome Biology*. 2017;18(1):220.
139. Love MI, Huber W, Anders S. Moderated estimation of fold change and dispersion for RNA-seq data with DESeq2. *Genome Biology*. 2014;15(12):550.
140. Yu G, Wang LG, Han Y, He QY. clusterProfiler: an R package for comparing biological themes among gene clusters. *Omics*. 2012;16(5):284-7.
141. Xie Y, Xie F, Zhang L, Zhou X, Huang J, Wang F, Jin J, Zhang L, Zeng L, Zhou F. Targeted Anti-Tumor Immunotherapy Using Tumor Infiltrating Cells. *Adv Sci (Weinh)*. 2021;8(22):e2101672-e.
142. Ma T, Renz BW, Ilmer M, Koch D, Yang Y, Werner J, Bazhin AV. Myeloid-Derived Suppressor Cells in Solid Tumors. *Cells*. 2022;11(2):310.

143. Dylag-Trojanowska K, Rogala J, Pach R, Siedlar M, Baran J, Sierzega M, Zybaczynska J, Lenart M, Rutkowska-Zapala M, Szczepanik AM. T Regulatory CD4(+)CD25(+)FoxP3(+) Lymphocytes in the Peripheral Blood of Left-Sided Colorectal Cancer Patients. *Medicina (Kaunas, Lithuania)*. 2019;55(6):307.
144. Krijgsman D, De Vries NL, Andersen MN, Skovbo A, Tollenaar RAEM, Møller HJ, Hokland M, Kuppen PJK. CD163 as a Biomarker in Colorectal Cancer: The Expression on Circulating Monocytes and Tumor-Associated Macrophages, and the Soluble Form in the Blood. *Int J Mol Sci*. 2020;21(16):5925.
145. Narasimhan PB, Eggert T, Zhu YP, Marcovecchio P, Meyer MA, Wu R, Hedrick CC. Patrolling Monocytes Control NK Cell Expression of Activating and Stimulatory Receptors to Curtail Lung Metastases. 2020;204(1):192-8.
146. Hanna RN, Cekic C, Sag D, Tacke R, Thomas GD, Nowyhed H, Herrley E, Rasquinha N, McArdle S, Wu R, Peluso E, Metzger D, Ichinose H, Shaked I, Chodaczek G, Biswas SK, Hedrick CC. Patrolling monocytes control tumor metastasis to the lung. 2015;350(6263):985-90.
147. Rosales C. Neutrophil: A Cell with Many Roles in Inflammation or Several Cell Types? 2018;9.
148. Bene NC, Alcaide P, Wortis HH, Jaffe IZ. Mineralocorticoid receptors in immune cells: emerging role in cardiovascular disease. *Steroids*. 2014;91:38-45.
149. Racioppi L, Means AR. Calcium/calmodulin-dependent kinase IV in immune and inflammatory responses: novel routes for an ancient traveller. *Trends Immunol*. 2008;29(12):600-7.
150. Koga T, Hedrich CM, Mizui M, Yoshida N, Otomo K, Lieberman LA, Rauen T, Crispín JC, Tsokos GC. CaMK4-dependent activation of AKT/mTOR and CREM- α underlies autoimmunity-associated Th17 imbalance. *J Clin Invest*. 2014;124(5):2234-45.
151. Koga T, Kawakami A. The role of CaMK4 in immune responses. *Modern Rheumatology*. 2018;28(2):211-4.
152. Kirchgessner H, Dietrich J, Scherer J, Isomäki P, Korinek V, Hilgert I, Bruyns E, Leo A, Cope AP, Schraven B. The transmembrane adaptor protein TRIM regulates T cell receptor (TCR) expression and TCR-mediated signaling via an association with the TCR zeta chain. *The Journal of experimental medicine*. 2001;193(11):1269-84.
153. Valk E, Leung R, Kang H, Kaneko K, Rudd CE, Schneider H. T cell receptor-interacting molecule acts as a chaperone to modulate surface expression of the CTLA-4 coreceptor. *Immunity*. 2006;25(5):807-21.
154. Gallois C, Pernot S, Zaanen A, Taieb J. Colorectal Cancer: Why Does Side Matter? *Drugs*. 2018;78(8):789-98.
155. Stintzing S, Tejpar S, Gibbs P, Thiebach L, Lenz H-J. Understanding the role of primary tumour localisation in colorectal cancer treatment and outcomes. *Eur J Cancer*. 2017;84:69-80.
156. Missiaglia E, Jacobs B, D'Ario G, Di Narzo AF, Sonesson C, Budinska E,

Popovici V, Vecchione L, Gerster S, Yan P, Roth AD, Klingbiel D, Bosman FT, Delorenzi M, Tejpar S. Distal and proximal colon cancers differ in terms of molecular, pathological, and clinical features. *Ann Oncol.* 2014;25(10):1995-2001.

157. Benedix F, Kube R, Meyer F, Schmidt U, Gastinger I, Lippert H, Group tCRCS. Comparison of 17,641 Patients With Right- and Left-Sided Colon Cancer: Differences in Epidemiology, Perioperative Course, Histology, and Survival. *2010;53(1):57-64.*

158. Sinicrope FA, Mahoney MR, Yoon HH, Smyrk TC, Thibodeau SN, Goldberg RM, Nelson GD, Sargent DJ, Alberts SR. Analysis of Molecular Markers by Anatomic Tumor Site in Stage III Colon Carcinomas from Adjuvant Chemotherapy Trial NCCTG N0147 (Alliance). *Clin Cancer Res.* 2015;21(23):5294-304.

159. Nitsche U, Stögbauer F, Späth C, Haller B, Wilhelm D, Friess H, Bader FG. Right Sided Colon Cancer as a Distinct Histopathological Subtype with Reduced Prognosis. *Dig Surg.* 2016;33(2):157-63.

160. Mouradov D, Sloggett C, Jorissen RN, Love CG, Li S, Burgess AW, Arango D, Strausberg RL, Buchanan D, Wormald S, O'Connor L, Wilding JL, Bicknell D, Tomlinson IP, Bodmer WF, Mariadason JM, Sieber OM. Colorectal cancer cell lines are representative models of the main molecular subtypes of primary cancer. *Cancer Res.* 2014;74(12):3238-47.

161. Lee MS, McGuffey EJ, Morris JS, Manyam G, Baladandayuthapani V, Wei W, Morris VK, Overman MJ, Maru DM, Jiang ZQ, Hamilton SR, Kopetz S. Association of CpG island methylator phenotype and EREG/AREG methylation and expression in colorectal cancer. *Br J Cancer.* 2016;114(12):1352-61.

162. Engstrom PF, Arnoletti JP, Benson AB, 3rd, Chen YJ, Choti MA, Cooper HS, Covey A, Dilawari RA, Early DS, Enzinger PC, Fakih MG, Fleshman J, Jr., Fuchs C, Grem JL, Kiel K, Knol JA, Leong LA, Lin E, Mulcahy MF, Rao S, Ryan DP, Saltz L, Shibata D, Skibber JM, Sofocleous C, Thomas J, Venook AP, Willett C. NCCN Clinical Practice Guidelines in Oncology: colon cancer. *J Natl Compr Canc Netw.* 2009;7(8):778-831.

163. Tejpar S, Stintzing S, Ciardiello F, Tabernero J, Van Cutsem E, Beier F, Esser R, Lenz H-J, Heinemann V. Prognostic and Predictive Relevance of Primary Tumor Location in Patients With RAS Wild-Type Metastatic Colorectal Cancer: Retrospective Analyses of the CRYSTAL and FIRE-3 Trials. *JAMA Oncol.* 2017;3(2):194-201.

164. Petrelli F, Tomasello G, Borgonovo K, Ghidini M, Turati L, Dallera P, Passalacqua R, Sgroi G, Barni S. Prognostic Survival Associated With Left-Sided vs Right-Sided Colon Cancer: A Systematic Review and Meta-analysis. *JAMA Oncol.* 2017;3(2):211-9.

165. Wang K, Fan X, Fan Y, Wang B, Han L, Hou Y. Study on the function of circulating plasmacytoid dendritic cells in the immunoactive phase of patients with chronic genotype B and C HBV infection. *J Viral Hepat.* 2007;14(4):276-82.

166. Fang Q, Deng Y, Liang R, Mei Y, Hu Z, Wang J, Sun J, Zhang X, Bellanti JA, Zheng SG. CD19(+)/CD24(hi)/CD38(hi) regulatory B cells: a potential immune predictive marker of severity and therapeutic responsiveness of hepatitis C. *Am J Transl Res.* 2020;12(3):889-900.
167. Ge J, Wang K, Meng QH, Qi ZX, Meng FL, Fan YC. Implication of Th17 and Th1 cells in patients with chronic active hepatitis B. *J Clin Immunol.* 2010;30(1):60-7.
168. Chen M, Zhang D, Zhen W, Shi Q, Liu Y, Ling N, Peng M, Tang K, Hu P, Hu H, Ren H. Characteristics of circulating T cell receptor gamma-delta T cells from individuals chronically infected with hepatitis B virus (HBV): an association between V(delta)2 subtype and chronic HBV infection. *J Infect Dis.* 2008;198(11):1643-50.
169. Choi YS, Lee J, Lee HW, Chang DY, Sung PS, Jung MK, Park JY, Kim JK, Lee JI, Park H, Cheong JY, Suh KS, Kim HJ, Lee JS, Kim KA, Shin EC. Liver injury in acute hepatitis A is associated with decreased frequency of regulatory T cells caused by Fas-mediated apoptosis. *Gut.* 2015;64(8):1303-13.
170. Vacchi E, Burrello J, Burrello A, Bolis S, Monticone S, Barile L, Kaelin-Lang A, Melli G. Profiling Inflammatory Extracellular Vesicles in Plasma and Cerebrospinal Fluid: An Optimized Diagnostic Model for Parkinson's Disease. 2021;9(3):230.
171. Vacchi E, Burrello J, Di Silvestre D, Burrello A, Bolis S, Mauri P, Vassalli G, Cereda CW, Farina C, Barile L, Kaelin-Lang A, Melli G. Immune profiling of plasma-derived extracellular vesicles identifies Parkinson disease. *Neurology(R) neuroimmunology & neuroinflammation.* 2020;7(6).
172. Yang X, Song X, Zhang X, Shankar V, Wang S, Yang Y, Chen S, Zhang L, Ni Y, Zare RN, Hu Q. In situ DESI-MSI lipidomic profiles of mucosal margin of oral squamous cell carcinoma. *EBioMedicine.* 2021;70:103529.

7. Appendix

Table 8 Identification of circulating immune subsets to differentiate CRC patients from healthy controls through univariable logistic regression

Immune cells	<i>P</i> value
B_Leucocytes	0.053
Pre_B	0.23
Transitional_B	0.179
Plasmablast_B	0.187
NCSM_B	0.869
CSM_B	0.894
Naive_B	0.475
Breg_B10_B	0.086
Breg_Immature_B	0.438
T_Leucocytes	0.021
CD8T_Leucocytes	0.076
Activated_CD8T	0.021
Naive_CD8T	0.803
EM_CD8T	0.579
E_CD8T	0.522
CM_CD8T	0.152
Th_Leucocytes	0.012
Activated_Th	0.018
Naive_Th	0.017
EM_Th	0.034
E_Th	0.037
CM_Th	0.007
Th1_Th	0.739
Th2_Th	0.567
Th17_Th	0.853
Tregs_Th	0.221
Naive_Tregs	0.062
Memory_Tregs	0.066
Activated_Tregs	0.645
Non-Classical Monocyte_Leucocytes	0.038
Intermediate Monocyte_Leucocytes	0.453
Classical Monocyte_Leucocytes	0.639
Total Monocyte_Leucocytes	0.328
Neutrophil_Leucocytes	0.184
NK_Leucocytes	0.628

CD56 ^{dim} _NK	0.268
CD69_CD56 ^{dim} NK	0.568
CD16_CD56 ^{dim} NK	0.076
CD8_CD56 ^{dim} NK	0.778
CD56 ^{bright} _NK	0.269
CD69_CD56 ^{bright} NK	0.944
CD16_CD56 ^{bright} NK	0.172
CD8_CD56 ^{bright} NK	0.681
NKT_Leucocytes	0.345
CD69_NKT	0.594
CD16_NKT	0.693
CD8_NKT	0.107
DC_Leucocytes	0.079
MDSC_Leucocytes	0.349
PMN.MDSC_MDSC	0.006
M.MDSC_MDSC	0.058
Early-stage MDSC	0.037

Note: Each immune subset was expressed as the percentage of source cells annotated following the underscore.

Abbreviation: NCSM: non-class switched memory; CSM: class switched memory; Breg, regulatory B cells; EM, effector memory; E, effector; CM, central memory; Tregs, regulatory T cells; NK, natural killer; NKT, natural killer T; DC, Dendritic cell; PMN.MDSC, polymorphonuclear MDSC; M.MDSC, mononuclear MDSC.

Table 9 Correlation analysis between circulating Th cells and common DEGs in healthy controls

Genes	Immune cells	Correlation coefficient	<i>P</i> -value
GRINA	Th cells	-0.51	2.07E-05
PDCD4	Th cells	0.65	1.24E-08
MIER3	Th cells	0.65	9.88E-09
NR3C2	Th cells	0.81	8.88E-16
ABHD3	Th cells	0.21	1.09E-01
NAP1L2	Th cells	0.66	4.26E-09
P2RY14	Th cells	0.44	3.21E-04
GIMAP7	Th cells	0.73	1.25E-11
ACADM	Th cells	0.69	5.76E-10
PRKACB	Th cells	0.77	3.04E-13
MGAT4A	Th cells	0.69	4.99E-10
GPRASP1	Th cells	0.65	1.48E-08
NAP1L3	Th cells	0.69	4.09E-10
SYTL2	Th cells	0.37	2.83E-03
KLRB1	Th cells	0.60	2.17E-07
BEX4	Th cells	0.63	4.87E-08
KLRF1	Th cells	0.40	1.23E-03
MS4A1	Th cells	0.55	3.39E-06
SH2D1B	Th cells	0.11	4.02E-01
TGFBR3	Th cells	0.15	2.36E-01
CAMK4	Th cells	0.83	0.00E+00
FCRL3	Th cells	0.39	1.82E-03
SMCHD1	Th cells	-0.11	3.95E-01
CD96	Th cells	0.77	3.14E-13
P2RY10	Th cells	0.67	1.82E-09
ZNF304	Th cells	0.50	3.40E-05
RGS18	Th cells	0.13	2.96E-01
ABCA5	Th cells	0.55	3.06E-06
GZMA	Th cells	0.54	6.13E-06

CD52	Th cells	0.71	7.96E-11
ZNF831	Th cells	0.37	2.82E-03
GIMAP5	Th cells	0.32	1.22E-02
THEMIS	Th cells	0.73	1.39E-11
EVI2A	Th cells	0.52	1.26E-05
GPR183	Th cells	0.80	8.44E-15
TRAT1	Th cells	0.83	0.00E+00
ZNF439	Th cells	0.58	7.30E-07
CD69	Th cells	0.69	6.96E-10
GPR174	Th cells	0.71	1.22E-10

Abbreviation: Th cells, T helper cells.

Table 10 Correlation analysis between circulating Th cells and common DEGs in CRC patients

Genes	Immune cells	Correlation coefficient	<i>P</i> -value
GRINA	Th cells	-0.64	8.78E-10
PDCD4	Th cells	0.77	3.11E-15
MIER3	Th cells	0.63	3.00E-09
NR3C2	Th cells	0.87	0.00E+00
ABHD3	Th cells	0.33	4.21E-03
NAP1L2	Th cells	0.63	2.96E-09
P2RY14	Th cells	0.39	5.93E-04
GIMAP7	Th cells	0.84	0.00E+00
ACADM	Th cells	0.68	2.96E-11
PRKACB	Th cells	0.77	2.66E-15
MGAT4A	Th cells	0.61	8.06E-09
GPRASP1	Th cells	0.72	5.09E-13
NAP1L3	Th cells	0.76	8.88E-15
SYTL2	Th cells	0.61	9.26E-09
KLRB1	Th cells	0.67	1.27E-10
BEX4	Th cells	0.73	3.44E-13
KLRF1	Th cells	0.66	1.65E-10

MS4A1	Th cells	0.64	7.71E-10
SH2D1B	Th cells	0.50	6.13E-06
TGFBR3	Th cells	0.58	9.26E-08
CAMK4	Th cells	0.85	0.00E+00
FCRL3	Th cells	0.58	9.12E-08
SMCHD1	Th cells	0.08	5.14E-01
CD96	Th cells	0.82	0.00E+00
P2RY10	Th cells	0.77	1.11E-15
ZNF304	Th cells	0.68	2.42E-11
RGS18	Th cells	0.18	1.32E-01
ABCA5	Th cells	0.57	1.06E-07
GZMA	Th cells	0.63	2.16E-09
CD52	Th cells	0.60	2.59E-08
ZNF831	Th cells	0.70	3.95E-12
GIMAP5	Th cells	0.54	9.13E-07
THEMIS	Th cells	0.80	0.00E+00
EVI2A	Th cells	0.32	5.11E-03
GPR183	Th cells	0.88	0.00E+00
TRAT1	Th cells	0.86	0.00E+00
ZNF439	Th cells	0.68	3.25E-11
CD69	Th cells	0.70	4.48E-12
GPR174	Th cells	0.77	3.11E-15

Abbreviation: Th cells, T helper cells.

Acknowledgement

I would first like to express my sincere gratitude to Prof. Dr. Alexandr Bazhin and Prof. Dr. med. Jens Werner for giving me the precious opportunity to pursue an M.D. degree at the Ludwig Maximilian University of Munich. They offered significant support to successfully conduct this project, including but not limited to financial support and project design.

Meanwhile, I would like to thank my supervisor, PD Dr. med. Florian Kühn, for patient instruction and coordinating the recruitment of patients. Your wisdom and critical thinking enabled me to scrutinize every detail related to the projects and broaden the scope of my scientific research. I also want to thank Dr. med. Josefine Schardey and Dr. med. Ulrich Wirth for their significant contribution to this project.

Furthermore, I would like to extend thanks to Michaela Svihla and Nadine Gesse for offering the technical support of the flow cytometry operation, thank Anna Christina Schmidt, Dennis Nothdurft, Saskia Dörbecker for providing tremendous help to collect patients' blood samples, and thank Nicole Sylvia Strobl and Peter Iffelsberger for administrative support.

In addition, I feel like to show appreciation to my parents, Mingxia Fu and Erhua Lu, and my dear girlfriend, Xin Li, for their continuous support and uninterrupted encouragement throughout three years' study abroad.

Last but not least, I need to acknowledge the LMU-China Scholarship Council program for the full financial support of my doctoral study.

This dissertation would not have been accomplished without their considerable support.

Affidavit



Affidavit

Lu, Can

Surname, first name

Street

310000, Hangzhou

Zip code, town

China

Country

I hereby declare, that the submitted thesis entitled

Characterization of Peripheral Immune Events in Primary Colorectal Cancer Patients

is my own work. I have only used the sources indicated and have not made unauthorised use of services of a third party. Where the work of others has been quoted or reproduced, the source is always given.

I further declare that the submitted thesis or parts thereof have not been presented as part of an examination degree to any other university.

Hangzhou, 22.09.2022

Place, date

Can Lu

Signature doctoral candidate

Confirmation of Congruency



Confirmation of congruency between printed and electronic version of the doctoral thesis

Lu, Can

Surname, first name

Street

310000, Hangzhou

Zip code, town

China

Country

I hereby declare that the electronic version of the submitted thesis, entitled
Characterization of Peripheral Immune Events in Primary Colorectal Cancer Patients

is congruent with the printed version both in content and format.

Hangzhou, 22.09.2022

Place, date

Can Lu

Signature doctoral candidate

List of publications

1. Yang S, Gu Z, **Lu C**, Zhang T, Guo X, Xue G, Zhang L. Neutrophil Extracellular Traps Are Markers of Wound Healing Impairment in Patients with Diabetic Foot Ulcers Treated in a Multidisciplinary Setting. *Adv Wound Care (New Rochelle)*. 2020;9(1):16-27. (IF: 4.730)
2. **Lu C**, Schardey J, Zhang T, Crispin A, Wirth U, Karcz KW, Bazhin AV, Andrassy J, Werner J, Kühn F. Survival Outcomes and Clinicopathological Features in Inflammatory Bowel Disease-Associated Colorectal Cancer: A Systematic Review and Meta-Analysis. *Ann Surg*. 2021. (IF: 13.787)
3. **Lu C**, Zhang X, Luo Y, Huang J and Yu M. Identification of CXCL10 and CXCL11 as the candidate genes involving the development of colitis-associated colorectal cancer. *Front. Genet*. 2022; 13:945414. (IF: 4.772)